공학박사학위논문

Robust Consensus and Synchronization in Heterogeneous Multi-Agent Systems

이종 다개체 시스템의 상태 일치 및 동기화에 대한 강인성 연구

2016년 8월

서울대학교 대학원

전기컴퓨터공학부

김 재 용

ABSTRACT

Robust Consensus and Synchronization in Heterogeneous Multi-Agent Systems

by

Jaeyong Kim

Department of Electrical and Computer Engineering
College of Engineering
Seoul National University

August 2016

Consensus and synchronization both refer to the property that individuals in a group reach agreement in some sense, and the phenomena in large communities of interacting systems appear in various areas of biology, social sciences, engineering, and so on. Flocking of birds, schooling of fish, and swarming of bees are fascinating phenomena to be observed in nature. Sometimes, the consensus theory is a useful tool for understanding social phenomena. In engineering world, consensus and synchronization are relevant in an extremely wide range of applications from various disciplines including sensor networks, unmanned vehicles, robot cooperation teams, mobile communication systems, and so on.

In particular, it is a common belief in biophysics and systems biology that synchronization makes the behavior of an interconnected system robust to perturbation, which has often been verified in simulations and experiments. Motivated by this, the dissertation addresses the robust consensus and synchronization problems of multi-agent systems. A multi-agent system consists of several

non-identical individuals, each of which has the ability that can interact with its neighboring systems. We consider consensus and synchronization in networks of individual dynamical systems interconnected according to a specific communication topology, where the individual systems are described by nonlinear ordinary differential equations and the communication topology is modeled by a graph.

We devote the first part of this dissertation to explain how synchronization may help protect interconnected multi-agent systems from heterogeneities in individuals and randomly determined variations. In fact, it is emphasized that the robustness comes, rather than from the synchronization itself, from two specific components that lead to synchronization; that is, "multi"-agents and "coupling" among them. In particular, it is mathematically proved that (i) the solutions of individual agents get closer to each other as the coupling gain gets larger, so that practical synchronization is achieved, even under large heterogeneity among the agents, and (ii) as the number of agents becomes larger, the achieved synchronization becomes less affected by the variations in the individual agents.

In general, the consensus and synchronization problems of the heterogeneous network systems are possessed of intrinsic complexities compared to controlling a single system. The complexities arise from, for example, the number of systems involved, system dynamics, and topological structure of the network. Thus, a new notion of averaged dynamics which is a useful tool for understanding the collective behavior of the heterogeneous multi-agent systems is introduced.

In the second part of the dissertation, we propose a design method to implement optimal distributed sensor network as an application of the robust consensus and synchronization. Even though centralized Kalman-Bucy filter is an optimal filter, it is not useful since a fundamental problem in distributed sensor network is to achieve estimation of target by using distributed algorithms. Since the underlying philosophy for designing distributed Kalman-Bucy filter is similar to the robust consensus and synchronization, we introduce the averaged distributed Kalman-Bucy filter which is the average of all distributed Kalman-Bucy filters' dynamics, so as to recover the optimality of centralized Kalman-Bucy filter. The proposed algorithm finds out that the strong coupling makes the error covariance matrix approximately (but arbitrarily closely) converge to that of the centralized

Kalman-Bucy filter and the optimality can be recovered. Moreover, we propose a flexible distributed Kalman-Bucy filter so as to expand and reduce the scale of the sensor network. Numerical simulations demonstrate the performance of the proposed scheme.

Keywords: multi-agent systems, consensus, synchronization, robustness, averaged dynamics, distributed sensor network, distributed Kalman-Bucy filter
Student Number: 2010–20777

Contents

List of Tables

List of Figures

Symbols and Acronyms

Symbols

$\mathbb{R}$	field of real numbers
$\mathbb{R}_{\geq 0}$	non–negative real numbers
$\mathbb{R}^n$	real Euclidean space of dimension n
$\mathbb{R}^{m\times n}$	space of $m \times n$ matrices with real entries
$\mathbb{S}$	the circle
$\mathrm{Re}(s)$	real part of the complex number s
C^1	continuously differentiable
$\mathbb{C}$	field of complex numbers
$\mathbb{C}^{m\times n}$	space of $m \times n$ matrices with complex entries
$\mathbb{C}_{\geq 0}$	closed right-half complex plane; i.e., $\mathbb{C}_{>0} \bigcup \mathbb{C}_{=0}$
$\forall$	for all
I_n	$n \times n$ identity matrix (subscript n is omitted when there is no confusion.)
$0_{m\times n}$	$m \times n$ zero matrix (subscript $m \times n$ is omitted when there is no confusion.)
A^{-1}	inverse of the square matrix A
A^T	transpose of the matrix A

$\mathrm{col}(x_1, \ldots, x_k)$	stacking of vectors $x_i \in \mathbb{R}^{m_i}$, $i = 1, 2, \ldots, k$; *i.e.*, $[x_1^T, \ldots, x_k^T]^T$
$\mathrm{v}(A)$	stacking the columns of the $m \times n$ matrix A; *i.e.*, $[a_{1,1}, \cdots, a_{m,1}, a_{1,2}, \cdots, a_{m,2}, \cdots, a_{1,n}, \cdots, a_{m,n}]^\top$ where $a_{i,j}$ represents the (i,j)-th element of A
$\mathrm{diag}(A_1, \ldots, A_k)$	block diagonal matrix with diagonal blocks A_1 to A_k
$\mathrm{sign}(x)$	signum function of $x \in \mathbb{R}$; i.e., -1 if $x < 0$, 0 if $x = 0$, and 1 if $x > 0$
P(A)	probability of the event A
E{X}	expectation value of the random variable X
V{X}	variance value of the random variable X
$A \otimes B$	Kronecker product of matrices A and B
$\sum_{i=m}^{n} x_i$	summation of the sequence x_i; *i.e.*, $x_m + x_{m+1} + \cdots + x_{n-1} + x_n$ if $m < n$, x_m if $m = n$, and 0 if $m > n$
$\prod_{i=m}^{n} x_i$	product of the sequence x_i; *i.e.*, $x_m \cdot x_{m+1} \cdot \cdots \cdot x_{n-1} \cdot x_n$ if $m < n$, x_m if $m = n$, and 1 if $m > n$
$\lvert x \rvert$	Euclidean norm of the vector x
$\lVert A \rVert$	induced 2-norm of the matrix A
$\lVert A \rVert_F$	Frobenius norm of the matrix A
$\max\{a_1, \ldots, a_k\}$	maximum value among $a_1, a_2, \cdots, a_k$
$\min\{a_1, \ldots, a_k\}$	minimum value among $a_1, a_2, \cdots, a_k$
$:=$	defined as
$\Leftrightarrow$	identically equal
$\Rightarrow$	implies
$\Diamond$	designation of the end of theorem, lemma, proposition, assumption, remark, and so on
$\square$	designation of the end of proof

- A scalar continuous function $\gamma : [0, a) \to [0, \infty)$ is a class-$\mathcal{K}$ function if it is strictly increasing and $\gamma(0) = 0$.
- Let f and g be two functions on some subset of real numbers, $f(k) = \mathcal{O}(g(k))$ means that there exist constant c and K such that $f(k) \leq cg(k)$ for all $k > K$.
- A square matrix A is said to be Hurwitz (matrix) if every eigenvalue λ of A has strictly negative real parts, i.e., $\mathrm{Re}(\lambda) < 0$.
- For a matrix $A \in \mathbb{R}^{m\times n}$, $\|A\| \leq \|A\|_F \leq \sqrt{\min\{m, n\}}\|A\|$.
- For arbitrary matrices A_i and A_j, $\|A_i \otimes A_j\| = \|A_i\|\|A_j\|$ [LS04].
- For matrices $A,\ B$ and C, $\mathrm{v}(ABC) = (C^T \otimes A)\mathrm{v}(B)$.
- For a positive constant r, $B_r := \{x \in \mathbb{R}^n : |x| \leq r\}$.
- For any state variable $x(t)$, its initial condition will be denoted by $x(0)$.
- In order to messy notation, the time symbol t is omitted when there in no confusion.

Acronyms

CKBF	Centralized Kalman-Bucy filter
KCF	Kalman-Consensus filter
O-DKBF	Optimal distributed Kalman-Bucy filter
F-DKBF	Flexible distributed Kalman-Bucy filter
LTI	Linear time-invariant
LTV	Linear time-varying

Chapter 1

Introduction

1.1 Research Background

1.1.1 Consensus and Synchronization

What is the difference between the notions of consensus and synchronization in the networked system? Many researchers who are interested in the consensus and synchronization problems may have this question. As expected, the two terms are closely related in some sense. Both describe the effect of reaching agreement in a group of individual systems. In the case of consensus, it deals with the problem of agreement about the value of the members while synchronization deals with the problem of the exact coincidence in time or rate, when the members take a specific value. Therefore, we can argue that consensus with the coincidence in time yields synchronization, and synchronized trajectory yields consensus. As a result, whether some phenomenon is termed consensus or synchronization often depends on the point of view one decides to take.

Cooperative collective behaviors in networks of individual agents have received considerable attention in recent years due to their broad applications to biological systems, neuroscience, social science, engineering, and so on. Flocking of birds, schooling of fish, swarming of bees, and fireflies flashing in synchrony are fascinating phenomena to be observed in nature [Rey87, HBSM04, JMB05, Buc88]. In biological systems and neuroscience, complex networks are found at different scales from the molecular level up to the population level. In some of these net-

works, dynamical interactions between units, which are crucial for our current understanding of living systems, can be analyzed in the framework of synchronization phenomena like, e.g., circadian rhythm [Str03, LWK+07], neuronal network [IM08], and so on. Gossip-based algorithms [AYSS08] to achieve consensus over a set of agents have recently received attention in social science.

In engineering area, distributed consensus and coordination control of multi-agent systems over the complex networks have received a lot of attention in recent years. Consensus and synchronization problems of coordinated motion of individual mobile agents is the most commonly cited example in its various occurrences [FM04, JLM03, OSFM07, RBA07, QWH08, SPL08]. Advances in wireless communications and microelectromechanical systems technology have enabled the use of distributed sensor nodes, and the distributed estimation is one of the most fundamental collaborative information processing problems in wireless sensor networks [OS07, BFL11, Geo13, YKK15]. In addition, many consensus and synchronization algorithms were developed and studied under various circumstances, *e.g.,* switching topology [Kim12, KSBS13, Wie10, WSA11, KA15], communication delay [MPA10, LJ08], packet drop communication [FZ09], and so on.

1.1.2 Complexity of Analysis

Even though the consensus and synchronization of individual systems are relevant in an extremely wide range of applications, it is difficult to tackle the consensus and synchronization problems in large communities with interacting systems. The intrinsic complexities of consensus and synchronization can be identified with the 2-dimensional space: complexity of the individual system dynamics, and complexity of the network. These two dimensions of complexity and the related references are depicted in Figure 1.1[1]. The system complexity can be ranged from the simple linear integrator models to heterogeneous[2] stochastic nonlinear systems or hybrid systems. The network complexity deals with the kind of topologies and communication link constraint, and thus the range can be determined from two

[1] The definitions of the terms of network complexity can be found in Chapter 2.

[2] The terms, heterogeneous, non-identical, have the same meaning in this dissertation. In addition, homogeneous, identical, have the same meaning, too. We will use them interchangeably.

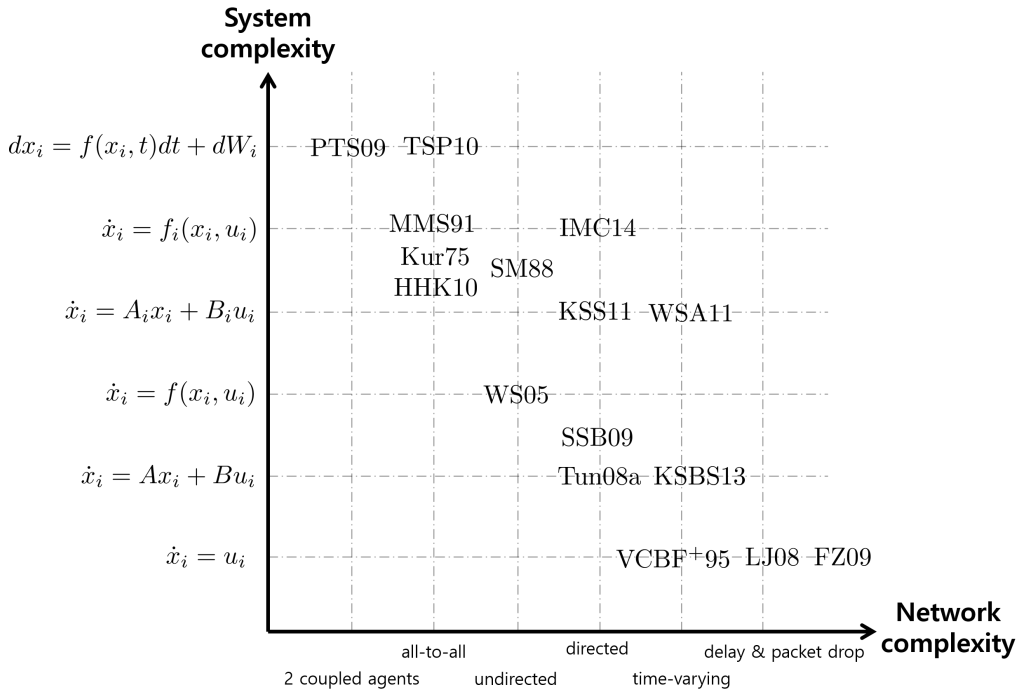

Figure 1.1: The complexity plane for networked systems and related references.

coupled agents to time-varying topologies with communication delay and packet drop.

Consensus and synchronization problems have been usually classified very differently in the complexity plane. Consensus problems are often focused on network complexity, in particular communication constraints, while individual system dynamics are usually fairly simple that the individual agents modeled as simple integrator [JLM03, OSFM07, RBA07]. This is because many researchers in control systems were inspired by the *Vicsek model* [VCBJ+95] and it triggered the interest of consensus problems. This model is composed of N autonomous subsystems which are driven by a constant absolute velocity (in discrete-time), and updating the head angle by the average direction of motion of the agents in its neighborhood with some random noises added, i.e.,

$$\theta_i(k+1) - \theta_i(k) = \delta_i(k) + \frac{1}{1 + |\mathcal{N}_i(k)|} \sum_{j \in \mathcal{N}_i(k)} (\theta_j(k) - \theta_i(k)) \,, \tag{1.1.1}$$

where $\theta_i \in \mathbb{S}$ is the heading angle of the i-th subsystem, $\delta_i \in \mathbb{S}$ represents temperature-like noise, and $\mathcal{N}_i(k)$ is the set of indices of the neighbors of the i-th subsystem at time k. The Vicsek model can be modeled as a simple integrator (without noise) with the time-varying communication network, and thus many consensus problems are more focused on network complexity.

Nevertheless, the following results have struggled to develop the system complexity in consensus problems.

i) In virtue of the graph theory, the consensus problem of identical LTI systems can be considered as simultaneous stabilizability problem of certain $(N-1)$ systems. It can be seen from [Tun08a][3] that

$$\begin{aligned}\dot{x}_i &= Ax_i + Bu_i,\\ u_i &= kB^TP\sum_{j\in\mathcal{N}_i}(x_j - x_i),\end{aligned}$$

where $x_i \in \mathbb{R}^n$ is the state, $k > 0$ is the coupling strength, and $P > 0$ is the solution of the following algebraic Riccati equation

$$A^TP + PA - PBB^TP + I_n = 0.$$

ii) Output consensus of heterogeneous multi-agent systems was addressed by introducing an internal model into the consensus problem in [KSS11, WSA11, IMC14], for example, consider a group of heterogeneous LTI systems

$$\begin{aligned}\dot{x}_i &= A_ix_i + B_iu_i,\\ y_i &= C_ix_i,\end{aligned}$$

where $x_i \in \mathbb{R}^{n_i}$ is the state, $y_i \in \mathbb{R}$ the output of the i-th agent, and output

[3]Here, the assumptions are (A, B) is stabilizable and the graph is connected.

feedback controller written as (relative degree 1 case of [KSS11])

$$\dot{\zeta}_i = F\zeta_i + Gy_i + H\sum_{j\in\mathcal{N}_i}(y_j - y_i)$$
$$u_i = J\zeta_i + Ky_i.$$

Even though they dealt with asymptotic consensus of the non-identical agents with output information, an identical internal model requirement is necessary for consensusability [WSA11], *i.e.,* the models of the individual systems together with their local controllers must embed an identical internal model of that virtual exosystem.

In contrast to consensus, the problems of synchronization usually deal with more complex system dynamics, *e.g.,* nonlinear oscillators, while putting less emphasis on the network complexity. Often, in order to simplify the analysis, the extreme case of all-to-all topology is assumed, which can be considered as unconstrained communication. Similar to the Vicsek model (1.1.1), there is a famous model for synchronization, namely the *Kuramoto model*[4] [Kur75, HHK10],

$$\dot{\theta}_i = \omega_i + \frac{K}{N}\sum_{j=1}^{N}\sin(\theta_j - \theta_i), \tag{1.1.2}$$

where $\theta_i \in \mathbb{S}$ is the phase of the i-th oscillator, $\omega_i \in \mathbb{R}$ is the randomly drawn i-th natural frequency of the oscillator, and $K \in \mathbb{R}$ is the coupling gain. Some efforts to expand the network compelxity and system complexity of the synchronization problems are as follows.

i) A natural extension of the Kuramoto model with short-range interaction effects was discussed in [SM88]. The authors considered the case in which interactions occur between nearest neighbors. The model equation is

$$\dot{\theta}_i = \omega_i + K\sum_{j\in\mathcal{N}_i}\sin(\theta_j - \theta_i).$$

[4] In fact, Kuramoto model was simplified from Winfree model [Win67] for the system of weakly coupled and nearly identical limit-cycle oscillators. See [Str00] for more details.

Compare to the Kuramoto model (1.1.2) the coupling strength K does not need to be scaled by the total number N of oscillators.

ii) When the coupling is strong enough, the amplitude of each oscillator may be affected, and thus a more comprehensive and general model was introduced by [MMS91]. The authors considered limit-cycle oscillator with all-to-all coupling,

$$\dot{z}_i = \left(1 - |z_i|^2 + \sqrt{-1}\omega_i\right) z_i + \frac{K}{N}\sum_{j=1}^{N}(z_j - z_i), \tag{1.1.3}$$

where z_i is the position of the i-th oscillator in the complex plane, ω_i its natural frequency (assumed to be randomly selected from a frequency distribution), and K is the coupling gain.

With $\bar{z} := \sum_{i=1}^{N} z_i/N$, the system (1.1.3) can be written as

$$\dot{z}_i = \left(1 - |z_i|^2 + \sqrt{-1}\omega_i\right) z_i + K(\bar{z} - z_i). \tag{1.1.4}$$

Define the amplitude and phase of the average position by $\bar{z} =: Re^{\sqrt{-1}\phi}$, which enables (1.1.4) to be written in polar form

$$\dot{r}_i = (1 - r_i^2 - K)r_i + KR\cos(\phi - \theta_i), \tag{1.1.5a}$$

$$\dot{\theta}_i = \omega_i + \frac{KR}{r_i}\sin(\phi - \theta_i). \tag{1.1.5b}$$

Therefore, with the limit of weak coupling and narrowly distributed frequencies, all the oscillators approach the unit circle and the system (1.1.5b) becomes the Kuramoto phase model (1.1.2). In particular, the limit-cycle oscillator (1.1.3) was derived from the weakly coupled Van der Pol oscillators [Aiz76].

iii) In [WS05], the authors considered the synchronization problems of nonlinear networked systems including Van der Pol oscillator under a general coupling

structure. A network containing identical individuals is given as

$$\dot{x}_i = f(x_i, t) + \sum_{j \in \mathcal{N}_i} K_{ji}(x_j - x_i), \tag{1.1.6}$$

where K_{ji} is the gain associated with coupling from node i to j. In this case, if the couplings are strong enough, then a generally coupled network (1.1.6) will achieve synchronization.

From the above researches, it is observed that consensus and synchronization studies often focus on either network or system complexity, but rarely deal with both at the same time. In particular, it seems that there is an intrinsic limitation in the interconnected dynamical systems composed of non-identical dynamics. We will devote to investigate the collective behavior of nonlinear and non-identical systems with general communication network[5], and the limitation will be partly solved in this dissertation.

1.1.3 Robustness of Interconnected Dynamical Systems

It is a common belief in biophysics and systems biology that synchronization makes the behavior of an interconnected system robust to perturbation, which has often been verified in simulations and experiments. Circadian rhythm is one of the most well known example of this feature [LWK$^+$07, AWJ$^+$15, KHHPB07]. Studies have found that the circadian rhythm is governed by a biological clock, which in mammals is located in brain area called the suprachiasmatic nuclei (SCN), and have a period of approximately 24 hours. In addition, these circadian cycles can be synchronized to external time signals but also can persist in the absence of such signals. Moreover, it is robust against the mutations [LWK$^+$07] and noises [AWJ$^+$15, KHHPB07]. This robustness of synchronization in circadian rhythm is important in determining the sleeping and feeding patterns of all animals, including human beings, and thus we need to figure out a way of obtaining the robustness.

[5] In this dissertation, we consider the system $\dot{x}_i = f_i(x_i, u_i)$ with undirected network in Figure 1.1.

This dissertation is devoted to explain how synchronization may help protect an interconnected multi-agent system from uncertainties and external disturbances. Tabareau, Slotine, and Pham in [TSP10] mathematically analyze the robustness of synchronization for a diffusive network of noisy identical nonlinear systems. The authors showed that under specific, quantified conditions, the impact of noise on individual interconnected systems and on their spatial mean can essentially be canceled through synchronization. The main assumption is that the dynamics is resistant to small perturbations, and thus all individual systems have to be the 'same' and 'good' agents in some sense. As mentioned in Section 1.1.2, however, the non-identical nature of individuals is intrinsic phenomenon in biological systems. Motivated by this, we will tackle the robustness problem of the network including 'different' and 'bad' agents in this dissertation.

1.2 Outline and Contributions

The following overview reveals the outline of this dissertation and briefly summarizes the contributions of each chapter.

Chapter 2. Graph Theory for Consensus and Synchronization Problems

In this chapter, we review basic definitions from graph theory and provide new interpretations of consensus and synchronization problems. Parts of this chapter are based on [KYKS12, KKYS13, KS15, KYS$^+$]

i) We review basic definitions of graph theory, as far as they are relevant for consensus and synchronization problems. In addition, a relation between algebraic graph properties and the number of nodes is established.

ii) We provide new interpretations of the solvability of the consensus and synchronization problems by introducing the useful coordinate transformation.

Chapter 3. Robustness by Strong Coupling

This chapter addresses one of the main ingredients of robust synchronization against heterogeneity. In particular, we discuss the key factors of synchronized

behavior and provide reliable computations to be carried out even in the presence of significant heterogeneity. Most of this chapter is based on [KYKS12, KKYS13, KS15, KYS$^+$].

i) We introduce the new notion of the averaged dynamics which is a useful tool for understanding the collective behavior of the non-identical multi-agent systems.

ii) We provide the conditions to achieve robust consensus and synchronization with strong coupling. From the results, we explain why strong coupling enhances the robustness of the synchronized behavior.

iii) In order to deal with physical systems, we provide similar results of strong coupling for high-order heterogeneous agents.

Chapter 4. Robustness by A Large Number of Agents

In this chapter, we consider the robust synchronization against randomly selected variations in individuals, and show that strong coupling and a large number of agents imply robustness of synchronization against heterogeneity. This chapter is mainly based on [KYS$^+$].

i) A new notion of expected averaged dynamics is introduced as a reference system which is not affected by the variations of the agents.

ii) We provide the effect of a large number of agents for the robustness of averaged dynamics by using probability theory.

iii) We explain why strong coupling and a large number of agents need to be used in robustness of consensus and synchronization problems.

Chapter 5. Optimal Distributed Kalman-Bucy Filter in Sensor Network

This chapter mainly deals with the distributed Kalman-Bucy filter which the application of the results in Chapter 3. We focus on the optimal recovery problem in the sense of distributed sensor network.

i) As a preliminary of the subsequent sections, we recall some background materials on Kalman-Bucy filter in distributed sensor network.

ii) We derive sufficient condition for semi-global ultimate boundedness of heterogeneous multi-agent systems with locally Lipschitz nonlinearity.

iii) We propose a design method to implement optimal distributed Kalman-Bucy filter with strong coupling.

iv) In order to expansion and reduction of scale, we propose a design method of flexible distributed Kalman-Bucy filter.

Chapter 6. Conclusions

This final chapter provides some conclusive remarks summarizing the thesis and hints to possible future directions of research.

Chapter 2

Graph Theory for Consensus and Synchronization Problems

In order to effectively deal with the consensus and synchronization problems in large communities of interacting systems, we need to consider networks of inidividual dynamical systems, which are interconnected according to a specific *communication topology*. The communication topology is chacracterized by the links between the individual systems, and the systems can send or receive the information through the links. Based on the links of the communication topology, the set of neighbors (or senders if links are directional) can be determined for every member of the network.

Graph theory is a useful tool for understanding or modeling the communication topology in a network of individual systems (see [Bon76, Bol02, Die06, GR01, Gro04, Big93, Moh92, Moh91, Mer95, New00] and the references therein for details about graph theory), and it has been used in the consensus and synchronization problems (refer to, *e.g.*, [FM04, RBA07, OS07, JLM03, SSB09, WSA11, FYL06, Tun08a, Tun08b, KSS11, Kim12, Wie10, ME10]). In particular, the *algebraic connectivity* has been used in analysing the robustness and synchronizability of networks. The theory related to the algebraic connectivity was introduced by Miroslav Fiedler [Fie73, Fie89].

In this chapter, we summarize the basic definitions and results from graph theory for the study of the consensus and synchronization problems, and the results will be used throughout this dissertation.

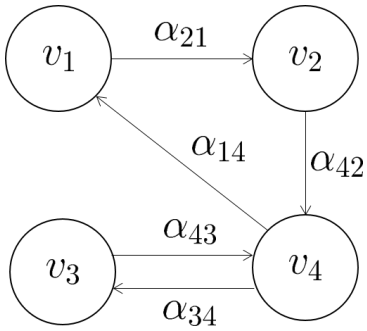

Figure 2.1: Fixed weighted directed graph with four nodes.

2.1 Basic Definitions of Graph Theory

Graph consist of *nodes* (or vertices), *edges* (or arcs) connecting the nodes, and *weights* assigned to their corresponding edges. Time-varying weighted directed graph is the most general case, because it contains fixed (or time-invariant), unweighted, and undirected graphs as special cases.

Definition 2.1.1. (Communication graph). A time-varying weighted directed graph $\mathcal{G}(t)$ is a 3-tuple $\mathcal{G}(t) := (\mathcal{N}, \mathcal{E}(t), \mathcal{A}(t))$ of nodes $\mathcal{N} := \{1, 2, \ldots, N\}$, edge set $\mathcal{E}(t) \subseteq \mathcal{N} \times \mathcal{N}$, and weighted *adjacency matrix* $\mathcal{A}(t) = [\alpha_{ij}(t)] \in \mathbb{R}^{N \times N}$, where $t \in \mathbb{R}$ represents time, satisfying the following properties:

(a) The graph contains no self-loops, *i.e.*, $(i, i) \notin \mathcal{E}(t)$ and $\alpha_{ij}(t) = 0$ for all $i \in \mathcal{N}$ and $t \geq 0$.

(b) The elements $\alpha_{ij}(t)$ of the adjacency matrix $\mathcal{A}(t)$ are nonnegative, bounded, and piecewise continuous function for $t \geq 0$.[1]

(c) The edge (j, i) is contained in $\mathcal{E}(t)$ at time t if and only if $\alpha_{ij}(t)$ is positive at time t. Otherwise, $\alpha_{ij}(t) = 0$.

□

[1] A function $f(t)$ is said to be a piecewise continuous function on a closed interval $[a, b] \subset \mathbb{R}$, if there exists finite number of points $a = t_0 < t_1 < t_2 < \cdots < t_N = b$ such that $f(t)$ is continuous in each of the intervals (t_{i-1}, t_i) for $1 \leq i \leq N$ and has finite limits as t approaches the end points. A function $f(t)$ is said to be a piecewise continuous function for $t \geq 0$, if $f(t)$ is a piecewise continuous function on every closed interval $[a, b] \subset [0, \infty)$.

In the above definition, the nodes $i \in \mathcal{N}$ represent the individual systems and the edges $(i, j) \in \mathcal{E}(t)$ are modelled on the interconnections between the individual systems. For a given edge $(i, j) \in \mathcal{E}(t)$, j is called the *head* and i is called the *tail* and (i, j) represents the *information flow* from the tail to the head of an edge. Usually, an edge (i, j) is represented by an arrow pointing from the tail i to the head j. An example of a fixed weighted directed graph with four nodes, with edges represented by arrows, is depicted in Figure 2.1.

The special classes of graphs can be defined from Definition 2.1.1. A graph is said to be *fixed* (or time-invariant) if it does not change over time t. In this case, it is simply denoted by $\mathcal{G} = (\mathcal{N}, \mathcal{E}, \mathcal{A})$. A graph $\mathcal{G}(t)$ is *unweighted* if $\alpha_{ij}(t) \in \{0, 1\}$ for all $i, j \in \mathcal{N}$ and for $t \geq 0$ and thus, one can simply write $\mathcal{G}(t) = \{\mathcal{N}, \mathcal{E}(t)\}$. Consequently, a fixed unweighted graph can be denoted by $\mathcal{G} = \{\mathcal{N}, \mathcal{E}\}$. The special case of an *undirected* graph is obtained by imposing $\alpha_{ij}(t) = \alpha_{ji}(t)$ for all $i, j \in \mathcal{N}$ and for $t \geq 0$, *i.e.*, $\mathcal{A}^T(t) = \mathcal{A}(t)$. Throughout this dissertation, we consider the fixed, unweighted, and undirected graph which is denoted by $\hat{\mathcal{G}} = \{\mathcal{N}, \mathcal{E}\}$.

2.1.1 Graph Connectedness

In order to achieve consensus or synchronization among the individual systems, it is necessary to share a minimum amount of information with all individuals. As explained before, the common information propagates through the network modeled by the graph which represents the communication topology. To ensure the propagation of the common information to all individuals, the graph needs to be connected in some sense. Here, we first define the neighbors of a node and a path of the graph.[2]

Definition 2.1.2. (Neighbors). Let $\hat{\mathcal{G}} = \{\mathcal{N}, \mathcal{E}\}$ be a graph. For a given $i \in \mathcal{N}$, a node $j \in \mathcal{N}$ is called *neighbor* of the node i if $(j, i) \in \mathcal{E}$. The *neighbors* of the node i is the set that contains every neighbor of the node i, and denoted by $\mathcal{N}_i$; *i.e.*, $\mathcal{N}_i := \{j \in \mathcal{N} : (j, i) \in \mathcal{E}\}$. □

[2]For a fixed weighted directed graph $\mathcal{G} = \{\mathcal{N}, \mathcal{E}, \mathcal{A}\}$, the definitions of the neighbors and the path are the same as Definition 2.1.2 and Definition 2.1.3, respectively.

Definition 2.1.3. (Path). Let $\hat{\mathcal{G}} = \{\mathcal{N}, \mathcal{E}\}$ be a graph. For a given $i, j \in \mathcal{N}$, a *path* of *length* l from the node i to the node j is a sequence of nodes of the form $\{i_0, i_1 \ldots, i_l\}$ such that $i_0 = i$, $i_l = j$, $i_k \in \mathcal{N}_{i_{k+1}}$ for $k = 0, 1, \ldots, l-1$, and i_k's are distinct for all k. □

In networked systems, existence of a path from the node $i \in \mathcal{N}$ to the node $j \in \mathcal{N}$ in the graph $\hat{\mathcal{G}}$ implies that the information can propagate from the system represented by the node i to the system represented by the node j. By using the definition of the path, we can define the connectedness of the graph as follows [ME10, GR01, Die06, Bol02, RBA07, RB08].

Definition 2.1.4. (Connected graph). A graph $\hat{\mathcal{G}} = \{\mathcal{N}, \mathcal{E}\}$ is said to be *connected* if there is a path between any two nodes of the graph $\hat{\mathcal{G}}$, otherwise *disconnected*. □

For a directed graph, the connected graph in Definition 2.1.4 is also called *quasi strongly connected* graph, and a different but equivalent statement of the connected graph is that a graph has a *directed spanning tree*. See [TS11, Lin06, Wu05, RBA07, RB08, SSB09] for more details of the definitions.

2.1.2 Laplacian Matrix

As was mentioned in Chapter 1, the diffusive coupling is the most commonly used mechanism potentially leading to consensus and synchronization. Therefore, we need to establish the connection between the diffusive coupling and the algbraic graph theory. To this end, consider the most common continuous consensus algorithm [OSM04, FM04, JLM03, RBA07] and assume the communication topology is modeled by a graph $\hat{\mathcal{G}} = \{\mathcal{N}, \mathcal{E}\}$. Then, the consensus algorithm can be expressed as

$$\dot{x}_i(t) = \sum_{j \in \mathcal{N}_i} (x_j(t) - x_i(t)), \quad i \in \mathcal{N},$$

where $x_i \in \mathbb{R}$ it the state of the i-th agent. The *collective dynamics* of the group of agents can be written as

$$\dot{x}(t) = -\mathcal{L}x(t) \tag{2.1.1}$$

where $x(t) := \mathrm{col}(x_1(t), \ldots, x_N(t))$ and $\mathcal{L} = [l_{ij}] \in \mathbb{R}^{N\times N}$ is a matrix, the so-called Laplacian matrix.

Definition 2.1.5. (Laplacian matrix). Given a graph $\hat{\mathcal{G}} = \{\mathcal{N}, \mathcal{E}\}$, the matrix

$$\mathcal{L} := \mathcal{D} - \mathcal{A}$$

is called the *Laplacian matrix* of the graph $\hat{\mathcal{G}}$, where $\mathcal{D} \in \mathbb{R}^{N\times N}$ is the degree matrix of the graph $\hat{\mathcal{G}}$, which is defined as $\mathcal{D} := \mathrm{diag}(\mathcal{A}1_N)$. □

Note that the Laplacian matrix $\mathcal{L}$ is symmetric, because of the undirected graph. The Laplacian matrix can also be defined by element-wise

$$l_{kj} := \begin{cases} \sum_{i=1}^{N} \alpha_{ki}, & j = k, \\ -\alpha_{kj}, & j \neq k. \end{cases}$$

In (2.1.1), the collective behavior of $x(t)$ is determined by the Laplacian matrix $\mathcal{L}$. Moreover, since the Laplacian matrix $\mathcal{L}$ can uniquely determines the adjacency matrix $\mathcal{A}$, it completely characterizes the graph $\hat{\mathcal{G}}$, and therefore characterizes the communication topology. Hence, the Laplacian graph can be a useful tool for understanding the behavior of interconnection dynamics for linearly diffusively coupled system. In order to figure out the relation between the algebric properties of $\mathcal{L}$ and the properties of the graph $\hat{\mathcal{G}}$, they will be discussed in the next section.

2.2 Algebraic Properties of Graph

The Laplacian matrix of a graph and its eigenvalues can be used in various areas, and according to Mohar [Moh91], the Laplacian spectrum is much more natural and more important than the spectrum of the adjacency matrix. Among all eigenvalues of the Laplacian matix of a graph, one of the most popular is the

second smallest, called by Fiedler [Fie73, Fie89], the algebraic connectivity of a graph. It is very important in the sense that it is a good parameter to measure how well a graph is connected.

2.2.1 Algebraic Connectivity

In order to introduce the algebraic connectivity, we need to start with the spectrum of the Laplacian matrix. By the construction of the Laplacian matrix, all rows of the Laplacian sum up to zero. Then, the all ones vector 1_N is an eigenvector of the Laplacian matrix $\mathcal{L}$ with corresponding eigenvalue 0 (*i.e.,* $\mathcal{L}1_N = 0$). In consensus and synchronization problems, this eigenvector 1_N spans the subspace in which all individual systems have reached to a certain trajectory in the subspace. Moreover, the zero eigenvalue of the Laplacian matrix can be interpreted as that if all individuals are reached to the common trajectory in the subspace, then the diffusive couplings vanish.

To analyze the locations of the eigenvalues of the Laplacian matrix, the following lemma, called the *Gershgorin disk theorem*, can be used.

Lemma 2.2.1. [HJ12, Theorem 6.1.1] Let $A = [a_{ij}] \in \mathbb{C}^{n\times n}$ and let $D_i := \{z \in \mathbb{C} : |z - a_{ii}| \leq \sum_{j\neq i} |a_{ij}|\}$ be the closed disk, called the i-th *Gershgorin disk*, in the complex plane centered at a_{ii}. Then all the eigenvalues of A lie in the union of the disks D_i for $i = 1, \ldots, n$, that is, $\lambda(A) \subset \bigcup_{i=1}^{n} D_i$, where $\lambda(A)$ is the spectrum of the matrix A. ◊

Since the Laplacian matrix has the properties that the off-diagonal elements are nonpositive and the diagonal elements are nonnegative, and each row sum of the Laplacian matrix is zero, we have

$$\lambda(\mathcal{L}) \subset \bigcup_{i\in\mathcal{N}} \left\{ z \in \mathbb{C} : |z - l_{ii}| \leq \sum_{j\neq i} |l_{ij}| \right\} \subset \mathbb{C}_{\geq 0}.$$

Hence, every nonzero eigenvalue of $\mathcal{L}$ lies in $\mathbb{C}_{>0}$. Based on this, we can sort the eigenvalues of the Laplacain matrix as $0 = \lambda_1(\mathcal{L}) \leq \lambda_2(\mathcal{L}) \leq \cdots \leq \lambda_N(\mathcal{L})$.[3]

[3]Since the Laplacian matrix is symmetric, all eigenvalues are real.

Table 2.1: The algebraic connectivity for some types of graphs

graph topology	$\lambda_2(\mathcal{L})$
path	$2(1-\cos(\pi/N))$
circle	$2(1-\cos(2\pi/N))$
star	1
all-to-all	N

The *algebraic connectivity* of a graph $\hat{\mathcal{G}}$ is the second-smallest eigenvalue $\lambda_2(\mathcal{L})$ of the Laplacian matrix $\mathcal{L}$. It is related to several important graph invariants and connectivity of the graph. The generalization of the algebraic connectivity (see [Wu05, DA07]) is defined as

$$\lambda_2(\mathcal{L}) = \min_{v\in\mathbb{R}^N, v\neq 0, v\perp 1_N} \frac{v^T\mathcal{L}v}{v^Tv}.$$

In general, adding new edges to a graph may increase the algebraic connectivity, and higher $\lambda_2(\mathcal{L})$ indicates graphs with smaller diameter (the greatest distance between any pair of nodes) and higher connectivity. It has pointed out in [Fie73, Hol06] that the algebraic connectivity may be dependent on the number of nodes, as well as the way in which nodes are connected. In Table 2.1, the algebraic connectivity with respect to the number of nodes for some types of graphs are presented. According to Table 2.1, except for the case of star topology, the algebraic connectivity $\lambda_2(\mathcal{L})$ is dependent on the number of nodes N. Increasing N decreases $\lambda_2(\mathcal{L})$ in the case of path and circle topologies. On the other hand, increasing N increases $\lambda_2(\mathcal{L})$ in the case of all-to-all topology.

In random graphs, the randomness is another factor of fundamental importance in $\lambda_2(\mathcal{L})$. Small-world network is one of the famous random networks in which any two arbitrary nodes can be connected using a few links. In [WS98], Watts & Strogatz introduced a model for small-world phenomenon that interpolates between these two extremes, in which the edges of the network are divided into 'local' and 'long-range' contacts (or a regular lattice and a random network, respectively) using a probability p. Watts & Strogatz model can be constructed

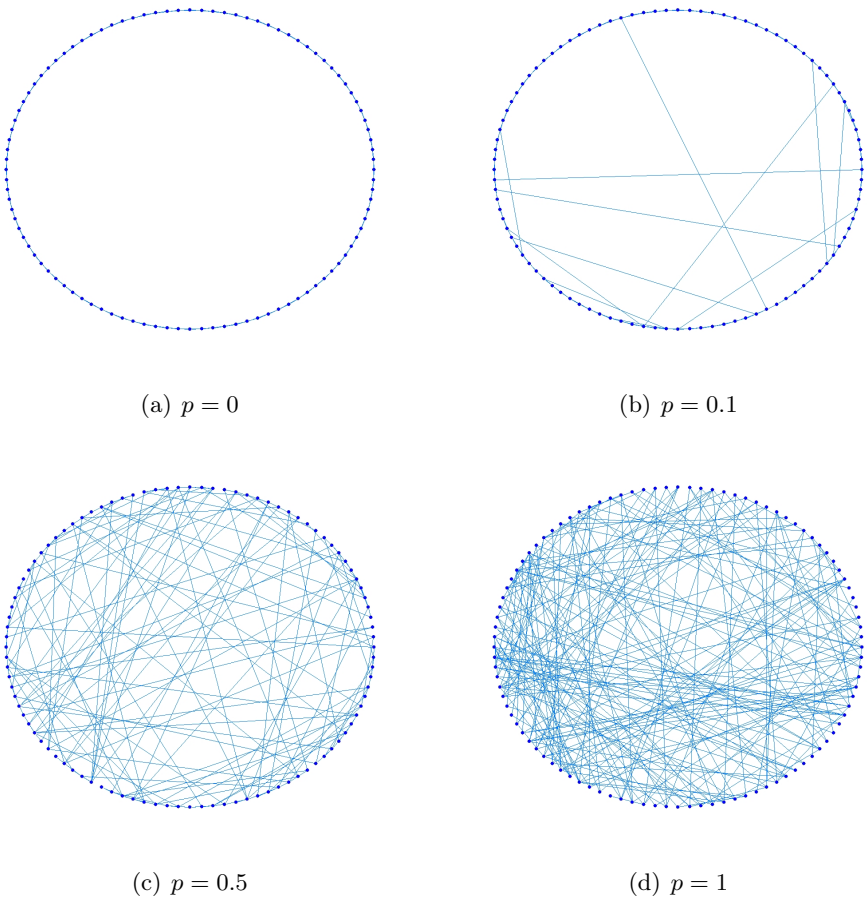

(a) $p = 0$ (b) $p = 0.1$

(c) $p = 0.5$ (d) $p = 1$

Figure 2.2: Small-world networks with $(N, d) = (100, 2)$ for $p = 0, 0.1, 0.5, 1$.

with the following steps:

(1) One starts with a one dimensional lattice on a ring with N nodes in which every node is connected to its nearest neighbors up to the distance d.

(2) One removes every edges with probability p.

(3) One rewires the removed edges by changing the endpoints uniformly at random (without self-loops or repeated links).

Figure 2.2 demonstrates small-world networks obtained by the above steps for various values of probability p.

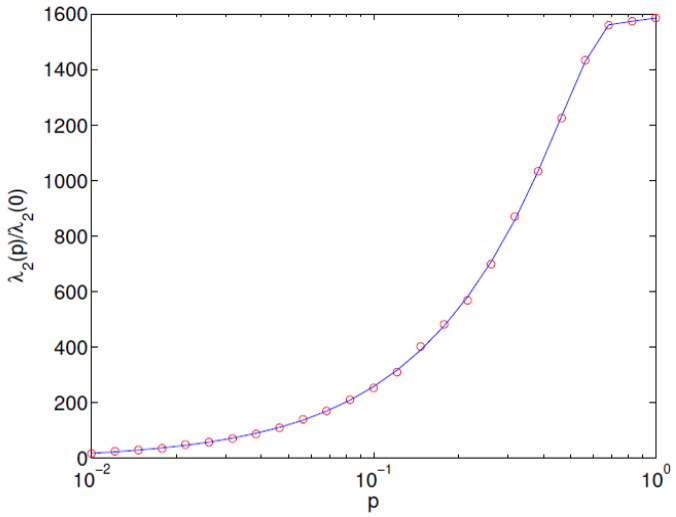

Figure 2.3: The S-shape curve of algebraic connectivity gain $\lambda_2(p)/\lambda_2(0)$ for small-world network with $(N, d) = (1000, 5)$ [OS05].

In small-world networks, the algebraic connectivity $\lambda_2(p)$[4] can be made more than 1000 times greater than a regular network by increasing randomness [OS05]. By defining the algebraic connectivity gain $\lambda_2(p)/\lambda_2(0)$, the curve of $\lambda_2(p)/\lambda_2(0)$ has S-shape in Figure 2.3. Thus, it can be observed that the algebraic connectivity increases as the randomness of the network increases.

Moreover, the algebraic connectivity is also affected by the number of nodes N and the distance d. The effects of N and d can be shown in Figures 2.4 and 2.5[5], respectively. In Figure 2.4, the algebraic connectivity has decreasing tendency as N increase, and it can also be seen from [Hol06] that the algebraic connectivity decreases with increasing the number of nodes in random network. On the other hand, an increase in d leads to a considerable increase in the algebraic connectivity in Figure 2.5.

[4]Here, instead of the Laplacian matrix index $\mathcal{L}$, we use the probability p as the parameter of the algebraic connectivity.

[5]Each data point in these figures are obtained by averaging over 10 randomly rewired networks

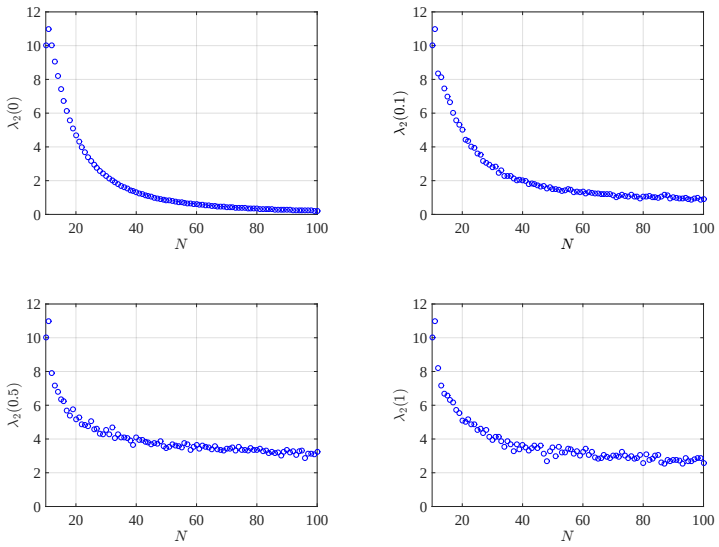

Figure 2.4: Small-world networks with $(N, d) = (100, 2)$ for $p = 0, 0.1, 0.5, 1$.

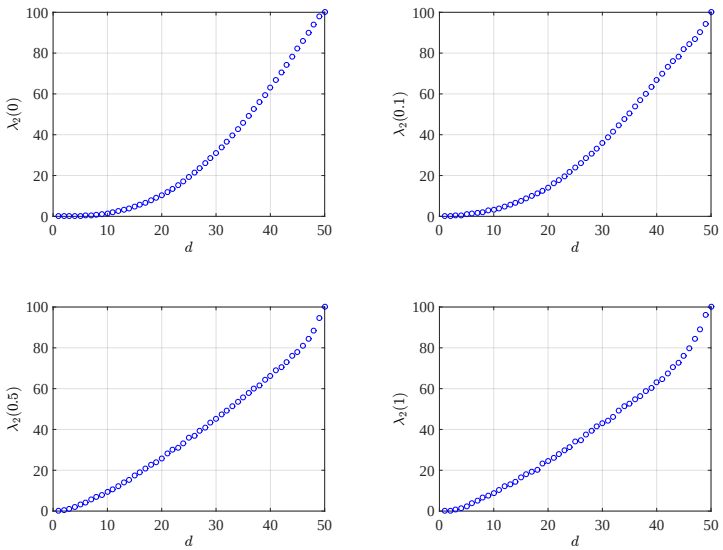

Figure 2.5: Small-world networks with $(N, d) = (100, 2)$ for $p = 0, 0.1, 0.5, 1$.

2.2.2 Useful Properties for Consensus and Synchronization

As a next step, we will establish some useful properties for consensus and synchronization problems. The algebraic connectivity $\lambda_2(\mathcal{L})$ is completely related to the graph connectivity as mentioned in 2.2.1. The following theorem is well-known result in spectral graph theory.

Theorem 2.2.2. Let $\hat{\mathcal{G}} = (\mathcal{N}, \mathcal{E})$ be a graph, and let $\mathcal{L}$ be the Laplacian matrix of the graph $\hat{\mathcal{G}}$. Then, $\lambda_2(\mathcal{L}) > 0$ if and only if $\hat{\mathcal{G}}$ is connected. $\Diamond$

Proof. ($\Rightarrow$) We first show that $\lambda_2(\mathcal{L}) = 0$ if $\hat{\mathcal{G}}$ is disconnected. If $\hat{\mathcal{G}}$ is disconnected, then it can be described as the disjoint union of graphs, $\hat{\mathcal{G}}_1$ and $\hat{\mathcal{G}}_2$. Without loss of generality, after suitably re-numbering the nodes, we have

$$\mathcal{L} = \begin{bmatrix} \mathcal{L}_{\hat{\mathcal{G}}_1} & 0 \\ 0 & \mathcal{L}_{\hat{\mathcal{G}}_2} \end{bmatrix}.$$

In this case, we obtain

$$\begin{bmatrix} \mathcal{L}_{\hat{\mathcal{G}}_1} & 0 \\ 0 & \mathcal{L}_{\hat{\mathcal{G}}_2} \end{bmatrix} \begin{bmatrix} 1_{N_1} \\ 0 \end{bmatrix} = \begin{bmatrix} 0 \\ 0 \end{bmatrix} \text{ and } \begin{bmatrix} \mathcal{L}_{\hat{\mathcal{G}}_1} & 0 \\ 0 & \mathcal{L}_{\hat{\mathcal{G}}_2} \end{bmatrix} \begin{bmatrix} 0 \\ 1_{N_2} \end{bmatrix} = \begin{bmatrix} 0 \\ 0 \end{bmatrix},$$

where $N_1 = \dim(\mathcal{L}_{\hat{\mathcal{G}}_1})$ and $N_2 = \dim(\mathcal{L}_{\hat{\mathcal{G}}_2})$. Hence, there are at least two orthogonal eigenvectors, $\mathrm{col}(1_{N_1}, 0)$ and $\mathrm{col}(0, 1_{N_2})$, of $\mathcal{L}$ corresponding to the eigenvalue zero, *i.e.,* at least two eigenvalues are zero, we know that $\lambda_1\mathcal{L} = \lambda_2\mathcal{L} = 0$.

($\Leftarrow$) Assume that $v \in \mathbb{R}^N$ is an eigenvector of $\mathcal{L}$ corresponding to the eigenvalue zero. Since $\mathcal{L}v = 0$, we have

$$v^T\mathcal{L}v = \sum_{(i,j)\in\mathcal{E}} (v_i - v_j)^2 = 0.$$

Consequently, $v_i - v_j = 0$ for each $(i, j) \in \mathcal{E}$. As there is a path between any two nodes of the graph $\hat{\mathcal{G}}$, we may inductively use this result to show that $v_i = v_j$ for all nodes $i, j \in \mathcal{N}$. Thus, every eigenvector for zero eigenvalue is multiple of 1_N. This shows that eigenspace corresponding to zero eigenvalue has dimension 1, that is, the geometric multiplicity of zero eigenvalue is 1. Since the Laplacian

matrix is symmetric, it is diagonalizable, and therefore algebraic and geometric multiplicity are the same. □

As was mentioned in 2.2.1, the algebraic connectivity $\lambda_2(\mathcal{L})$ may decrease as the number of nodes N increases in some cases (*e.g.,* path and circle topologies in Table 2.1). However, Theorem 2.2.2 ensures that as long as the graph is connected, the algebraic connectivity is always positive ($\lambda_2(\mathcal{L}) > 0$).

In order to achieve the consensus and synchronization problems by using the algebraic properties of the Laplacian matrix, we introduce the following useful theorem which will be used throughout this dissertation. To develop this, we first recall the following decomposition lemma of linear algebra.

Lemma 2.2.3. (Schur decomposition [HJ12]). If $A \in \mathbb{C}^{n\times n}$, then A can be expressed as $A = UTU^{-1}$ where U is a unitary matrix (*i.e.,* U^{-1} is also the conjugate transpose U^*, $U^{-1} = U^*$), and T is an upper triangular matrix. Moreover, since T is similar to A, it has the same eigenvalues as A, and therefore those eigenvalues are the diagonal entries of T. ◊

Theorem 2.2.4. Let $\hat{\mathcal{G}} = \{\mathcal{N}, \mathcal{E}\}$ and $\mathcal{L}$ be a connected graph and the Laplacian matrix of $\hat{\mathcal{G}}$. Then, there exists a nonsingular matrix W such that

$$W\mathcal{L}W^{-1} = \begin{bmatrix} 0 & 0 \\ 0 & \Lambda \end{bmatrix},$$

where $\Lambda = \mathrm{diag}(\lambda_2(\mathcal{L}), \ldots, \lambda_N(\mathcal{L}))$. In particular, the nonsingular matrices W and W^{-1} can be expressed as

$$W = \begin{bmatrix} \frac{1}{N}1_N^T \\ R^T \end{bmatrix}, \quad \text{and} \quad W^{-1} = [1_N,\ Q], \tag{2.2.1}$$

where R and Q are real matrices of size $N \times (N-1)$ such that $R^TR = (1/N)I$, $Q^TQ = NI$, $R^T1_N = 0$, $Q^T1_N = 0$, and $R^TQ = I$. ◊

Proof. A direct consequence of the connected graph $\hat{\mathcal{G}}$ is that the Laplacian matrix $\mathcal{L}$ is symmetric and has zero eigenvalue which is simple. By Schur decomposition, we can write the Laplacian matrix as $\mathcal{L} = UTU^T$ where U is a unitary matrix

and T is an upper triangular matrix. Since the Laplacian matrix $\mathcal{L}$ is symmetric, one sees that $\mathcal{L}\mathcal{L}^T = \mathcal{L}^T\mathcal{L}$, and therefore it ensures $TT^T = T^TT$. It means that T must be diagonal matrix since a normal upper triangular matrix is diagonal, and $T = \text{diag}(0, \Lambda)$. Without loss of generality, we can express the first row of the orthogonal matrix U as $(1/\sqrt{N})1_N^T$ from the property of the Laplacian matrix that all rows of the Laplacian sum up to zero. Define the matrix $W := (1/\sqrt{N})U$. Then,

$$W = \begin{bmatrix} \frac{1}{N}1_N^T \\ R^T \end{bmatrix}, \qquad W^{-1} = \sqrt{N}U^T = [1_N,\ Q]$$

where R and Q are real matrices of size $N \times (N-1)$. Since U is a unitary matrix and $UU^T = U^TU = I$, it follows that $R^TR = (1/N)I$, $Q^TQ = NI$, $R^T1_N = 0$, $Q^T1_N = 0$, and $R^TQ = I$. From above properties, we can also find that $\|Q\| = \sqrt{N}$ and $\|R\| = 1/\sqrt{N}$. □

Theorem 2.2.4 ensures that the problems of consensus and synchronization can be considered as the convergence to a invariant subspace $\mathcal{M}$ which implies that any trajectory starting in $\mathcal{M}$ remains in $\mathcal{M}$. We call this invariant subspace $\mathcal{M}$ as the *consensus subspace* which is spanned by the eigenvector 1_N of $\mathcal{L}$ with corresponding eigenvalue zero.

For example, consider the consensus algorithm (2.1.1) with a connected graph $\hat{\mathcal{G}}$. By the coordinate transformation in (2.2.1)

$$\xi = \begin{bmatrix} \xi_1 \\ \tilde{\xi} \end{bmatrix} = Wx = \begin{bmatrix} \frac{1}{N}1_N^T \\ R^T \end{bmatrix} x$$

where $\tilde{\xi} = [\xi_2, \ldots, \xi_N]^T$, the overall system (2.1.1) is transformed into

$$\dot{\xi}_1 = 0 \tag{2.2.2a}$$

$$\dot{\tilde{\xi}} = -\Lambda\tilde{\xi} \tag{2.2.2b}$$

because $1_N^T\mathcal{L} = 0$ and $R^T\mathcal{L}Q = \Lambda$. Since Λ is a positive definite matrix, it is easy to see from (2.2.2a) and (2.2.2b) that $\xi_1(t) = (1/N)\sum_{i=1}^N x_i(0)$ and $\tilde{\xi}(t) \to 0$ as

$t \to \infty$. Therefore, it explains the following properties:

i) Since $x = 1_N \xi_1 + Q\tilde{\xi}$, if $\tilde{\xi}(t) \to 0$ as $t \to \infty$, then the consensus and synchronization is achieved. Thus, the consensus and synchronization problem can be considered as the convergence problem, and the transformed system (2.2.2b) can be also considered as the error dynamics between agents.

ii) Consensus (or synchronized) trajectory can be expressed as $\xi_1(t)$ due to the fact that $\tilde{\xi}(t) \to 0$ implies $x_i(t) \to \xi_1(t)$.

iii) Since the solution of the transformed system (2.2.2b) is $\tilde{\xi}(t) = e^{-\Lambda t}\tilde{\xi}(0)$, the inequality

$$|\tilde{\xi}(t)| \leq |\tilde{\xi}(0)| e^{-\lambda_2(\mathcal{L})t}$$

holds for all $t \geq 0$. Therefore, the algebraic connectivity $\lambda_2(\mathcal{L})$ of the graph $\hat{\mathcal{G}}$ is related to the rate of convergence to consensus subspace $\mathcal{M}$, as well as the connectivity of the graph.

Based on these properties, a generalization to heterogeneous agents will be developed in Chapter 3.

Chapter 3

Robustness by Strong Coupling

In this chapter, we deal with the robust consensus and synchronization of heterogeneous multi-agent systems by strong coupling. In fact, strong coupling is somewhat well-known condition to achieve asymptotic consensus and synchronization with static diffusive coupling [WS05, PS07, TSP10, DdG09, DdBR11]. Static diffusive couplings with strong interaction have been used in several setups. *Contraction theory* has been shown to be an effective tool for understanding synchronization in terms of convergence properties of all solutions between each other rather than toward some asymptotic solution [WS05, PS07, TSP10]. In [DdG09, DdBR11], the so-called *QUAD condition* is assumed to be satisfied as a starting point to derive conditions for synchronization of the network of interest.

Even though the above studies provided strong coupling condition, the authors assumed that the dynamical model of the individual systems are identical and have some stability properties (*e.g.,* contraction system or QUAD condition). Unfortunately, in many real-world networks, it is often unrealistic to assume that all nodes share the same identical dynamics. For example, between the agents, there are parameter mismatches which cannot avoid and rather large in biochemical or power networks [KHHPB07, DB12, HC06]. Moreover, the networked system may have some abnormal agents, and therefore it will cause some problems which are propagated through the communication network. Nevertheless, practical consensus and synchronization is still possible as observed from nature such as flashing in fireflies, flocking of birds, schooling of fishes, and swarming of insects.

In order to effectively deal with the robust consensus and synchronization

of heterogeneous (non-identical) agents against the heterogeneities, we introduce the notion of *averaged dynamics*, which is the average of the vector fields of each agents. The aim of this chapter is to introduce the concept of the averaged dynamics and investigate the robustness of heterogeneous multi-agent systems by strong coupling. This chapter has its origin in these papers [KYKS12, KKYS13, KS15, KYS$^+$].

3.1 Problem Formulation

In this section, we address the robust consensus and synchronization problem of heterogeneous multi-agent systems. We consider a group of non-identical individual systems represented by

$$\dot{x}_i = f_i(t, x_i) + u_i, \quad i \in \mathcal{N} := \{1, 2, \dots, N\} \tag{3.1.1}$$

where N is the number of agents, $x_i \in \mathbb{R}$ is the state[1] and $u_i \in \mathbb{R}$ represents interactions with other agents through the network. Here the function $f_i : [0, \infty) \times \mathbb{R} \to \mathbb{R}$ may include time-varying signals persistently exciting the agent, and disturbances to the agent, as well as parametric variations or uncertainties of each agent.

The local interaction among the agents (3.1.1) is modeled by a fixed unweighted undirected graph $\hat{\mathcal{G}}$. In this section, it is supposed that the agents are interconnected by static diffusive-type coupling [Hal97]

$$u_i = k \sum_{j=1}^{N} \alpha_{ij}(x_j - x_i) \tag{3.1.2}$$

where k represents the coupling strength and α_{ij} is the (i, j)-th entry of the adjacency matrix of the given network.

[1]The class of systems considered in this section is restrictive in the sense that it is a scalar dynamics. Actually, this restriction arose because we have focused on the simplest case, which is because we wanted to find the main ingredients that yield practical consensus and synchronization in spite of heterogeneity of the agents and its robustness against heterogeneity (that includes external disturbances and parametric uncertainties), leaving aside the relaxation of these restrictions to Section 3.3.

Definition 3.1.1. (Robust consensus and synchronization). The N individuals (3.1.1) are said to achieve *robust consensus and synchronization* if there exists some trajectory $\zeta : \mathbb{R} \to \mathbb{R}$ such that for any given $\epsilon > 0$,

$$\limsup_{t\to\infty} |x_i(t) - \zeta(t)| \leq \epsilon$$

for all $i \in \mathcal{N}$. □

Note that Definition 3.1.1 is equivalent to the ultimate boundedness problem with arbitrary ultimate bound, *i.e.,* the robust consensus and synchronization of (3.1.1) can be achieved if there exist some trajectory $\zeta : \mathbb{R} \to \mathbb{R}$ and $T \geq 0$ such that for any given $\epsilon > 0$,

$$|x_i(t) - \zeta(t)| \leq \epsilon, \quad \forall t \geq T$$

for all $i \in \mathcal{N}$. On the other hand, the considered problem can be viewed as achieving the *practical consensus* from the viewpoint of achieving the asymptotic consensus problems. Since the terminology 'practical consensus' is used differently in [XJZY11] where just boundedness of the difference $|x_i(t) - x_j(t)|$ is of interest, we emphasize that the error could be made arbitrarily small in Definition 3.1.1.

We study the problem under the following assumptions.

Assumption 3.1.1. (Individual agent). The function $f_i(t, x_i)$ of the individual system (3.1.1) is uniformly bounded in t, continuously differentiable, and globally Lipschitz in x_i uniformly in t; *i.e.*, there exist a non-decreasing continuous function $M : \mathbb{R}_{\geq 0} \to \mathbb{R}_{\geq 0}$ and a constant $L > 0$ such that

$$|f_i(t, x_i)| \leq M(|x_i|), \qquad \left|\frac{\partial f_i}{\partial x_i}(t, x_i)\right| \leq L, \quad \forall t \geq 0 \tag{3.1.3}$$

for all $x_i \in \mathbb{R}$ and $i \in \mathcal{N}$. ◊

Assumption 3.1.1 also guarantees uniqueness of the solutions $x_i(t)$ for all $i \in \mathcal{N}$, for (3.1.1) and (3.1.2). By letting $x := \mathrm{col}(x_1, \ldots, x_N) \in \mathbb{R}^{Nn}$ and $f(t, x) := \mathrm{col}(f_1(t, x_1), \ldots, f_N(t, x_N)) \in \mathbb{R}^{Nn}$, the dynamics of the overall system, composed

of (3.1.1) and (3.1.2), is written as

$$\dot{x} = -k\mathcal{L}x + f(t, x) \tag{3.1.4}$$

where $\mathcal{L}$ is the Laplacian matrix describing the network connection.

Assumption 3.1.2. (Connected network). Given a graph $\hat{\mathcal{G}}$, the coupling network topology under consideration is connected. ♢

A direct consequence of the assumption is that the Laplacian matrix $\mathcal{L}$ is symmetric and has zero eigenvalue which is simple (see the results of the graph theory in Chapter 2), and therefore there exists a nonsingular matrix W such that

$$W = \begin{bmatrix} \frac{1}{N}1_N^T \\ R^T \end{bmatrix}, \quad W^{-1} = [1_N,\ Q], \quad \text{and} \quad W\mathcal{L}W^{-1} = \begin{bmatrix} 0 & 0 \\ 0 & \Lambda \end{bmatrix}$$

where $\Lambda = \mathrm{diag}(\lambda_2(\mathcal{L}), \ldots, \lambda_N(\mathcal{L}))$. From now on, we will drop the Laplacian matrix index of the eigenvalues for simplicity of notation, *i.e.,* $\lambda_i := \lambda_i(\mathcal{L})$ for all $i \in \mathcal{N}$.

Note that since the heterogeneities of $f(t, x)$, the collective dynamics (3.1.4) is no longer possible to decouple the synchronized trajectory dynamics and the error dynamics between agents (See the transformed system (5.2.24) in Section 2.2.2). Therefore, one hardly can predict the collective behavior of (3.1.4), and thus we need to think a new concept of the group behavior.

3.2 Averaged Dynamics

In this section, we introduce the concept of the averaged dynamics which is a useful tool for understanding the collective behavior of the heterogeneous multi-agent systems. In general, it is not easy to achieve asymptotic consensus and synchronization between non-identical agents. Therefore, while most of the results of consensus and synchronization problems have focused on the homogeneous multi-agent systems, only a few papers [KSS11, WSA11, ZHL12, IMC14, DDBL15] considered heterogeneous cases. In particular, Kim *et al.* and Wieland *et al.*

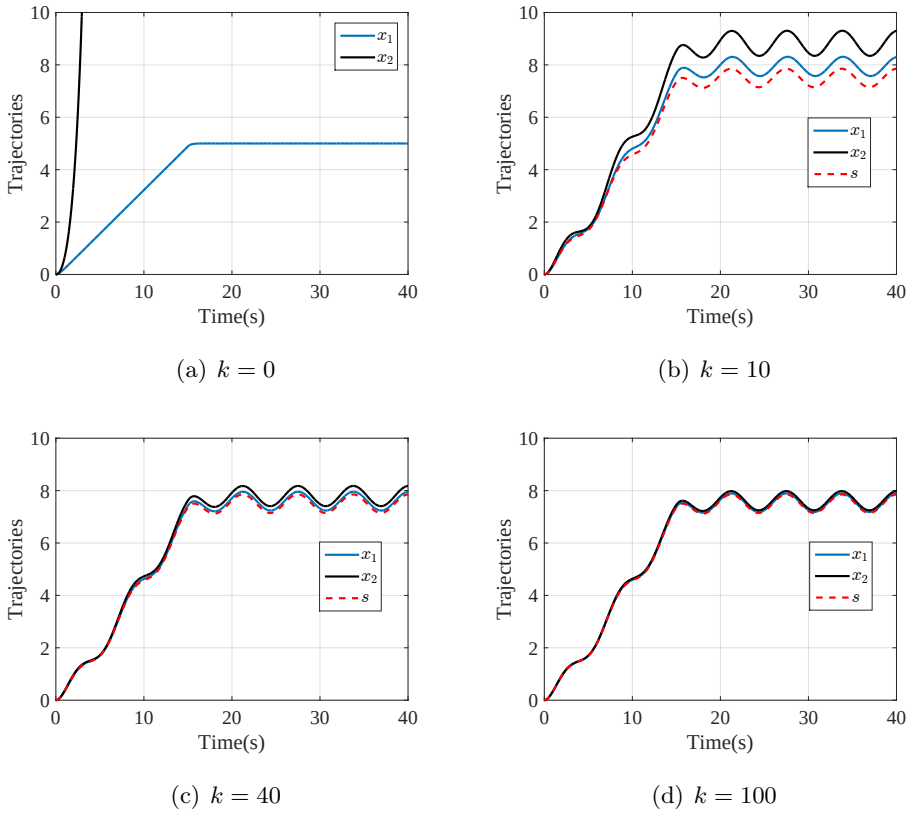

(a) $k = 0$ (b) $k = 10$

(c) $k = 40$ (d) $k = 100$

Figure 3.1: Trajectories of 2-agent systems with coupling strength k are depicted as solid curves, and the trajectory $s(t)$ of the averaged dynamics is given as the dashed curve.

[KSS11, WSA11] introduced the *internal model* into the consensus problem in order to achieve asymptotic consensus. Instead of achieving asymptotic consensus, bounded convergence of networks of heterogeneous multi-agent systems is considered in [ZHL12, DDBL15]. However, the bounded convergence condition cannot give the information of the collective behavior of the heterogeneous multi-agent systems. Therefore, it is important to know the synchronized trajectory of the heterogeneous agent, as well as the bounded convergence. Then, how to find out the group behavior in the case of non-identical individual systems? The following example gives us the insight of the solution to this problem.

Consider a group of 2 agents given by

$$\dot{x}_1(t) = -3x_1(t) + \phi(t) + k(x_2(t) - x_1(t)), \quad x_1(0) = 0,$$
$$\dot{x}_2(t) = x_2(t) + \sin(t) + k(x_1(t) - x_2(t)), \quad x_2(0) = 0,$$

where

$$\phi(t) = \begin{cases} t, & t \geq 15, \\ 15, & t > 15. \end{cases}$$

Here, k is the coupling strength. In many studies of the heterogeneous multi-agent systems, the average of the states $\bar{x}(t) := (1/N)\sum_{i=1}^{N} x_i(t)$ has been considered as a reference of the collective behavior. However, since the trajectory $\bar{x}(t)$ is dependent on the coupling strength k, it cannot be the proper reference signal. This observation can be seen in the Figure 3.1. Figure 3.1(a) shows the trajectories of the uncoupled agents (*i.e.,* $k = 0$). If we consider $\bar{x}(t)$ as the reference of the collective behavior, we may expect that the synchronized trajectory will diverge, and therefore the trajectories of the agents will diverge, too. However, as we can see in Figure 3.1(b), the actual trajectories are bounded if $k = 10$. Furthermore, by comparing Figures 3.1(b), 3.1(c), and 3.1(d), it can be observed that increasing k makes the trajectories $x_1(t)$ and $x_2(t)$ converge to a trajectory $s(t)$. It is interesting that $s(t)$ is not the average of the states but the trajectory which is generated by the average of the vector fields of each agent, *i.e.,*

$$\dot{s}(t) = -s(t) + \frac{\phi(t) + \sin(t)}{2}, \quad s(0) = \frac{x_1(0) + x_2(0)}{2}. \tag{3.2.1}$$

Note that the system (3.2.1) can be a reference system which is not affected by the coupling strength k.

Motivated by this observation, the *averaged dynamics* (or, so-called 'blended dynamics') of (3.1.1) is defined as

$$\dot{s} = \frac{1}{N}\sum_{i=1}^{N} f_i(t, s) = \frac{1}{N} 1_N^T f(t, 1_N s) =: \bar{f}(t, s) \tag{3.2.2}$$

with the averaged initial condition $s(0) = \sum_{i=1}^{N} x_i(0)/N$. It is natural that $\bar{f}(t, s)$

is not the same as any of $f_i(t,s)$ so that $s(t)$ is different from any of $x_i(t)$.

We assume stability of the averaged dynamics stated in the following way.

Assumption 3.2.1. (Stability of averaged dynamics). There exists a constant $p > 0$ such that, for all $s \in \mathbb{R}$ and $t \geq 0$,

$$\frac{\partial \bar{f}}{\partial s}(t,s) = \frac{1}{N}\frac{\partial 1_N^T f(t, 1_N s)}{\partial s} = \frac{1}{N}\sum_{i=1}^{N}\frac{\partial f_i}{\partial x_i}(t,s) \leq -p. \tag{3.2.3}$$

$\Diamond$

Note that this assumption does not require stability of individual systems, and allows unstable agents if their instability is compensated by the stability of other agents so that their sum is somehow stable in the sense of (3.2.3). A direct consequence of Assumption 3.2.1 is ultimate boundedness of the solution $s(t)$ of (3.2.2) as seen in the following lemma.

Lemma 3.2.1. For a scalar system $\dot{s} = F(t,s)$ with C^1 function F satisfying $(\partial F)/(\partial s) \leq -p < 0$ for all s and $t \geq 0$,

$$\limsup_{t\to\infty} |s(t)| \leq \frac{\limsup_{t\to\infty} |F(t,0)|}{p}. \tag{3.2.4}$$

$\Diamond$

Proof. Since, by the mean-value theorem,

$$\begin{aligned}\frac{d|s|}{dt} &= \mathrm{sign}(s)\left(F(t,0) + \frac{\partial F(t,s)}{\partial s}\Big|_{s=q}\cdot s\right)\\ &\leq |F(t,0)| - p|s(t)|, \quad \text{almost everywhere,}\end{aligned}$$

with some $q \in \mathbb{R}$, the comparison lemma [Kha02] yields $|s(t)| \leq w(t)$, $\forall t \geq 0$, where $w(t)$ is the solution of $\dot{w} = -pw + |F(t,0)|$ with $w(0) = |s(0)|$. This concludes the claim. $\square$

As a reference system of the collective behavior, there are some advantages of the averaged dynamics:

- By constructing averaged dynamics, trading stability among heterogeneous agents is clearly seen, and thus, it could be dealt with unstable agent in the framework. Note that it is a unique feature of the averaged dynamics that an unstable node dynamics is allowed, because there is no result that allows unstable agent in the literature (to the author's knowledge up to now). For example, if $f_1(t, x_1) = 2x_1$, $f_2(t, x_2) = -2x_2$, and $f_3(t, x_3) = -x_3$, then we can easily see that the averaged dynamics

$$\dot{s} = \bar{f}(t, s) = (2 - 2 - 1)s = -s$$

  is stable, and so, one immediately knows (from the result of Section 3.3) that strong coupling will ensure (practical) synchronization. Even if the averaged dynamics is not used, one may check the stability (or, contracting property) of the overall system, but this is quite complicated and tedious task (see [WS05, PTS09] for more details).

- Note that $s(t)$ is the solution to the averaged dynamics (3.2.2), while $\bar{x}(t)$ is the averaged trajectory of individual solution $x_i(t)$ to individual dynamics (3.1.1) with diffusive input (3.1.2). They are the same at $t = 0$; *i.e.*, $s(0) = \bar{x}(0)$, but they become different for $t > 0$ in general when the agents are different. We will claim in Section 3.3 that working with $s(t)$ as the reference is more convenient than $\bar{x}(t)$, because $s(t)$ is not dependent on the value of k while $\bar{x}(t)$ is. (However, since $\limsup_{t\to\infty} |s(t) - \bar{x}(t)|$ converges to zero as $k \to \infty$, both will eventually result in the same conclusion with sufficiently large k. The issue is the level of difficulty in the analysis.)

- Use of $s(t)$, that is the solution to the averaged dynamics, makes prediction of the collective behavior much easier when the coupling is strong (since just solving $\dot{s} = \bar{f}(t, s)$ gives the answer). This is again because $s(t)$ is not dependent on k. (The average trajectory $\bar{x}(t)$ plays similar role, but it is not simple to compute $\bar{x}(t)$ before choosing k.)

Overall, since the contribution of the averaged dynamics is not just dealing with the heterogeneous multi-agent, we will emphasize the contributions such as

treatment of unstable agent, the quantitative analysis about the size of residual error versus the size of the coupling gain k (in Section 3.3), and the analysis of the robustness from large number of agents (in Chapter 4).

3.3 Analysis of Robustness by Strong Coupling

The following particular ultimate boundedness lemma, whose proof is found in the Appendix A.1, will play a key role for the main result in this section.

Lemma 3.3.1. Let

$$\rho_\kappa(x,y) = -\begin{bmatrix}|x|\\|y|\end{bmatrix}^T \begin{bmatrix}p & a\\ a & \kappa\end{bmatrix}\begin{bmatrix}|x|\\|y|\end{bmatrix} + \theta(t)|y|$$

with $x \in \mathbb{R}^l$, $y \in \mathbb{R}^m$, $p > 0$, $\theta(t) \geq 0$, and a is a constant. Then, there are a class-$\mathcal{K}$ function r and a positive number c such that

$$\rho_\kappa(x,y) \leq -c(|x|^2 + |y|^2) \quad \text{if } |x|^2 + |y|^2 > \theta^2(t) r\left(\frac{1}{\kappa}\right)$$

for all $\kappa > 3a^2/p$. $\lozenge$

Now one of the two main ingredients of the robustness is presented in the following theorem, which shows strong coupling among agents makes the trajectories of all agents remain in an arbitrarily small neighborhood of the trajectory of the averaged dynamics.

Theorem 3.3.2. Under Assumptions 3.1.1, 3.1.2, and 3.2.1, there exists a class-$\mathcal{K}$ function γ_N such that the solutions of the overall system, composed of (3.1.1) and (3.1.2), with arbitrary initial conditions, and the solution $s(t)$ to the averaged dynamics (3.2.2) with $s(0) = \sum_{i=1}^N x_i(0)/N$ satisfy

$$\limsup_{t\to\infty} |x_i(t) - s(t)| \leq \gamma_N\left(\frac{1}{k\lambda_2 - L}\right), \quad \forall k > \bar{K}, \tag{3.3.1}$$

for all $i = 1, \ldots, N$, where

$$\bar{K} = \frac{3L^2}{p\lambda_2} + \frac{L}{\lambda_2}. \tag{3.3.2}$$

In particular, the function γ_N is defined on $[0, p/3L^2)$ and given by

$$\gamma_N(\chi) = M\left(\frac{M(0)}{p}\right)\sqrt{N}\sqrt{r(\chi)} \tag{3.3.3}$$

in which,

$$r(\chi) = \begin{cases} 0, & \chi = 0, \\ \frac{4\chi}{p-3L^2\chi}, & 0 < \chi \leq \frac{4p}{p^2+20L^2}, \\ \frac{(p^2+8L^2)\chi^2}{(p-3L^2\chi)^2}, & \frac{4p}{p^2+20L^2} < \chi < \frac{p}{3L^2}. \end{cases} \tag{3.3.4}$$

$\Diamond$

Remark 3.3.1. The following remarks are intended to clarify the meaning of the parameters and the significances in Theorem 3.3.2:

(a) Theorem 3.3.2 asserts that for any given $\epsilon > 0$, there is a sufficiently large k such that $\limsup_{t\to\infty} |x_i(t) - s(t)| \leq \epsilon$ for all $i \in \mathcal{N}$, and therefore the robustness of the N individuals is achieved from Definition 3.1.1.

(b) The ultimate bound in (3.3.1) expressed by the function γ_N of (3.3.3), and the value of $\bar{K}$ of (3.3.2) may be conservative. However, the expressions (3.3.2) and (3.3.3) yield a reasonable interpretation. For example, (3.3.2) indicates that the minimal coupling strength $\bar{K}$ increases as the Lipschitz constant L increases while it decreases as the degree of stability p and the algebraic connectivity λ_2 of the network get larger.

(c) It should be noted that the function γ_N and the value of $\bar{K}$ are affected by the number N. The former is obvious due to the appearance of $\sqrt{N}$ in (3.3.3), but the latter is indirect through the value of λ_2. As was mentioned in Chapter 2, the second smallest eigenvalue λ_2 of the Laplacian matrix is called the algebraic connectivity (or, density) of a graph $\mathcal{G}$, which indicates how well connected the graph is. It depends both on the topology of the graph and the number N of the nodes. In Table 2.1, for the all-to-all network (with unit weights), λ_2 is the same as the number N, but for the ring network, increasing N decreases λ_2 (because $\lambda_2 = 2\,(1 - \cos(2\pi/N))$).

(d) Remark 3.3.1(c) implies that, in order to maintain the same level of error while

the number N increases, the coupling strength k may need to be increased. In fact, the ultimate error bound is given in (3.3.1) and it can be seen that $\gamma_N\left(1/(k\lambda_2 - L)\right) = \mathcal{O}\left(\sqrt{N/(k\lambda_2)}\right)$ when k is large enough (so that χ is small enough). Therefore, for the ring network where $\lambda_2 = 2\left(1 - \cos(2\pi/N)\right)$, we have $\gamma_N = \mathcal{O}\left(\sqrt{N^3/k}\right)$, and for the same level of error, k should be increased when N is increased. This phenomenon is observed in the simulations of Chapter 4 as well. On the other hand, for the all-to-all network, the error bound is $\mathcal{O}\left(\sqrt{1/k}\right)$ since $\lambda_2 = N$.

(e) In the particular case where $k = 1$ (*e.g.,* [WS05, RBA07]), Theorem 3.3.2 can also be used to deal with the robustness of networked system when the coupling strength cannot be available such as biological systems, existence of limitation in communication network, and so on. In this case, we have

$$\limsup_{t\to\infty} |x_i(t) - s(t)| \leq \gamma_N\left(\frac{1}{\lambda_2 - L}\right), \quad \forall \lambda_2 > \frac{3L^2}{p} + L. \tag{3.3.5}$$

Instead of increasing the coupling strength k, we can design the robust network by increasing the algebraic connectivity λ_2 in (3.3.5). Therefore, it follows from Section 2.2.1 that the robustness of the heterogeneous multi-agent systems can be enhanced by adding and rewiring (or increasing randomness) links to the underlying network structure.

$\Diamond$

Proof. By the coordinate transformation in (2.2.1)

$$\xi = \begin{bmatrix} \xi_1 \\ \tilde{\xi} \end{bmatrix} = Wx = \begin{bmatrix} \frac{1}{N} 1_N^T \\ R^T \end{bmatrix} x$$

where $\tilde{\xi} = \mathrm{col}(\xi_2, \ldots, \xi_N)$, the overall system (3.1.4) is transformed into

$$\dot{\xi}_1 = \frac{1}{N} 1_N^T f\left(t, 1_N \xi_1 + Q\tilde{\xi}\right) \tag{3.3.6a}$$

$$\dot{\tilde{\xi}} = -k\Lambda\tilde{\xi} + R^T f\left(t, 1_N \xi_1 + Q\tilde{\xi}\right) \tag{3.3.6b}$$

because $W^{-1}\xi = 1_N\xi_1 + Q\tilde{\xi}$. With $e := \xi_1 - s$, equation (5.2.24a) can be rewritten

as

$$\dot{e} = \frac{1}{N} 1_N^T f\left(t, 1_N e + 1_N s + Q\tilde{\xi}\right) - \frac{1}{N} 1_N^T f\left(t, 1_N s\right) \tag{3.3.7a}$$

$$\dot{\tilde{\xi}} = -k\Lambda\tilde{\xi} + R^T f\left(t, 1_N e + 1_N s + Q\tilde{\xi}\right). \tag{3.3.7b}$$

Let $V(e, \tilde{\xi}) := (1/2)e^2 + (1/2)|\tilde{\xi}|^2$. Then, the time derivative of V along (3.3.7) becomes

$$\begin{aligned}\dot{V} = \frac{e}{N}\Big[1_N^T f\left(t, 1_N e + 1_N s + Q\tilde{\xi}\right) - 1_N^T f(t, 1_N e + 1_N s) \\ + 1_N^T f(t, 1_N e + 1_N s) - 1_N^T f(t, 1_N s)\Big] - k\tilde{\xi}^T\Lambda\tilde{\xi} + \tilde{\xi}^T R^T f(t, 1_N s) \\ + \left[\tilde{\xi}^T R^T f\left(t, 1_N e + 1_N s + Q\tilde{\xi}\right) - \tilde{\xi}^T R^T f(t, 1_N s)\right]\end{aligned}$$

which leads, by the mean-value theorem, to

$$\begin{aligned}\dot{V} = \frac{e}{N}\frac{\partial(1_N^T f)}{\partial x}\Big|_z \cdot Q\tilde{\xi} + \frac{e}{N}\frac{\partial(1_N^T f)}{\partial e}\Big|_q \cdot e - k\tilde{\xi}^T\Lambda\tilde{\xi} \\ + \frac{\partial(\tilde{\xi}^T R^T f)}{\partial x}\Big|_w \cdot \left(1_N e + Q\tilde{\xi}\right) + \tilde{\xi}^T R^T f(t, 1_N s)\end{aligned}$$

with some $z \in \mathbb{R}^N$, $w \in \mathbb{R}^N$, and $q \in \mathbb{R}$. Since

$$\frac{\partial(\tilde{\xi}^T R^T f)}{\partial x}\Big|_w = \tilde{\xi}^T R^T \mathrm{diag}\left(\frac{\partial f_1}{\partial x_1}(t, w_1), \ldots, \frac{\partial f_N}{\partial x_N}(t, w_N)\right),$$

it is seen by (3.1.3) that

$$\left|\frac{\partial(\tilde{\xi}^T R^T f)}{\partial x}\Big|_w\right| \le L\|R\||\tilde{\xi}|, \quad \forall t \ge 0$$

and similarly that

$$\left|\frac{\partial(1_N^T f)}{\partial x}\Big|_z\right| \le L\sqrt{N}, \quad \forall t \ge 0.$$

Therefore, using (3.2.3) and the fact that $\|Q\| = \sqrt{N}$ and $\|R\| = 1/\sqrt{N}$,

$$\begin{aligned}\dot{V} &\leq -p|e|^2 + \frac{L\|Q\|}{\sqrt{N}}|e||\tilde{\xi}| - k\lambda_2|\tilde{\xi}|^2 + L\|R\||\tilde{\xi}|\left(\sqrt{N}|e| + \|Q\||\tilde{\xi}|\right) \\ &\quad + |R^T f(t, 1_N s)||\tilde{\xi}| \\ &\leq -p|e|^2 + 2L|e||\tilde{\xi}| - (k\lambda_2 - L)|\tilde{\xi}|^2 + |R^T f(t, 1_N s)||\tilde{\xi}|.\end{aligned}$$

Lemma 3.3.1 is employed with $a := -L$, $\kappa := k\lambda_2 - L$, and $\theta(t) := |R^T f(t, 1_N s(t))|$, and we obtain that

$$\dot{V} \leq -2cV \quad \text{if } 2V = e^2 + |\tilde{\xi}|^2 > |R^T f(t, 1_N s)|^2 r\left(\frac{1}{\kappa}\right) \tag{3.3.8}$$

where $c > 0$ and the function r is given by (3.3.4) (which can be seen by following the proof of Lemma 3.3.1 in the Appendix A.1). Inequality (3.3.8) implies that

$$\limsup_{t\to\infty} 2V(t) \leq \limsup_{t\to\infty} |R^T f(t, 1_N s(t))|^2 r\left(\frac{1}{\kappa}\right).$$

By (3.1.3) and Lemma 3.2.1, we have that

$$\begin{aligned}\limsup_{t\to\infty} |R^T f(t, 1_N s(t))| &\leq \|R\|\sqrt{N} M\left(\limsup_{t\to\infty} |s(t)|\right) \\ &\leq M\left(\limsup_{t\to\infty} \frac{|\bar{f}(t, 0)|}{p}\right) \leq M\left(\frac{M(0)}{p}\right).\end{aligned}$$

Finally, since

$$x - 1_N s = W^{-1}\xi - 1_N s = 1_N \xi_1 - 1_N s + Q\tilde{\xi} = [1_N, Q]\begin{bmatrix} e \\ \tilde{\xi} \end{bmatrix},$$

and the vector norm of the i-th row of $[1_N, Q]$ is $\sqrt{N}$ by the construction of W, we have

$$|x_i - s| \leq \sqrt{N}\sqrt{|e|^2 + |\tilde{\xi}|^2} = \sqrt{N}\sqrt{2V}.$$

Therefore, for any $i \in \mathcal{N}$,

$$\limsup_{t\to\infty} |x_i(t) - s(t)| \le M\left(\frac{M(0)}{p}\right)\sqrt{N}\sqrt{r\left(\frac{1}{\kappa}\right)}$$

if $\kappa = k\lambda_2 - L > 3L^2/p$. This completes the proof with (3.3.2) and (3.3.3). □

The proof of Theorem 3.3.2 enlightens the following. The quantity $|R^T f(t, 1_N s)|$ has the meaning of 'measure of heterogeneity' in the sense that, if all agents are identical; $f_i(t, s) = f_0(t, s)$ for all s and $i \in \mathcal{N}$, then

$$R^T f(t, 1_N s) = R^T 1_N f_0(t, s) = 0.$$

More specifically, if we denote the first column of R^T by r_1 so that $R^T = [r_1, \tilde{R}]$ with a matrix $\tilde{R}$, then it follows from $R^T 1_N = 0$ that $r_1 = -\tilde{R}1_{N-1}$. Hence,

$$R^T f(t, 1_N s) = [r_1, \tilde{R}]\begin{bmatrix} f_1(t,s) \\ \vdots \\ f_N(t,s) \end{bmatrix} = \tilde{R}\begin{bmatrix} f_2(t,s) - f_1(t,s) \\ \vdots \\ f_N(t,s) - f_1(t,s) \end{bmatrix}.$$

In particular, if $R^T f(t, 1_N s) = 0$, then it can be seen that

$$\lim_{t\to\infty} |x_i(t) - x_j(t)| = 0,$$

$\forall i, j \in \mathcal{N}$, with some $k > 0$. While this can be seen directly from (3.3.8), it also follows from (3.3.6b) by appending $R^T f(t, 1_N \xi_1)$ (which is 0) and utilizing the Lipschitzness of f (Assumption 3.1.1). (Indeed, if $\tilde{\xi}(t) \to 0$ then $x_i(t) \to x_1(t)$, $\forall i$, since $\tilde{\xi} = R^T x = \tilde{R}[x_2 - x_1, \ldots, x_N - x_1]^T$.) The latter approach reveals that convergence of $\tilde{\xi}(t)$ to zero is in fact regardless of the behavior of $\xi_1(t)$. Under the stability property of f_0 (Assumption 3.2.1), the state $\xi_1(t)$ reaches a certain steady state forgetting the effect of the initial condition of $\xi_1(0)$ and $\tilde{\xi}(0)$, and this is in contrast to the 'average consensus' of [SSB09, OS07, WSA11, KSS11, ZHL11], in which the agreed trajectory reflects the initial conditions of the networked agents.

Corollary 3.3.3. (Asymptotic convergence to $s(t)$). Under Assumptions 3.1.1,

3.1.2, and 3.2.1, the trajectories of the individual systems (3.1.1) with (3.1.2) and arbitrary initial conditions asymptotically converge to the solution $s(t)$ of the averaged dynamics (3.2.2) with $s(0) = \sum_{i=1}^{N} x_i(0)/N$, if all agents are identical ($f_i(t,s) = f_0(t,s)$ for all s and $i \in \mathcal{N}$) and $k > \bar{K}$, that is,

$$\lim_{t\to\infty} |x_i(t) - s(t)| = 0, \quad \forall k > \bar{K},$$

for all $i = 1, \ldots, N$, where

$$\bar{K} = \frac{3L^2}{p\lambda_2} + \frac{L}{\lambda_2}.$$

$\Diamond$

In particular, if we only care about the asymptotic consensus and synchronization between individual systems in the case of homogeneous multi-agent systems, the averaged dynamics and the stability property (Assumption 3.2.1) are no longer needed.

Corollary 3.3.4. (Asymptotic consensus and synchronization). Under Assumptions 3.1.1 and 3.1.2, the trajectories of the individual systems (3.1.1) with (3.1.2) and arbitrary initial conditions asymptotically converge to each other, if all agents are identical and $k > L/\lambda_2$, that is,

$$\lim_{t\to\infty} |x_i(t) - x_j(t)| = 0, \quad \forall k > \frac{L}{\lambda_2},$$

for all $i, j = 1, \ldots, N$. $\Diamond$

3.4 Illustrative Example

3.4.1 Effect of strong coupling

In this section, we illustrate, through simulation studies, that strong coupling enhances the robustness among heterogeneous multi-agent systems. In computational neuroscience, one often uses the following simplified leaky integrate-and-fire

model [OBH09].

$$c_m \dot{V}_i(t) = -g_{m_i} V_i(t) + I_i^{ext}(t) + I_i^{int}(t)$$

where V_i is the membrane potential of the i-th cell, c_m and g_{m_i} are the membrane capacitance and conductance which can be perturbed by variations, I_i^{ext} is an external input current flowing into each cell, and I_i^{int} is the current due to the interactions with other cells within the network. The external current I_i^{ext} represents the collective effect of inputs coming from other areas, outside of the studied network, and is modeled as

$$I_i^{ext}(t) = I_i^{mean}(t) + \Delta \eta_i(t)$$

where $I_i^{mean}(t)$ is the mean value of the input, Δ measures the amplitude of input fluctuation, $\eta_i(t)$ is the noise of unit intensity. The interaction current I_i^{int} represents the effect of gap junctions connecting neuron i and other neurons within the network, which is usually modeled as a simple ohmic conductance between their membranes,

$$I_i^{int}(t) = \gamma_{gap} \sum_{j=1}^{N} \alpha_{ij} \left(V_j(t) - V_i(t) \right)$$

where γ_{gap} is a strength parameter and α_{ij} is the (i,j)-th entry of the adjacency matrix of the given network.[2] This model fits to the system (3.1.1)–(3.1.2) considered in Section 3.3 with $V_i = x_i$ and $\gamma_{gap} = k$. In particular, if $I_i^{ext}(t) = 10 \sin t + 10 m_i \sin(\omega_i t + \theta_i)$ where $m_i,\ \omega_i$ are realizations of standard normal distribution $N(0,1)$ and θ_i is a realization of uniform distribution on $[0, 2\pi]$, then it is the same as the model in the following group of heterogeneous subsystems with $c_m = 1$ and $g_{m_1} = -1,\ g_{m_2} = -0.75,\ g_{m_3} = -0.5,\ g_{m_4} = 0.5,\ g_{m_5} = 0.75$:

[2] In this model, the membrane potential is known only in the subthreshold domain, as the precise voltage trace of the spike is ignored.

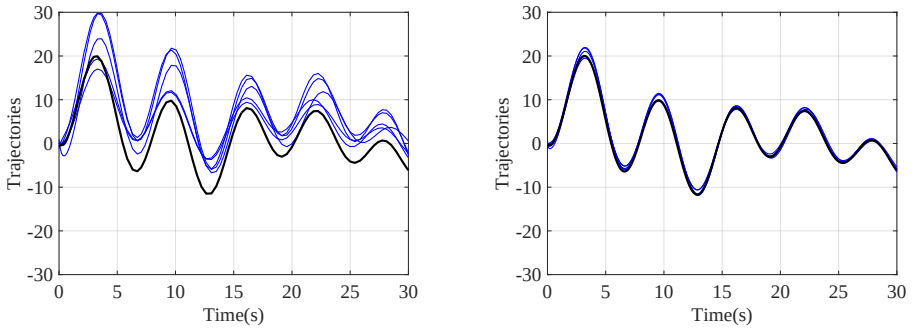

(a) $N = 5,\ k = 2$ (b) $N = 5,\ k = 10$

Figure 3.2: Simulation results with $k = 2$ and $k = 10$. The blue and the black curves represent the trajectories of 5-agent systems and the trajectory $s(t)$ of the averaged dynamics, respectively.

$$
\begin{aligned}
f_1(t, x_1) &= -x_1 + 10\sin(t) + 7.15\sin(-0.38t + 1.90),\\
f_2(t, x_2) &= -0.75x_2 + 10\sin(t) + 3.72\sin(0.80t + 1.85),\\
f_3(t, x_3) &= -0.5x_3 + 10\sin(t) - 18.25\sin(-0.94t + 1.63),\\
f_4(t, x_4) &= 0.5x_4 + 10\sin(t) - 1.42\sin(-0.87t + 2.91),\\
f_5(t, x_5) &= 0.75x_5 + 10\sin(t) + 6.01\sin(0.90t + 6.21).
\end{aligned}
\tag{3.4.1}
$$

Note that there are two unstable agents ($i = 4, 5$) in the group (3.4.1). In this case, the averaged dynamics of the subsystems is obtained as

$$
\begin{aligned}
\dot{s} = -\frac{1}{5}s + 10\sin(t) + \frac{1}{5}\big\{&7.15\sin(-0.38t + 1.90) + 3.72\sin(0.80t + 1.85)\\
&- 18.25\sin(-0.94t + 1.63) - 1.42\sin(-0.87t + 2.91) + 6.01\sin(0.90t + 6.21)\big\}.
\end{aligned}
$$

Although the group includes two unstable agents, the averaged dynamics is stable in the sense of averaging effect. Therefore, we can predict the bounded collective behavior when the coupling is strong. Here, we assume the network topology is the undirected connected ring graph with unit weights.

The effect of strong coupling k is seen clearly by comparing Figure 3.2(a) with 3.2(b). The simulation results show that by increasing the coupling strength, the

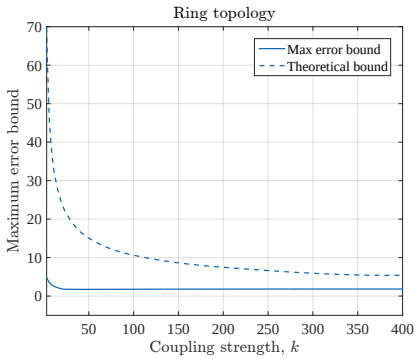

(a) Error bounds, ring topology

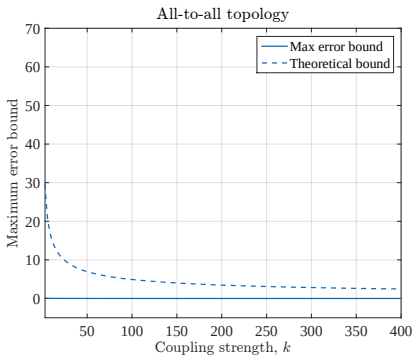

(b) Error bounds, all-to-all topology

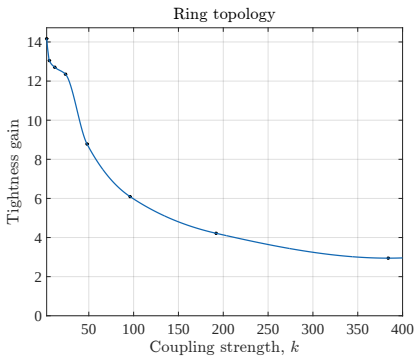

(c) Tightness gain, ring topology

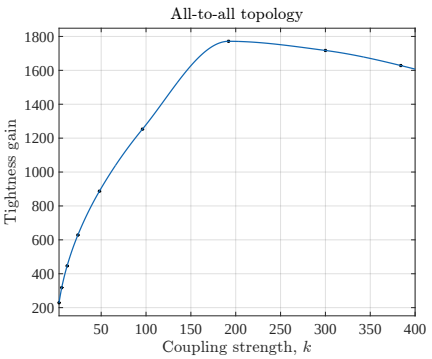

(d) Tightness gain, all-to-all topology

Figure 3.3: (a)–(b): The solid and dashed curves represent the maximum error distance between $x_i(t)$ and $s(t)$ (*i.e.,* $\max_{0\le t\le 10, i\in\mathcal{N}} |x_i(t) - s(t)|$) of 30-agent systems and the theoretical upper bound in Theorem 3.3.2 with respect to the coupling gain k. (c)–(d): Tightness gain curves, $E_g(k, 30)$.

behaviors of all agents approach the trajectory of the averaged dynamics.

3.4.2 Tightness of upper bound

Our remaining task is to verify whether the proposed upper bound (3.3.1) in Theorem 3.3.2 can be a tight upper bound. We consider a group of heterogeneous multi-agent systems with

$$f_i(t, x_i) = (-1 + \delta_i)x_i + m_i \sin(\omega_i t + \theta_i), \quad i \in \{1, \dots, 30\},$$

where $\delta_i, \omega_i \sim N(0,1)$, $\theta_i \sim$ uniform$[0, 2\pi]$, and $m_i \sim$ uniform$[1, 10]$. The tightness of upper bound can be calculated by defining the *tigtness gain* as

$$\begin{aligned} E_g(k,N) :&= \frac{\text{Theoretical upper bound with } k \text{ and } N}{\text{Maximum error bound with } k \text{ and } N} \\ &= \frac{\gamma_N(k)}{\max_{0\le t\le 10,\ i\in\mathcal{N}} |x_i(t) - s(t)|}. \end{aligned}$$

Figures 3.3(a) and 3.3(b) illustrate the theoretical upper bound in (3.3.1) and the maximum error distance between $x_i(t)$ and $s(t)$ when the coupling gain k is given. Even though the theoretical upper bound can be determined conservatively when the coupling gain k is small, but for a large k, the theoretical upper bound can be tight, as seen in Figures 3.3(c) and 3.3(d) . Furthermore, by comparing Figure 3.3(c) with 3.3(d), we can see that ring topology gives more tight bound than all-to-all topology.

The effect of increasing the number of agents about the upper bound can be seen in Figure 3.4. As mentioned in Remark 3.3.1(d), in Figures 3.4(a) and 3.4(b), the upper bound for the ring and the all-to-all topologies has $\mathcal{O}(\sqrt{N^3})$ and $\mathcal{O}(1)$ when k is large enough and fixed. In Figures 3.4(c) and 3.4(d), the upper bound can hardly be "tightened" as the number of agents increases.

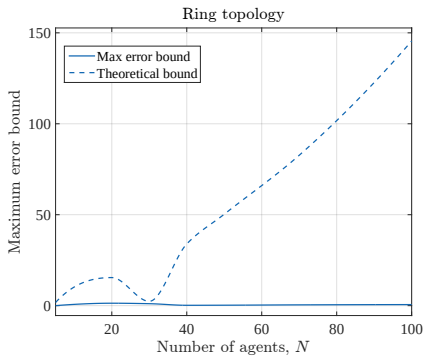

(a) $k = 100$, ring topology

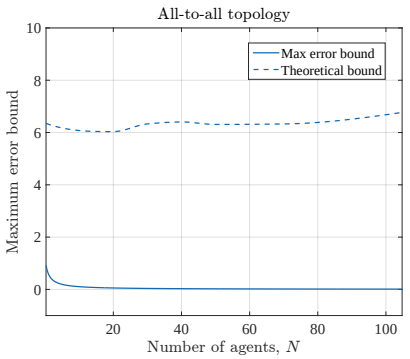

(b) $k = 100$, all-to-all topology

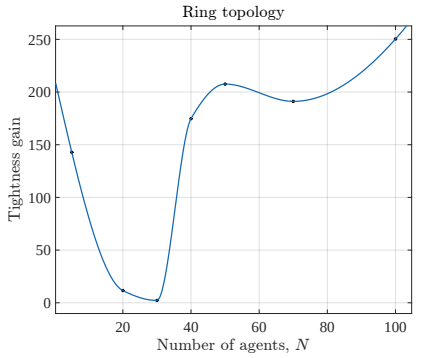

(c) Tightness gain, ring topology

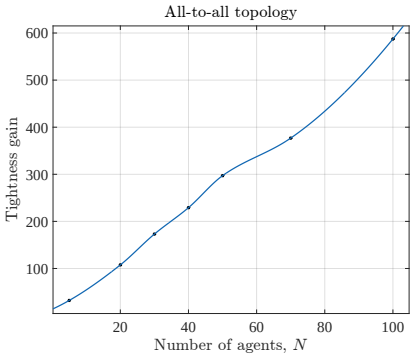

(d) Tightness gain, all-to-all topology

Figure 3.4: (a)–(b): The solid and dashed curves represent the maximum error distance between $x_i(t)$ and $s(t)$ (*i.e.*, $\max_{0\le t\le 10, i\in\mathcal{N}} |x_i(t) - s(t)|$) with the coupling strength $k = 100$ and the theoretical upper bound in Theorem 3.3.2 with respect to the number of agents N. (c)–(d): Tightness gain curves, $E_g(100, N)$.

3.5 High-Order Heterogeneous Multi-Agent Systems

In previous sections of Chapter 3, the robustness of the heterogeneous multi-agent systems composed of first-order dynamics has been considered. However, many physical systems usually result in complex high-order dynamic models, *e.g.,* pendulum equation, mass-spring system, oscillators, and so on.

In this section, we establish a mathematical framework for robust consensus and synchronization of high-order heterogeneous multi-agent systems and investigating the interplay between robustness and strong coupling.

We consider a group of N dynamic objects represented by

$$\dot{x}^i = f^i(t, x^i) + u^i, \quad i \in \mathcal{N} = \{1, 2, \dots, N\}, \tag{3.5.1}$$

where $x^i = \mathrm{col}(x^i_1, \dots, x^i_n) \in \mathbb{R}^n$ is the state and $u^i \in \mathbb{R}^n$ indicates interactions with other objects through the network. Let $f^i_j : \mathbb{R}^n \to \mathbb{R}$ be the j-th component function of f^i, so that $f^i(t, x^i) = \mathrm{col}(f^i_1(t, x^i), \dots, f^i_n(t, x^i))$.

Assumption 3.5.1. (Individual system). The function $f^i(t, x^i)$ of the individual system (3.5.1) is uniformly bounded in t, continuously differentiable, and globally Lipschitz in x^i uniformly in t; *i.e.*, there exist a non-decreasing function $\beta(a)$ and a constant L such that

$$|f^i(t, a)| \le \beta(a), \quad \left\| \frac{\partial f^i}{\partial x^i}(t, x^i) \right\| \le L, \quad \forall x^i \in \mathbb{R}^n, \ \forall t \ge 0, \ \forall i \in \mathcal{N}, \tag{3.5.2}$$

where $\frac{\partial f^k}{\partial x^k}(t, x^k)$ is a $n \times n$ matrix whose (i, j)-entry is $\frac{\partial f^k_i}{\partial x^k_j}(t, x^k)$. $\Diamond$

By letting $x := \mathrm{col}(x^1, \dots, x^N)$ and $f(t, x) := \mathrm{col}(f^1(t, x^1), \dots, f^N(t, x^N))$, the inequalities (3.5.2) can be written as

$$\begin{aligned} &|f(t, (1_N \otimes I_n)a)| \le \sqrt{N}\beta(a), \\ &\left\| \frac{\partial f}{\partial x}(t, x) \right\| = \left\| \mathrm{diag}\left(\frac{\partial f^1}{\partial x^1}(t, x^1), \dots, \frac{\partial f^N}{\partial x^N}(t, x^N) \right) \right\| \le L. \end{aligned} \tag{3.5.3}$$

We assume that the agent i collects only the relative state information between

the i-th agent and its neighborhood by diffusive coupling input

$$u^i = k\sum_{j=1}^{N}\alpha_{ij}(x^j - x^i), \tag{3.5.4}$$

where k represents the coupling strength and α_{ij} is the (i,j)-entry of the adjacency matrix of the given network.

Let $s(t)$ be the solution of the following *averaged dynamics* of (3.5.1)

$$\dot{s} = \frac{1}{N}\sum_{i=1}^{N} f^i(t,s) = \left(\frac{1}{N}1_N^T \otimes I_n\right) f\big(t,(1_N\otimes I_n)s\big) =: \bar{f}(t,s), \tag{3.5.5}$$

with the averaged initial condition $s(0) = \sum_{i=1}^{N} x^i(0)/N$.

Assumption 3.5.2. (Stability of averaged dynamics). There exist positive definite matrices $P(t)$ and $F(t)$ such that

$$0 < c_1 I_n \le P(t) \le c_2 I_n, \quad F(t) \ge c_3 I_n > 0, \quad \forall t \ge 0, \tag{3.5.6}$$

which satisfies the matrix differential equation

$$\begin{aligned} -\dot{P}(t) \ge P(t)&\left\{\left(\frac{1}{N}1_N^T\otimes I_n\right)\frac{\partial f}{\partial s}(t,(1_N\otimes I_n)s)(1_N\otimes I_n)\right\} \\ &+\left\{\left(\frac{1}{N}1_N^T\otimes I_n\right)\frac{\partial f}{\partial s}(t,(1_N\otimes I_n)s)(1_N\otimes I_n)\right\}^T P(t) \\ &+F(t), \quad \forall s\in\mathbb{R}^n, \end{aligned} \tag{3.5.7}$$

where c_1, c_2 and c_3 are positive constants. ◊

In fact, the Jacobian matrix of the averaged dynamics in (3.5.7) is a $n\times n$ matrix whose (i,j)-entry is

$$\left(\frac{1}{N}1_N^T\otimes I_n\right)\frac{\partial f}{\partial x}(t,x)(1_N\otimes I_n) = \left[\frac{1}{N}\sum_{k=1}^{N}\frac{\partial f_i^k(t,x^k)}{\partial x_j^k}\right] \in \mathbb{R}^{n\times n},$$

and equivalently, the matrix differential equation (3.5.7) can be written as

$$-\dot{P}(t) \geq P(t)\left(\frac{\partial \bar{f}}{\partial s}(t,s)\right) + \left(\frac{\partial \bar{f}}{\partial s}(t,s)\right)^T P(t) + F(t), \quad \forall s \in \mathbb{R}^n.$$

Notice that if the Jacobian matrix of the averaged dynamics is Hurwitz and constant, then there always exist positive definite matrices $P(t)$ and $F(t)$ satisfying Assumption 3.5.2. The following lemma is well-known mean-value theorem.

Lemma 3.5.1. (Mean-value theorem [Apo74]) Let $S \in \mathbb{R}^n$ be an open and assume that $f : S \to \mathbb{R}^m$ is differentiable at each point of S. Let x and y be two points in S such that the whole line segment $l(x,y) := \{tx + (1-t)y : 0 \leq t \leq 1\}$ remains in S. Then for every vector $a \in \mathbb{R}^m$, there is a point $z \in l(x,y)$ such that

$$a^T\{f(y) - f(x)\} = a^T\left\{\frac{\partial f(x)}{\partial x}\Big|_z (y-x)\right\}.$$

$\Diamond$

From the stability condition of Assumption 3.5.2, $s(t)$ can be ultimately bounded. The following lemma ensures the ultimate boundedness of the solution $s(t)$ of the averaged dynamics (3.5.5).

Lemma 3.5.2. Under Assumptions 3.5.1 and 3.5.2, the solution of the averaged dynamics $s(t)$ is globally ultimately bounded with ultimate bound $(4c_2/c_3)\beta(0)$, that is,

$$\limsup_{t\to\infty} |s(t)| \leq \frac{4c_2}{c_3}\beta(0). \tag{3.5.8}$$

$\Diamond$

Proof. We use $V = s^T P(t) s$ as a Lyapunov function candidate for the averaged dynamics (3.5.5). The derivative of V along the trajectory of the system is given by

$$\begin{aligned}
\dot{V} &= s^T P(t)\bar{f}(t,s) + s^T\dot{P}(t)s + \bar{f}^T(t,s)P(t)s \\
&= s^T P(t)\left(\bar{f}(t,s) - \bar{f}(t,0)\right) + s^T\dot{P}(t)s + \left(\bar{f}(t,s) - \bar{f}(t,0)\right)^T P(t)s \\
&\quad + 2s^T P(t)\bar{f}(t,0)
\end{aligned}$$

By Lemma 3.5.1, there is a point $z \in l(0, s)$ such that

$$\begin{aligned}\dot{V} &= s^T P(t) \left(\frac{\partial \bar{f}}{\partial s}\Big|_z s \right) + s^T \dot{P}(t) s + \left(\frac{\partial \bar{f}}{\partial s}\Big|_z s \right)^T P(t) s + 2 s^T P(t) \bar{f}(t, 0) \\ &= s^T \left\{ P(t) \left(\frac{\partial \bar{f}}{\partial s}\Big|_z \right) + \dot{P}(t) + \left(\frac{\partial \bar{f}}{\partial s}\Big|_z \right)^T P(t) \right\} s + 2 s^T P(t) \bar{f}(t, 0).\end{aligned}$$

Then, by Assumptions 3.5.1 and 3.5.2, we have

$$\begin{aligned}\dot{V} &\leq -s^T F(t) s + 2 s^T P(t) \bar{f}(t, 0) \\ &\leq -c_3 |s|^2 + 2 c_2 \beta(0) |s| \\ &\leq -\frac{1}{2} c_3 |s|^2, \quad \forall |s| \geq \frac{4 c_2}{c_3} \beta(0)\end{aligned}$$

which show that the conditions of [Kha02, Theorem 4.18] are satisfied globally with $(4c_2/c_3)\beta(0)$. Thus, we conclude that the solution of the averaged dynamics is globally ultimately bounded and the equation (3.5.8) is satisfied. □

The following theorem has the similar interpretation as Remark 3.3.1 in Theorem 3.3.2.

Theorem 3.5.3. Under Assumptions 3.5.1, 3.1.2, and 3.5.2, there exists a class-$\mathcal{K}$ function σ^* such that the solutions of (3.5.1) with arbitrary initial conditions and the solution $s(t)$ to the averaged system (3.5.5) with $s(0) = \sum_{i=1}^N x_i(0)/N$ satisfy

$$\limsup_{t \to \infty} |x_i(t) - s(t)| \leq \sigma^* \left(\frac{1}{k \lambda_2 - L} \right), \quad \forall k > \bar{K}, \tag{3.5.9}$$

for all $i = 1, \ldots, N$, where

$$\bar{K} = \frac{3 L^2 (2 c_2 + 1)^2}{4 c_3 \lambda_2} + \frac{L}{\lambda_2}. \tag{3.5.10}$$

In particular, the function σ^* is defined on $[0, 3L^2(2c_2 + 1)^2/4c_3)$ and given by

$$\sigma^*(\chi) = \sqrt{N} \sqrt{\frac{c_{\max}}{c_{\min}}} \beta \left(\frac{4 c_2}{c_3} \beta(0) \right) \sqrt{r(\chi)} \tag{3.5.11}$$

in which,

$$r(\chi)=\begin{cases}0, & \chi=0,\\ \frac{8\chi}{4c_3-L^2(2c_2+1)^2\chi}, & 0<\chi\le\frac{2c_3}{c_3^2+L^2(2c_2+1)^2},\\ \frac{\left\{16c_3^2+8L^2(2c_2+1)^2\right\}\chi^2}{\left\{4c_3-L^2(2c_2+1)^2\chi\right\}^2}, & \frac{2c_3}{c_3^2+L^2(2c_2+1)^2}<\chi<\frac{L^2(2c_2+1)^2}{4c_3},\end{cases} \tag{3.5.12}$$

where $c_{\max}:=\max\{c_2,(1/2)\},\ c_{\min}:=\min\{c_1,(1/2)\}$. ◊

Proof. The dynamics of the overall system, composed of (3.5.1) and (3.5.4), is written as

$$\dot{x}=-k(\mathcal{L}\otimes I_n)x+f(t,x). \tag{3.5.13}$$

By the coordinate transformation in (2.2.1)

$$\xi=\begin{bmatrix}\xi_1\\ \tilde{\xi}\end{bmatrix}=(W\otimes I_n)x=\begin{bmatrix}\frac{1}{N}1_N^T\otimes I_n\\ R^T\otimes I_n\end{bmatrix}x$$

where $\tilde{\xi}=\mathrm{col}(\xi_2,\dots,\xi_N)$, the overall system (3.5.13) is transformed into

$$\begin{aligned}\dot{\xi}_1&=\left(\frac{1}{N}1_N^T\otimes I_n\right)f\left(t,(1_N\otimes I_n)\xi_1+(Q\otimes I_n)\tilde{\xi}\right)\\ \dot{\tilde{\xi}}&=-k(\Lambda\otimes I_n)\tilde{\xi}+\left(R^T\otimes I_n\right)f\left(t,(1_N\otimes I_n)\xi_1+(Q\otimes I_n)\tilde{\xi}\right),\end{aligned} \tag{3.5.14}$$

because $x=(W^{-1}\otimes I_n)\xi=[1_N\otimes I_n,Q\otimes I_n]\xi$. With $e:=\xi_1-s$ and (3.5.5), equation (5.2.24b) can be rewritten as

$$\begin{aligned}\dot{e}&=\left(\frac{1}{N}1_N^T\otimes I_n\right)f\left(t,(1_N\otimes I_n)e+(1_N\otimes I_n)s+(Q\otimes I_n)\tilde{\xi}\right)\\ &\quad-\left(\frac{1}{N}1_N^T\otimes I_n\right)f\left(t,(1_N\otimes I_n)s\right)\\ \dot{\tilde{\xi}}&=-k(\Lambda\otimes I_n)\tilde{\xi}+\left(R^T\otimes I_n\right)f\left(t,(1_N\otimes I_n)e+(1_N\otimes I_n)s+(Q\otimes I_n)\tilde{\xi}\right).\end{aligned} \tag{3.5.15}$$

Let a Lyapunov function be

$$V(e,\tilde{\xi})=e^TP(t)e+\frac{1}{2}\tilde{\xi}^T\tilde{\xi}.$$

The time derivative of V along (3.5.15) becomes

$$\begin{aligned}
\dot{V} &= \dot{e}^T P(t)e + e^T \dot{P}(t)e + e^T P(t)\dot{e} + \frac{1}{2}\dot{\tilde{\xi}}^T\tilde{\xi} + \frac{1}{2}\tilde{\xi}^T\dot{\tilde{\xi}} \\
&= \Big\{ f^T\Big(t,(1_N\otimes I_n)e + (1_N\otimes I_n)s + (Q\otimes I_n)\tilde{\xi}\Big) - f^T\left(t,(1_N\otimes I_n)e + (1_N\otimes I_n)s\right) \\
&+ f^T\left(t,(1_N\otimes I_n)e + (1_N\otimes I_n)s\right) - f^T\big(t,(1_N\otimes I_n)s\big)\Big\}\left(\frac{1}{N}1_N^T\otimes I_n\right)^T P(t)e \\
&+ e^T\dot{P}(t)e + e^T P(t)\left(\frac{1}{N}1_N^T\otimes I_n\right)\Big\{ f\big(t,(1_N\otimes I_n)e + (1_N\otimes I_n)s + (Q\otimes I_n)\tilde{\xi}\big) \\
&- f\big(t,(1_N\otimes I_n)e + (1_N\otimes I_n)s\big) + f\big(t,(1_N\otimes I_n)e + (1_N\otimes I_n)s\big) - f\big(t,(1_N\otimes I_n)s\big)\Big\} \\
&- k\tilde{\xi}^T(\Lambda\otimes I_n)\tilde{\xi} + \tilde{\xi}^T\big(R^T\otimes I_n\big)\Big\{ f\big(t,(1_N\otimes I_n)e + (1_N\otimes I_n)s + (Q\otimes I_n)\tilde{\xi}\big) \\
&- f\big(t,(1_N\otimes I_n)s\big)\Big\} + \tilde{\xi}^T\big(R^T\otimes I_n\big)f\big(t,(1_N\otimes I_n)s\big).
\end{aligned}$$

By Lemma 3.5.1, we obtain

$$\begin{aligned}
\dot{V} &= e^T(1_N\otimes I_n)^T\frac{\partial f^T(t,(1_N\otimes I_n)e)}{\partial e}\Big|_z\left(\frac{1}{N}1_N^T\otimes I_n\right)^T P(t)e \\
&+ \tilde{\xi}^T(Q\otimes I_n)^T\frac{\partial f^T(t,x)}{\partial x}\Big|_w\left(\frac{1}{N}1_N^T\otimes I_n\right)^T P(t)e + e^T\dot{P}(t)e \\
&+ e^T P(t)\left(\frac{1}{N}1_N^T\otimes I_n\right)\frac{\partial f(t,(1_N\otimes I_n)e)}{\partial x}\Big|_z(1_N\otimes I_n)e \\
&+ e^T P(t)\left(\frac{1}{N}1_N^T\otimes I_n\right)\frac{\partial f(t,x)}{\partial x}\Big|_w(Q\otimes I_n)\tilde{\xi} - k\tilde{\xi}^T(\Lambda\otimes I_n)\tilde{\xi} \\
&+ \tilde{\xi}^T\big(R^T\otimes I_n\big)\frac{\partial f(t,x)}{\partial x}\Big|_q(1_N\otimes I_n)e + \tilde{\xi}^T\big(R^T\otimes I_n\big)\frac{\partial f(t,x)}{\partial x}\Big|_q(Q\otimes I_n)\tilde{\xi} \\
&+ \tilde{\xi}^T\big(R^T\otimes I_n\big)f\big(t,(1_N\otimes I_n)s\big),
\end{aligned}$$

with some $z\in\mathbb{R}^n$, $w\in\mathbb{R}^{Nn}$, and $q\in\mathbb{R}^{Nn}$. It is seen by (3.5.3), (3.5.6), and the

fact that $\|Q\| = \sqrt{N}$ and $\|R\| = 1/\sqrt{N}$ that

$$\begin{aligned}
\left|\tilde{\xi}^T(Q\otimes I_n)^T\frac{\partial f^T(t,x)}{\partial x}\Big|_w\left(\frac{1}{N}1_N^T\otimes I_n\right)^T P(t)e\right| &\le c_2L|\tilde{\xi}||e|, \quad \forall t\ge 0,\\
\left|\tilde{\xi}^T\big(R^T\otimes I_n\big)\frac{\partial f(t,x)}{\partial x}\Big|_q(1_N\otimes I_n)e\right| &\le L|\tilde{\xi}||e|, \quad \forall t\ge 0,\\
\left|\tilde{\xi}^T\big(R^T\otimes I_n\big)\frac{\partial f(t,x)}{\partial x}\Big|_q(Q\otimes I_n)\tilde{\xi}\right| &\le L|\tilde{\xi}|^2, \quad \forall t\ge 0.
\end{aligned} \tag{3.5.16}$$

Therefore, using (3.5.7), and (3.5.16), it follows that

$$\begin{aligned}
\dot{V} &\le -c_3|e|^2 + 2c_2L|e||\tilde{\xi}| - k\lambda_2|\tilde{\xi}|^2 + L|e||\tilde{\xi}| + L|\tilde{\xi}|^2 + \left|\big(R^T\otimes I_n\big)f\big(t,(1_N\otimes I_n)s\big)\right||\tilde{\xi}|\\
&= -c_3|e|^2 + L(2c_2+1)|e||\tilde{\xi}| - (k\lambda_2 - L)|\tilde{\xi}|^2 + \left|\big(R^T\otimes I_n\big)f\big(t,(1_N\otimes I_n)s\big)\right||\tilde{\xi}|\\
&= -\begin{bmatrix}|e|\\|\tilde{\xi}|\end{bmatrix}^T\begin{bmatrix}c_3 & -\frac{L(2c_2+1)}{2}\\ -\frac{L(2c_2+1)}{2} & k\lambda_2 - L\end{bmatrix}\begin{bmatrix}|e|\\|\tilde{\xi}|\end{bmatrix} + \left|\big(R^T\otimes I_n\big)f\big(t,(1_N\otimes I_n)s\big)\right||\tilde{\xi}|.
\end{aligned}$$

With $k_1 := k\lambda_2 - L$ and $a = -\frac{L(2c_2+1)}{2}$, the following lemma can be employed to find the region for $\dot{V} < 0$. By Lemma 3.3.1 and (3.5.6), it is seen that

$$\dot{V} \le -h(|e|^2+|\tilde{\xi}|^2) \quad \text{if} \quad |e|^2+|\tilde{\xi}|^2 \ge \frac{V}{c_{\max}} > \left|\big(R^T\otimes I_n\big)f\big(t,(1_N\otimes I_n)s\big)\right|^2 r\left(\frac{1}{k_1}\right),$$

which implies that

$$\limsup_{t\to\infty} V(t) \le \limsup_{t\to\infty} c_{\max}\left|\big(R^T\otimes I_n\big)f\big(t,(1_N\otimes I_n)s\big)\right|^2 r\left(\frac{1}{k_1}\right).$$

By (3.5.3) and (3.5.8), we have that

$$\begin{aligned}
\limsup_{t\to\infty} V(t) &\le c_{\max}\left|\big(R^T\otimes I_n\big)\sqrt{N}\beta(\limsup_{t\to\infty}|s(t)|)\right|^2 r\left(\frac{1}{k_1}\right)\\
&= c_{\max}\beta^2\left(\frac{4c_2}{c_3}\beta(0)\right)r\left(\frac{1}{k_1}\right).
\end{aligned}$$

Finally, note that

$$\begin{aligned} x - (1_N \otimes I_n)s &= (W^{-1} \otimes I_n)\xi - (1_N \otimes I_n)s \\ &= (1_N \otimes I_n)\xi_1 - (1_N \otimes I_n)s + (Q \otimes I_n)\tilde{\xi} \\ &= \left([1_N,\ Q] \otimes I_n\right) \begin{bmatrix} e \\ \tilde{\xi} \end{bmatrix}. \end{aligned}$$

Then, by the fact that $\|[1_N,\ Q] \otimes I_n\| \leq \sqrt{N}$ and (3.5.6),

$$|x_i - s| \leq |x - (1_N \otimes I_n)s| \leq \sqrt{N}\sqrt{|e|^2 + |\tilde{\xi}|^2} \leq \sqrt{N}\sqrt{\frac{V}{c_{min}}}.$$

Therefore, for any $i \in \mathcal{N}$,

$$\limsup_{t\to\infty} |x_i(t) - s(t)| \leq \sqrt{N}\sqrt{\frac{c_{\max}}{c_{\min}}}\beta\left(\frac{4c_2}{c_3}\beta(0)\right)\sqrt{r\left(\frac{1}{k_1}\right)}, \tag{3.5.17}$$

if $k_1 = k\lambda_2 - L > \frac{3L^2(2c_2+1)^2}{4c_3}$. From this, the class-$\mathcal{K}$ function σ^* in (3.5.11) and the constant $\bar{K}$ (3.5.10) are found. □

In this section, it is worthwhile to mention that Assumption 3.5.2 is more general assumption than Assumption 3.2.1 in Section 3.2, and Theorem 3.5.3 ensures that the robust properties with the strong coupling can be also hold for high-order heterogeneous multi-agent systems.

Chapter 4

Robustness by A Large Number of Agents

In this chapter, we extend the result of Chapter 3 to the case where the heterogeneities of multi-agent systems are affected by the parametric variations in the individual agents. This chapter is devoted to explain how a large number of agents may be robust to the variations which is realized by the random variables.

Consideration of heterogeneous agents in this way may explain one of the features of biological organs that they are meaningfully working well even though they consist of nonideal, imperfect, and fragile building blocks [PLS+07, BS11, PS07]. Indeed, the fact that any organ is composed of huge number of cells reduces the chance of ending up with abnormal averaged dynamics, and the fact that they are interconnected in a certain way (possibly with large coupling coefficients) implies the operations of the individual cells are not too different from others, and in this way, some malfunctioning cells can operate like normal ones within the network. If the lesson is transferred to another domain such as sensor networks [OSS05], it becomes clear that one can enhance accuracy not by equipping with precision device but by employing many (cheap) sensors (which may include a few of defective ones) and combining their internal filters, such as Kalman filters, through the strong consensus network.

The analysis of the effect of large number of agents is very rare in the literature, although there is only one paper [TSP10] in author's knowledge that deals with the similar problem. However, they dealt with identical node dynamics interconnected

with all-to-all network topology, by different analysis method. On the other hand, when we deal with large number of agents, the use of the averaged dynamics is very helpful. To see this, we note that the averaged dynamics is still affected by the variations of individual agents. For example, suppose that there is only one abnormal agent (*i.e.*, having different vector field from others) in a group of identical and normal agents. If N is not large, the averaged dynamics may be affected heavily by the abnormal dynamics of the agent. Then, how to make the averaged dynamics robust to the perturbations in the abnormal agents? This is where the large number N comes into the picture. Indeed, the law of large number plays a central role in the averaged dynamics, and therefore the robustness of the averaged dyanmics can be obtained.

In this chapter, only the parametric variations are dealt with for quantitative analysis, and the vector field $f_i(t, x_i)$ is supposed to be dependent on some parameters of random variables. With this setup, we additionally introduce the *expected averaged dynamics* as a reference system which is not affected by the variation of the agents, and show that amount of individual variation of each agent, that is contributed to the averaged dynamics, gets smaller as the number of agents increases, and thus, the averaged dynamics becomes close to the expected averaged dynamics. Finally, combining the results of Chapter 3 and Chapter 4, it is not difficult to infer that strong coupling and a large number of agents imply robustness of consensus and synchronization against heterogeneity (here, heterogeneity also includes uncertainty and/or external disturbance in each agent).

4.1 Problem Formulation

In this section we are more specific on the system diversity and derive quantitative robustness measure under a large number of agents. For this, we introduce random variables to represent the heterogeneous group of N dynamic agents[1] under

[1]For a similar reason as discussed above in Section 3.1, the class of systems considered in this section is scalar dynamics.

consideration as

$$\dot{x}_i = f_i(t, x_i) + u_i = g_0(t, x_i) + \sum_{j=1}^{d} \Delta_{ij} g_j(t, x_i) + u_i \tag{4.1.1}$$

for $i \in \mathcal{N}$, where g_j's are C^1 "generating functions" for the individual agent function f_i, and Δ_{ij}'s are random variables having the expectation $E\{\Delta_{ij}\} = 0$ (without loss of generality) and the variance $V\{\Delta_{ij}\} = \sigma_j^2$ ($\sigma_j \geq 0$) for all $i \in \mathcal{N}$ and $j \in \mathcal{D} := \{1, \ldots, d\}$.[2] It is assumed that Δ_{ij}'s are mutually independent for all i, but possibly dependent for j. The individual system (4.1.1) is divided into two parts: a deterministic model for heterogeneous multi-agent systems $g_0(t, x_i)$ and a sum of d randomly determined functions $\sum_{j=1}^{d} \Delta_{ij} g_j(t, x_i)$ depending on time and the state. In fact, this term cannot handle realistic noise (*e.g.,* white Gaussian noise), but can handle the sinusoidal signal with random phase (see Section 4.2.2 for more details).

The averaged dynamics of (4.1.1) is then given by

$$\dot{s} = \bar{f}(t, s) = \frac{1}{N} \sum_{i=1}^{N} f_i(t, s) = g_0(t, s) + \sum_{j=1}^{d} \bar{\Delta}_j g_j(t, s) \tag{4.1.2}$$

where $\bar{\Delta}_j := \sum_{i=1}^{N} \Delta_{ij}/N$. It should be noted from [YG05] that

$$E\{\bar{\Delta}_j\} = 0, \quad V\{\bar{\Delta}_j\} = \frac{\sigma_j^2}{N}. \tag{4.1.3}$$

Now let us consider the *expected averaged dynamics* which will be used as a reference for comparison:

$$\dot{s}_E = E\{\bar{f}(t, s_E)\} = g_0(t, s_E), \quad s_E(0) = s(0). \tag{4.1.4}$$

For the given dynamical system, we now define the notion of robustness in probability for multi-agent systems which has variations.

[2] It is noted that (4.1.1) is not a stochastic differential equation. Once those random variables are drawn (or, realized) when the system is created, it remains deterministic. In this sense, we share the philosophy of 'random differential equation' in [TS13].

Definition 4.1.1. (Robustness in probability). The N individuals (4.1.1) is said to achieve *robust consensus and synchronization in probability* if for any given $\epsilon > 0$,

$$\lim_{N\to\infty} P\left(\limsup_{t\to\infty} |x_i(t) - s_E(t)| \leq \epsilon\right) = 1.$$

for all $i \in \mathcal{N}$. □

Since we do not impose any particular conditions (such as probability distribution) on the random variables Δ_{ij}, they are unbounded, and thus, Assumptions 3.1.1 and 3.2.1 cannot hold for all cases. Instead, we impose assumptions on the generating functions.

Assumption 4.1.1. There exist non-decreasing continuous functions $M_j : \mathbb{R}_{\geq 0} \to \mathbb{R}_{\geq 0}$ and constants $L_j > 0$ such that

$$|g_j(t, x_i)| \leq M_j(|x_i|), \quad \left|\frac{\partial g_j}{\partial x_i}(t, x_i)\right| \leq L_j, \quad \forall t \geq 0, \tag{4.1.5}$$

for all $x_i \in \mathbb{R}$, and $j \in \mathcal{D} \cup \{0\}$. ◊

Assumption 4.1.2. There exists $p > 0$ such that

$$\frac{\partial g_0}{\partial s}(t, s) \leq -p, \tag{4.1.6}$$

for all $s \in \mathbb{R}$ and $t \geq 0$. ◊

4.2 Robustness of Averaged Dynamics

In this section, we develop the robustness of the averaged dynamics by a large number of agents. To show this, we first claim that as the number of agents N increases in the network, the averaged dynamics (4.1.2) with variations approaches the expected averaged dynamics (4.1.4) without them. For example, if $f_i(t, x_i) = a_i x_i + \Delta_i$, where a_i and Δ_i are independent and identically distributed random variables with the average $\bar{a}$ and 0, respectively, then the averaged dynamics

becomes

$$\dot{s} = \left(\frac{1}{N} \sum_{i=1}^{N} a_i \right) s + \frac{1}{N} \sum_{i=1}^{N} \Delta_i.$$

When N gets large, the effects of individual variations in a_i and Δ_i get weakened in the sense that the averaged dynamics can be regarded as

$$\dot{s}_E = \bar{a} s_E$$

which we may regard as a 'nominal' averaged dynamics with the standard deviations are in the order of $(1/\sqrt{N})$.

4.2.1 Probabilistic Analysis of Robust Averaged Dynamics

The objective of this section is to develop simple, but efficient procedures for probabilistic analysis of robust averaged dynamics. To develop, we recall a well-known fact for probability.

Lemma 4.2.1. (Chebyshev's inequality). Let X be a random variable with $E\{X\} = \mu$ and $V\{X\} = \sigma^2$ $(\sigma \geq 0)$. Then, for any $h > 0$, it holds that

$$P\left(|X - \mu| \geq h\right) \leq \frac{\sigma^2}{h^2},$$

and therefore,

$$1 - \frac{\sigma^2}{h^2} \leq P(|X - \mu| < h) \leq P(|X - \mu| \leq h).$$

$\Diamond$

The *weak law of large number* follows immediately from Lemma 4.2.1. By (4.1.3), for any given $\epsilon > 0$, we have

$$P\left(|\bar{\Delta}_j| \leq \epsilon\right) \geq 1 - \frac{\sigma_j^2}{N^2 \epsilon^2}, \quad \forall j \in \mathcal{D},$$

and

$$\lim_{N\to\infty} P\left(|\bar{\Delta}_j| \leq \epsilon\right) = 1, \quad \forall j \in \mathcal{D}.$$

It means that if the sample size increases, then the arithmetic average $\bar{\Delta}_j$ tends more and more closely to the expected value $E\{\bar{\Delta}_j\} = 0$. We note that the variations in the averaged dynamics can be smoothened by the weak law of large number.

The following lemma is the generalization of the addition rule for probability.

Lemma 4.2.2. *Let $A_1, \ldots, A_d$ be d arbitrary events. Then*

$$\sum_{i=1}^{d} P(A_i) - d + 1 \leq P\left(\bigcap_{i=1}^{d} A_i\right).$$

Proof. We will prove by induction. It is clearly true for $d = 1$. If it holds for $d = k - 1$, then

$$\begin{aligned}
\sum_{i=1}^{k} P(A_i) - k + 1 &= \sum_{i=1}^{k-1} P(A_i) - (k-1) + 1 + P(A_k) - 1 \\
&\leq P\left(\bigcap_{i=1}^{k-1} A_i\right) + P(A_k) - 1 \\
&\leq P\left(\left(\bigcap_{i=1}^{k-1} A_i\right) \bigcap A_k\right) \\
&= P\left(\bigcap_{i=1}^{k} A_i\right)
\end{aligned}$$

in which, the second inequality follows from the fact that

$$P(A) + P(B) - P(A \cap B) \leq 1$$

for any two events A and B. □

Now we compare two trajectories $s(t)$ and $s_E(t)$ and claim that they tend to be arbitrarily close with high probability when N is sufficiently large. For this,

note first that

$$\begin{aligned}\limsup_{t\to\infty}|s_E(t)| &\leq \limsup_{t\to\infty}\frac{|g_0(t,0)|}{p}\\ &\leq \frac{M_0(0)}{p},\end{aligned}$$

which follows from Lemma 3.2.1 for (4.1.4) under Assumptions 4.1.1 and 4.1.2.

Lemma 4.2.3. Under Assumptions 4.1.1 and 4.1.2, the solutions of the averaged dynamics (4.1.2) and the expected averaged dynamics (4.1.4) satisfy that, for any given $\epsilon > 0$,

$$\lim_{N\to\infty} P\left(\limsup_{t\to\infty}|s(t)-s_E(t)|\leq\epsilon\right)=1. \tag{4.2.1}$$

$\Diamond$

Proof. Let $\tilde{s} := s - s_E$ be the error between (4.1.2) and (4.1.4). Then,

$$\begin{aligned}\dot{\tilde{s}} &= g_0(t,\tilde{s}+s_E)-g_0(t,s_E)+\sum_{j=1}^{d}\bar{\Delta}_j g_j(t,\tilde{s}+s_E)\\ &=: \tilde{f}(t,\tilde{s})\end{aligned}$$

with $\tilde{s}(0)=0$. With this, suppose that

$$|\bar{\Delta}_j| \leq \frac{p}{2dL_j} =: \phi_j, \qquad \forall j\in\mathcal{D}. \tag{4.2.2}$$

Then, it follows from Asummptions 4.1.1 and 4.1.2 that

$$\begin{aligned}\frac{\partial\tilde{f}}{\partial\tilde{s}}(t,\tilde{s}) = \frac{\partial\bar{f}}{\partial s}(t,s) &= \frac{\partial g_0}{\partial s}(t,s)+\sum_{j=1}^{d}\bar{\Delta}_j\frac{\partial g_j}{\partial s}(t,s)\\ &\leq -p+\sum_{j=1}^{d}|\bar{\Delta}_j|L_j\\ &\leq -\frac{p}{2}.\end{aligned}$$

Lemma 3.2.1 now yields that

$$\begin{aligned}\limsup_{t\to\infty}|\tilde{s}(t)| &\le \limsup_{t\to\infty}\frac{\left|\tilde{f}(t,0)\right|}{p/2}\\ &= \limsup_{t\to\infty}\frac{\left|\sum_{j=1}^{d}\bar{\Delta}_j g_j(t,s_E(t))\right|}{p/2}.\end{aligned}$$

Therefore, if, in addition to (4.2.2),

$$|\bar{\Delta}_j| \le \frac{\epsilon p}{2dM_j\left(M_0(0)/p\right)} =: \varphi_j, \qquad \forall j\in\mathcal{D}, \tag{4.2.3}$$

with any $\epsilon > 0$, then

$$\begin{aligned}\limsup_{t\to\infty}|\tilde{s}(t)| &\le \frac{\sum_{j=1}^{d}|\bar{\Delta}_j|M_j(\limsup_{t\to\infty}s_E(t))}{p/2}\\ &\le \frac{\sum_{j=1}^{d}|\bar{\Delta}_j|M_j\left(M_0(0)/p\right)}{p/2}\\ &\le \epsilon.\end{aligned} \tag{4.2.4}$$

Finally,

$$\begin{aligned}&P\left(|\bar{\Delta}_j|\le\phi_j \text{ and } |\bar{\Delta}_j|\le\varphi_j,\ \forall j\in\mathcal{D}\right)\\ &= P\left(\bigcap_{j=1}^{d}\left\{\left(|\bar{\Delta}_j|\le\phi_j\right)\bigcap\left(|\bar{\Delta}_j|\le\varphi_j\right)\right\}\right)\\ &\ge \sum_{j=1}^{d}P\left(\left(|\bar{\Delta}_j|\le\phi_j\right)\bigcap\left(|\bar{\Delta}_j|\le\varphi_j\right)\right)-d+1 \qquad \text{by Lemma 4.2.2,}\\ &\ge \sum_{j=1}^{d}P\left(|\bar{\Delta}_j|\le\phi_j\right)P\left(|\bar{\Delta}_j|\le\varphi_j\right)-d+1\end{aligned}$$

since one event implies the other and probability is not larger than 1, and Lemma 4.2.1 leads to

$$\ge \sum_{j=1}^{d}\left(1-\frac{1}{\phi_j^2}\frac{\sigma_j^2}{N}\right)\left(1-\frac{1}{\varphi_j^2}\frac{\sigma_j^2}{N}\right)-d+1. \tag{4.2.5}$$

In summary, we conclude that

$$\sum_{j=1}^{d}\left(1-\frac{4d^2\sigma_j^2L_j^2}{p^2N}\right)\left(1-\frac{4d^2\sigma_j^2M_j(M_0(0)/p)^2}{\epsilon^2p^2N}\right)-d+1 \leq P\left(\limsup_{t\to\infty}|s(t)-s_E(t)|\leq\epsilon\right). \quad (4.2.6)$$

Note that this also implies (4.2.1). □

4.2.2 Simulation Results

In this section we illustrate, through simulation studies, that a large number of agents have robust averaged dynamics against the random variations which are the realizations of the random variables.

As an example, consider a group of N agents with

$$f_i(t,x_i)=(-1+\delta_i)x_i+10\sin t+10m_i^1\sin(0.1t+\theta_i^1)+10m_i^2\sin(10t+\theta_i^2),$$

for $i=1,2,\ldots,N$, where δ_i, m_i^1, and m_i^2 are realizations of independent random variables of standard normal distribution $N(0,1)$, and θ_i^1 and θ_i^2 are realizations of independent random variables of uniform distribution on $[0,2\pi]$. Since, from trigonometric addition formulas, we can handle the following sinusoidal signal with random phase such that

$$\begin{aligned}10m_i^1\sin(0.1t+\theta_i^1)&=10m_i^1\cos\theta_i^1\sin 0.1t+10m_i^1\sin\theta_i^1\cos 0.1t,\\ 10m_i^1\sin(10t+\theta_i^1)&=10m_i^1\cos\theta_i^1\sin 10t+10m_i^1\sin\theta_i^1\cos 10t.\end{aligned}$$

In order to represent the agent in the form of (4.1.1), we take

$$\begin{aligned}\Delta_{i1}&=\delta_i,\\ \Delta_{i2}&=10m_i^1\cos\theta_i^1,\\ \Delta_{i3}&=10m_i^1\sin\theta_i^1,\\ \Delta_{i4}&=10m_i^2\cos\theta_i^2,\\ \Delta_{i5}&=10m_i^2\sin\theta_i^2,\end{aligned}$$

with

$$
\begin{aligned}
g_0(t, x_i) &= -x_i + 10 \sin t, \\
g_1(t, x_i) &= x_i, \\
g_2(t, x_i) &= \sin 0.1t, \\
g_3(t, x_i) &= \cos 0.1t, \\
g_4(t, x_i) &= \sin 10t, \\
g_5(t, x_i) &= \cos 10t.
\end{aligned}
$$

Indeed, $E\{\Delta_{ij}\} = 0$ for all i and j since m_i^j and θ_i^j are independent and $E\{m_i^j\} = 0$. Also, Δ_{ij} are independent for i while it is not for j. The averaged dynamics is given by

$$
\begin{aligned}
\dot{s} = \left(-1 + \frac{1}{N} \sum_{i=1}^{N} \delta_i \right) s + 10 \sin t + \frac{1}{N} \sum_{i=1}^{N} 10 m_i^1 \sin(0.1t + \theta_i^1) \\
+ \frac{1}{N} \sum_{i=1}^{N} 10 m_i^2 \sin(10t + \theta_i^2), \quad s(0) = \frac{1}{N} \sum_{i=1}^{N} x_i(0)
\end{aligned}
$$

and thus the expected averaged dynamics is given as

$$
\dot{s}_E = -s_E + 10 \sin t, \quad s_E(0) = \frac{1}{N} \sum_{i=1}^{N} x_i(0).
$$

Assuming that these agents are interconnected by the ring network, and it can be observed by Monte Carlo experiments that the solution $s(t)$ tends to $s_E(t)$ as N increases. For example, Figure 4.1 is taken from six random samples of the group of 5 agents, and shows the trajectories of $s(t)$ (solid) and $s_E(t)$ (dashed), while Figure 4.2 is for the case of 100 agents. It is seen that, as N increases, (the solution of) the averaged dynamics from the random samples becomes closer to (the solution of) the expected averaged dynamics, as expected.

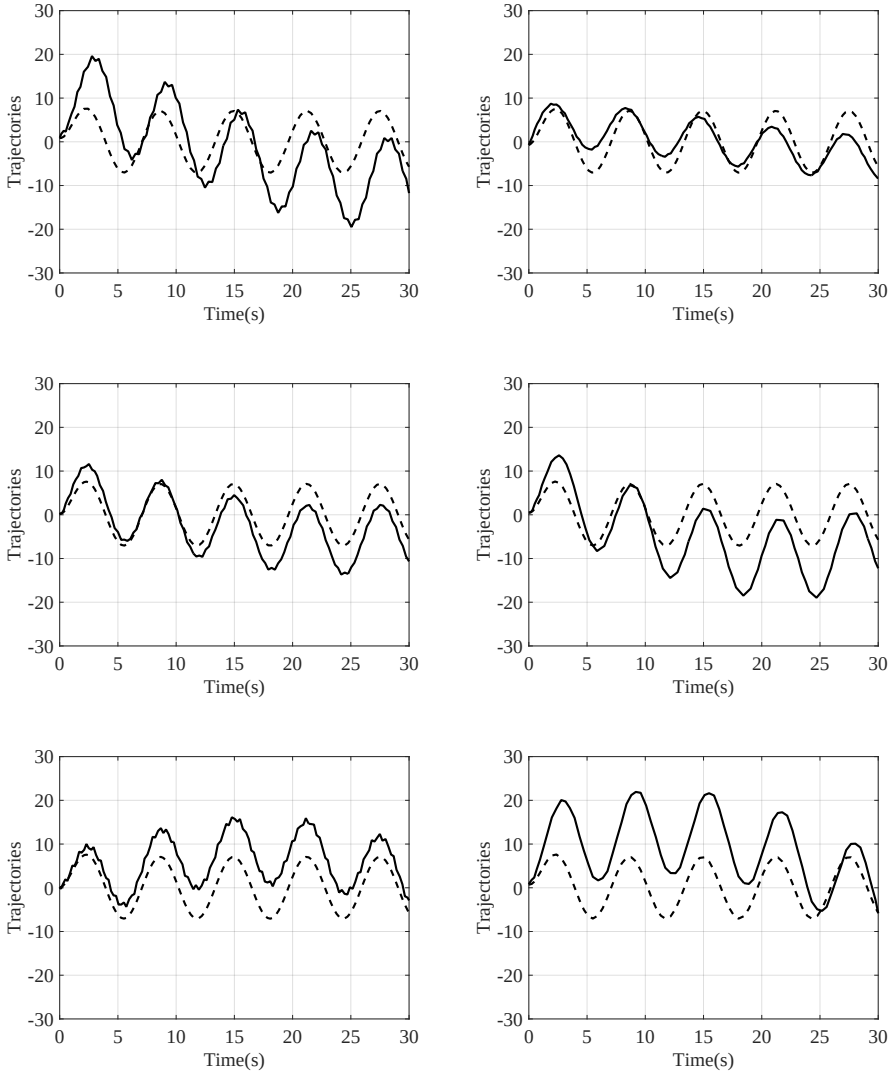

Figure 4.1: Plots of $s(t)$ (solid) from 6 sample runs for $N = 5$. The solution $s_E(t)$ of the expected averaged system is also drawn (dashed).

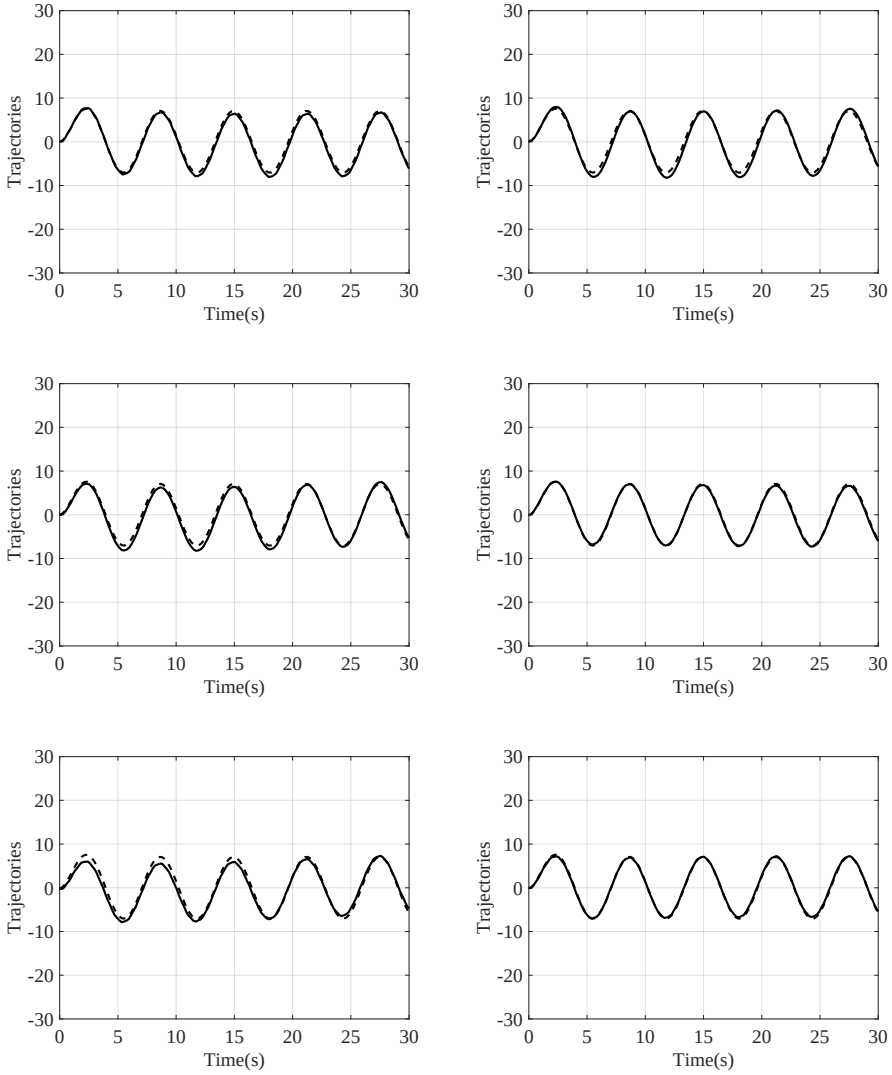

Figure 4.2: Plots of $s(t)$ (solid) from 6 sample runs for $N = 100$. The solution $s_E(t)$ is also drawn (dashed).

4.3 Strong Coupling with A Large Number of Agents

Until now, we have seen the effect of a large number of agents in the averaged dynamics. In this section, we combine two ingredients (*i.e.,* strong coupling and a large number of agents) in order to achieve robust consensus and synchronization in probability. As mentioned in Remark 3.3.1(a) of Section 3.3, strong coupling makes the trajectories of individuals close to that of the averaged dynamics, *i.e.,* for any $\epsilon > 0$, there is a sufficient large coupling gain k such that

$$\limsup_{t\to\infty} |x_i(t) - s(t)| \leq \frac{\epsilon}{2}, \quad \forall i \in \mathcal{N}.$$

Moreover, Lemma 4.2.3 ensures that the averaged dynamics can be robust if the number of agents N increases, that is to say, for the given ϵ,

$$\lim_{N\to\infty} P\left(\limsup_{t\to\infty} |s(t) - s_E(t)| \leq \frac{\epsilon}{2}\right) = 1.$$

Therefore, we can easily infer from the triangular inequality that for any given $\epsilon > 0$,

$$\lim_{N\to\infty} P\left(\limsup_{t\to\infty} |x_i(t) - s_E(t)| \leq \epsilon\right) = 1, \quad \forall i \in \mathcal{N}.$$

We note that the robust consensus and synchronization in probability can be achieved by Definition 4.1.1.

The following theorem characterizes the effect of strong coupling and a large number of agents and is the main result of this dissertation.

Theorem 4.3.1. Under Assumptions 4.1.1, 3.1.2, and 4.1.2, there exists a class-$\mathcal{K}$ function γ_N^* such that the solutions of the overall system, composed of (4.1.1) and (3.1.2), satisfy that

$$\begin{aligned} &P\left(\limsup_{t\to\infty} |x_i(t) - s_E(t)| \leq \gamma_N^*\left(\frac{1}{k\lambda_2 - \mathcal{L}_N}\right) + \epsilon,\ \forall k > \bar{\mathcal{K}}_N,\ \forall i \in \mathcal{N}\right) \\ &\geq \left(1 - \frac{d}{N^2}\right)^N + \sum_{j=1}^{d}\left(1 - \frac{4d^2\sigma_j^2 L_j^2}{p^2 N}\right)\left(1 - \frac{4d^2\sigma_j^2 M_j (M_0(0)/p)^2}{\epsilon^2 p^2 N}\right) - d \end{aligned} \tag{4.3.1}$$

where $s_E(t)$ is the solution of (4.1.4) with $s_E(0) = \sum_{i=1}^N x_i(0)/N$, ϵ is any positive number, and

$$\mathcal{L}_N := L_0 + N\sum_{j=1}^{d} \sigma_j L_j \quad \text{and} \quad \bar{\mathcal{K}}_N := \frac{6\mathcal{L}_N^2}{p\lambda_2} + \frac{\mathcal{L}_N}{\lambda_2}. \tag{4.3.2}$$

The function γ_N^* is defined on $[0, p/6\mathcal{L}_N^2)$ and given by

$$\gamma_N^*(\chi) = \mathcal{M}_N\left(\frac{2\mathcal{M}_N(0)}{p}\right)\sqrt{N}\sqrt{r_N(\chi)} \tag{4.3.3}$$

in which,

$$\mathcal{M}_N(a) := M_0(a) + N\sum_{j=1}^{d}\sigma_j M_j(a), \quad \text{and}$$

$$r_N(\chi) := \begin{cases} 0, & \chi = 0, \\ \frac{8\chi}{p-6\mathcal{L}_N^2\chi}, & 0 < \chi \le \frac{8p}{p^2+80\mathcal{L}_N^2}, \\ \frac{(p^2+32\mathcal{L}_N^2)\chi^2}{(p-6\mathcal{L}_N^2\chi)^2}, & \frac{8p}{p^2+80\mathcal{L}_N^2} < \chi < \frac{p}{6\mathcal{L}_N^2}. \end{cases} \tag{4.3.4}$$

$\Diamond$

A few factors are related to the upper bound of $\limsup_{t\to\infty}|x_i(t) - s_E(t)|$ and the probability estimation in (4.3.1). The upper bound tends to increase as N increases since $\mathcal{L}_N$ and $\mathcal{M}_N$ increase. (Also, λ_2 is affected.) The lower bound of the probability (the right-hand side of (4.3.1)) tends to decrease as the increment of d, σ_j, L_j, M_j and the decrement of p, which intuitively makes sense. It is also true that, with ϵ getting larger, the lower bound of the probability increases. In any case, as $k \to \infty$, the upper error bound in (4.3.1) tends to ϵ, and the probability of achieving this error bound tends to 1 as $N \to \infty$. The latter can be seen from the right-hand side of (4.3.1), with

$$\lim_{N\to\infty}\left(1 - \frac{d}{N^2}\right)^N = \lim_{N\to\infty}\left\{\left(1 - \frac{d}{N^2}\right)^{-\frac{N^2}{d}}\right\}^{-\frac{d}{N}} = 1.$$

Therefore, it is asserted that, with a large number of agents, it is more likely to

have $\limsup_{t\to\infty} |x_i(t) - s_E(t)|$ less than or equal to the error bound for all $i \in \mathcal{N}$, and the error bound can be made small with strong coupling k.

Remark 4.3.1. As in Remark 3.3.1(d) in Section 3.3, let us look into the ultimate error bound γ_N^* in more detail. For this, suppose that, without loss of generality, the function M_j in Assumption 4.1.2 is taken as an affine function of $|x_i|$ (for example, $M_j(|x_i|) = \sup_{t\geq 0} |g_j(t,0)| + L_j|x_i|$ does the job). Then, with sufficiently large k, one can show that $\gamma_N^*\left(1/(k\lambda_2 - \mathcal{L}_N)\right) = \mathcal{O}\left(\sqrt{N^5/(k\lambda_2)}\right)$.

$\Diamond$

Proof. In this proof we combine the analysis performed for Theorem 3.3.2 which discusses the closeness between $x_i(t)$ and $s(t)$, and the analysis about the closeness between $s(t)$ and $s_E(t)$. For this, let us first suppose that

$$|\Delta_{ij}| \leq N\sigma_j, \quad \forall i \in \mathcal{N},\ \forall j \in \mathcal{D}. \tag{4.3.5}$$

Then, it follows from Assumption 4.1.1 that

$$\begin{aligned} |f_i(t,x_i)| &= \left| g_0(t,x_i) + \sum_{j=1}^{d} \Delta_{ij} g_j(t,x_i) \right| \\ &\leq M_0(|x_i|) + N\sum_{j=1}^{d} \sigma_j M_j(|x_i|) = \mathcal{M}_N(|x_i|), \end{aligned}$$

and that

$$\begin{aligned} \left| \frac{\partial f_i}{\partial x_i}(t,x_i) \right| &= \left| \frac{\partial g_0}{\partial x_i}(t,x_i) + \sum_{j=1}^{d} \Delta_{ij} \frac{\partial g_j}{\partial x_i}(t,x_i) \right| \\ &\leq L_0 + N\sum_{j=1}^{d} \sigma_j L_j = \mathcal{L}_N, \end{aligned}$$

so that Assumption 3.1.1 holds with M and L replaced with $\mathcal{M}_N$ and $\mathcal{L}_N$, respectively. Moreover, if (4.2.2) holds as well, then $|(\partial \bar{f}/\partial s)| \leq -p/2$ (not $-p$!) as seen in Lemma 4.2.3. In this case, Theorem 3.3.2 guarantees that

$$\limsup_{t\to\infty} |x_i(t) - s(t)| \leq \gamma_N^*\left(\frac{1}{k\lambda_2 - \mathcal{L}_N}\right),\ \forall k > \bar{\mathcal{K}}_N,\ \forall i \in \mathcal{N}$$

in which, γ_N^*, $\bar{\mathcal{K}}_N$, and r_N are given by (4.3.3), (4.3.2), and (4.3.4), respectively (which are obtained simply by replacing p in Theorem 3.3.2 with $p/2$). Now, if (4.2.3) holds additionally with some $\epsilon > 0$, then we have seen that $\limsup_{t\to\infty} |s(t) - s_E(t)| \leq \epsilon$ in (4.2.4). Thus, combining these two by triangular inequality, we obtain that

$$\limsup_{t\to\infty} |x_i(t) - s_E(t)| \leq \gamma_N^* \left(\frac{1}{k\lambda_2 - \mathcal{L}_N} \right) + \epsilon$$

for all $k > \bar{\mathcal{K}}_N$ and $i \in \mathcal{N}$.

To see (4.3.1), it is left to compute the probability that all (4.2.2), (4.2.3), and (4.3.5) hold. For (4.3.5), it is seen that

$$\begin{aligned}
&P(|\Delta_{ij}| \leq N\sigma_j, \forall i \in \mathcal{N}, \forall j \in \mathcal{D}) \\
&\quad = \prod_{i=1}^{N} P(|\Delta_{ij}| \leq N\sigma_j, \forall j \in \mathcal{D}) \quad \text{by independency of } \Delta_{ij} \text{ for } i \\
&\quad \geq \prod_{i=1}^{N} \left(\sum_{j=1}^{d} P(|\Delta_{ij}| \leq N\sigma_j) - d + 1 \right) \quad \text{by Lemma 4.2.2} \\
&\quad \geq \prod_{i=1}^{N} \left(\sum_{j=1}^{d} \left(1 - \frac{1}{N^2} \right) - d + 1 \right) \quad \text{by Lemma 4.2.1} \\
&\quad = \left(1 - \frac{d}{N^2} \right)^N .
\end{aligned}$$

Finally, we have that

$$\begin{aligned}
&P\left(((4.3.5) \text{ holds}) \bigcap ((4.2.2) \text{ and } (4.2.3) \text{ hold}) \right) \\
&\quad \geq P\left((4.3.5) \text{ holds} \right) + P\left((4.2.2) \text{ and } (4.2.3) \text{ hold} \right) - 1 \\
&\quad \geq \left(1 - \frac{d}{N^2} \right)^N + \sum_{j=1}^{d} \left(1 - \frac{1}{\phi_j^2} \frac{\sigma_j^2}{N} \right) \left(1 - \frac{1}{\varphi_j^2} \frac{\sigma_j^2}{N} \right) - d \text{ from (4.2.5)}
\end{aligned}$$

which concludes (4.3.1). □

4.3.1 Simulation Results

Here, the simulations are performed the same as in Section 4.2.2. In order to see the effect of a large number of agent, the simulation results of two sample runs with $N = 5$ and $N = 100$ are depicted in Figure 4.3. In each case, the coupling gains of $k = 5$ and $k = 500$ are used, respectively.

The effect of strong coupling k is seen rather clearly by comparing Figure 4.3.(a) with (b), and (c) with (d), respectively. On the other hand, by comparing (a) with (c), and (b) with (d), it is seen that, when N is larger, the solutions of each agents (solid blue) tend closer to the dashed black curve, which is the solution of the expected averaged dynamics

$$\dot{s}_E = -s_E + 10\sin t, \quad s_E(0) = \frac{1}{N}\sum_{i=1}^{N} x_i(0).$$

This is because the averaged dynamics, given by

$$\begin{aligned}\dot{s} = &\left(-1 + \frac{1}{N}\sum_{i=1}^{N}\delta_i\right)s + 10\sin t + \frac{1}{N}\sum_{i=1}^{N} 10m_i^1 \sin(0.1t + \theta_i^1) \\ &+ \frac{1}{N}\sum_{i=1}^{N} 10m_i^2 \sin(10t + \theta_i^2),\end{aligned}$$

gets close to the expected averaged dynamics with large N. In the sample run for $N = 5$, it was

$$\begin{aligned}\dot{s} = &-0.437s + 10\sin t + 0.445\sin 0.1t + 6.005\cos 0.1t + 6.588\sin 10t \\ &- 5.523\cos 10t,\end{aligned}$$

and

$$\begin{aligned}\dot{s} = &-1.034s + 10\sin t + 0.608\sin 0.1t - 0.833\cos 0.1t - 0.671\sin 10t \\ &+ 0.08\cos 10t\end{aligned}$$

for $N = 100$.

It is also observed that increasing N (under the same k) results in more

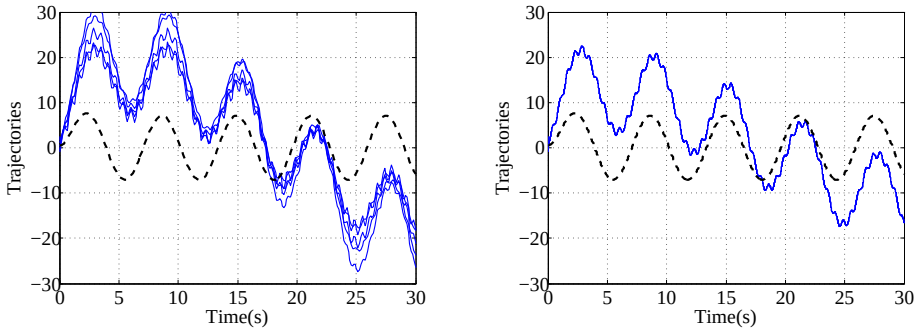

(a) $N = 5,\ k = 5$

(b) $N = 5,\ k = 500$

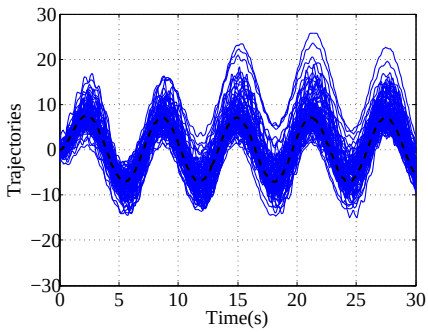

(c) $N = 100,\ k = 5$

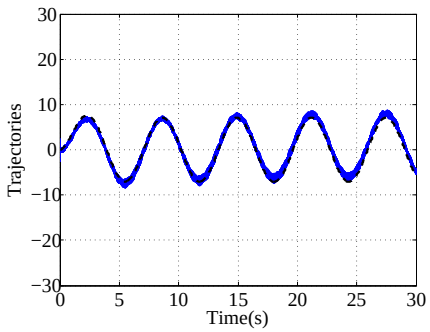

(d) $N = 100,\ k = 500$

Figure 4.3: Trajectories of N-agent systems with coupling strength k are depicted as blue solid curves, and the trajectory $s_E(t)$ of the expected averaged system is given as the black dashed curve.

deviation by comparing (a) and (c); (b) and (d), as discussed in Remark 3.3.1(d). Finally, it is stressed that there were 2 unstable agents out of 5 when $N = 5$, and 12 out of 100 when $N = 100$, in the sample run. By repeating the sample runs, we observe that the error $|x_i(t) - x_j(t)|$ is small for all $i, j \in \mathcal{N}$ when k is large, and the deviation of $x_i(t)$ from $s_E(t)$ is small *with high probability* when both N and k are large. Fig. 4.3 is a typical one of them.

Chapter 5

Optimal Distributed Kalman-Bucy Filter in Sensor Network

In the first part of the dissertation, the robustness of consensus and synchronization in the heterogeneous multi-agent systems has been addressed. As mentioned in Section 1.1.3, the phenomena of the robustness in networked systems appear in various areas. In engineering, distributed sensor network is one of the major application area of the robust consensus and synchronization, particularly in surveillance and monitoring of an environment, tracking of target, and so on [ASSC02, CHZ02, CMKB02, DW05, EGHK99, FOSPP06, GDW94, OSS05]. A fundamental problem in distributed sensor network is to achieve estimation of target by using distributed algorithms.

In [GDW94, RDWS93], the decentralized filtering problem involving the local Kalman filters is solved with the information topology which is all-to-all network, and thus it is not scalable[1] since the complexity of the communication is $\mathcal{O}(N^2)$. In order to deal with scalable sensor network, the authors of [OS07] proposed Kalman-Consensus filtering algorithm in which each node only communicates messages with its neighbors on a network. Furthermore, in accordance with the local measurement and error covariance matrices, some novel distributed Kalman filtering methods are provided to further improve the local estimation

[1] In the context of interconnected dynamical systems, scalability is the property that analysis and design complexity grows slowly as compared to system size, *i.e.*, number of subsystems. In practice, if there are a large number of things (N) that affect scaling, then resource requirements (for example, algorithmic time-complexity) must grow less than N^2 as N increases.

performance for each node by applying the internal model average consensus estimator [BFL11, Geo13].

This chapter addresses a design and analysis of distributed Kalman filter (Kalman-Bucy filter for continuous-time system) in the sensor network. In order to recover the optimality of the centralized Kalman-Bucy filter, we introduce the averaged distributed Kalman-Bucy filter which is the average of all distributed Kalman-Bucy filters' dynamics. The underlying philosophy for designing distributed Kalman-Bucy filter is similar to the robustness of the consensus and synchronization problem.

5.1 Reviews of Distributed Kalman-Bucy Based Filtering for Sensor Network

In this section, we briefly review the previously proposed Kalman-based filters in sensor network. To formulate the distributed sensor network, we consider a continuous-time linear system[2]

$$\dot{x} = Ax + Bw, \tag{5.1.1}$$

$$z = Hx + v = \begin{bmatrix} H_1 \\ \vdots \\ H_N \end{bmatrix} x + \begin{bmatrix} v_1 \\ \vdots \\ v_N \end{bmatrix} = \begin{bmatrix} z_1 \\ \vdots \\ z_N \end{bmatrix} \tag{5.1.2}$$

where $x = \mathrm{col}(x^1, \ldots, x^n) \in \mathbb{R}^n$ is the state, $z \in \mathbb{R}^p$ is the measurement output, $w \in \mathbb{R}^m$ is the input (process) noise, and $v \in \mathbb{R}^p$ is the measurement noise. The submatrix $H_i \in \mathbb{R}^{p_i \times n}$ is a partition of H such that $\sum_{i=1}^N p_i = p$, and $v_i, z_i \in \mathbb{R}^{p_i}$. The noise signals $\{w, v_1, \cdots, v_N\}$ are independent Gaussian signals of zero mean with

$$E\{w(t)w^T(\tau)\} = Q\delta(t-\tau), \quad E\{v_i(t)v_i^T(\tau)\} = R_i\delta(t-\tau)$$

for all $i \in \mathcal{N} := \{1, \ldots, N\}$, where $\delta(t-\tau) = 1$ if $t = \tau$ and $\delta(t-\tau) = 0$ otherwise.

The forthcoming discussion is based on the following assumption.

[2] We consider a time-invariant linear system here for simplicity.

Assumption 5.1.1. The matrix R_i is positive definite ($R_i > 0$) for all $i \in \mathcal{N}$, and Q is positive semi-definite ($Q \geq 0$). The pair $(A, B\sqrt{Q})$ is controllable, and the pair (A, H) is observable. $\lozenge$

Our assumption on the dynamical system to be estimated is that it is observable only in a centralized sense, that is, the state of the dynamical system may not be observable to individual agents but is observable when the measurements from the agents are fused (*i.e.,* (A, H_i) is not necessarily observable).

5.1.1 Centralized Kalman-Bucy Filter

We first review the centralized Kalman-Bucy filter (CKBF) [BJ68]. The CKBF of the plant (5.1.1) can be written as

$$\dot{\hat{x}} = A\hat{x} + PH^T R^{-1}(z - H\hat{x}) \tag{5.1.3a}$$

$$\dot{P} = AP + PA^T + BQB^T - PH^T R^{-1} HP \tag{5.1.3b}$$

with $P(0) = P_0 > 0$, where $\hat{x} \in \mathbb{R}^n$ is the estimated state vector of x and $R = \mathrm{diag}(R_1, \ldots, R_N)$.

It follows from optimal control theory that the CKBF is optimal in cases where i) the model perfectly matches the real system, ii) the entering noise is white and Gaussian, and iii) the covariances of the noise are exactly known. We note that the error covariance matrix $P(t)$ is the solution of the differential Riccati equation (5.1.3b), and converges to steady state (finite) covariance if the pair (A, H) is observable. Moreover, the steady state error covariance matrix P^* is the solution of the algebraic Riccati equation of (5.1.3b), and thus it gives the optimal gain. The following lemma is well-known result in optimal control theory.

Lemma 5.1.1. Under Assumption 5.1.1, it follows that

(a) [LXP07, Theorem 3.2] the origin of the system $\dot{x} = \left(A - P^* H^T R^{-1} H\right) x$ with the unique positive definite solution $P^* > 0$ to the algebraic Riccati equation of (5.1.3b) is exponentially stable.

(b) [BJ68, Theorem 3.1] the origin of the system $\dot{x} = \left(A - P(t) H^T R^{-1} H\right) x$ with the solution $P(t)$ of (5.1.3b) is exponentially stable.

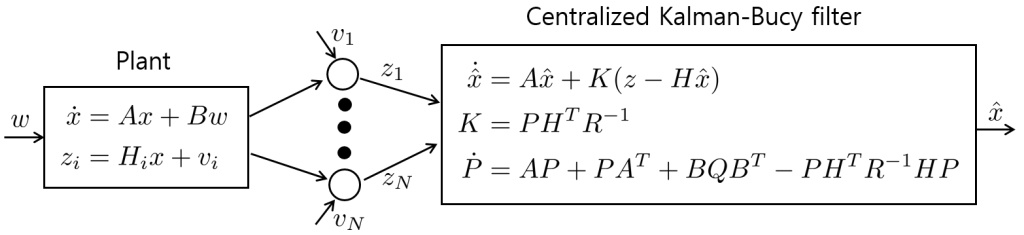

Figure 5.1: Centralized Kalman-Bucy filter.

(c) [BJ68, Thorem 5.1] $P_0 > 0$ ensures that the solution $P(t)$ of (5.1.3b) satisfies $P(t) > 0$ for all $t \geq 0$.

(d) [AM71, Theorem 5.3] $P(t) \to P^*$ as $t \to \infty$.

$\Diamond$

A centralized filter requires communicating the entire measurement vectors to a central node, and the implementation is depicted in Figure 5.1. Although CKBF is theoretically optimal, the CKBF is impractical in large-scale dynamical systems because it has some following disadvantages:

- CKBF requires long-distance communication since the sensors span a large geographical area, *e.g.,* surveillance and monitoring of an environment.
- A centralized scheme results in large latency.
- The centralized network cannot be robust under the malicious attack to the center node, and it will leave severe consequences in the network.

In [HRL88, RDW91], the authors focused on reducing the computational complexity of centralized Kalman filtering by parallelizing computations. However, they require all-to-all communication topology and assume that each subsystem has full knowledge of the whole dynamics.

5.1.2 Kalman-Consensus Filter

In the sensor network, the most fundamental problem was how to develop a distributed algorithm based on some traditional Kalman filtering schemes. A

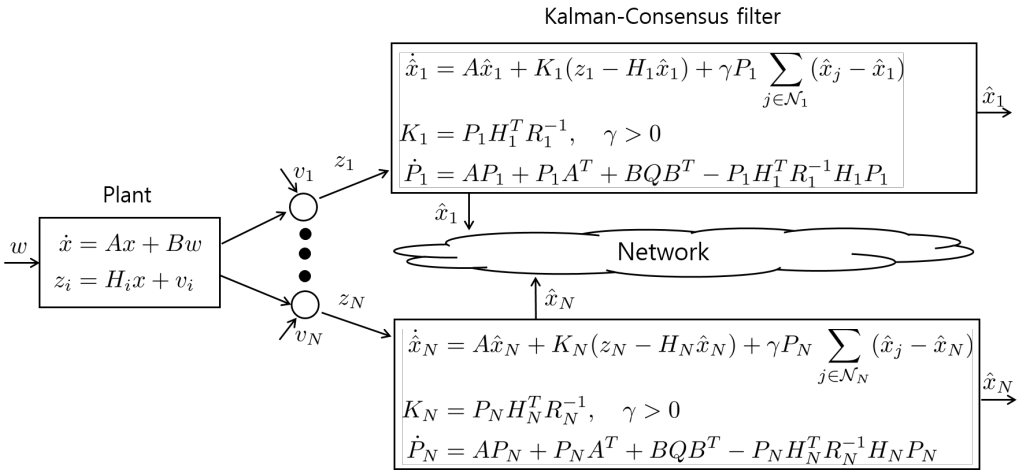

Figure 5.2: Kalman-Consensus filter.

distributed Kalman filter has been proposed by Olfati-Saber in [OS07], which has attracted a lot of attention in the literature.

The distributed Kalman-Bucy filter of [OS07] consists of N nodes, and each node i has the dynamics

$$\dot{\hat{x}}_i = A\hat{x}_i + P_iH_i^TR_i^{-1}(z_i - H_i\hat{x}_i) + \gamma P_i \sum_{j\in\mathcal{N}_i}(\hat{x}_j - \hat{x}_i), \quad \gamma > 0 \tag{5.1.4a}$$

$$\dot{P}_i = AP_i + P_iA^T + BQB^T - P_iH_i^TR_i^{-1}H_iP_i \tag{5.1.4b}$$

with

$$P_i(0) = P_0 > 0, \quad \hat{x}_i(0) = x(0), \quad \forall i \in \mathcal{N} \tag{5.1.4c}$$

where $\hat{x}_i = \mathrm{col}(\hat{x}_i^1, \ldots, \hat{x}_i^n) \in \mathbb{R}^n$ is the i-th estimated state vector of x and the set $\mathcal{N}_i$ is the neighboring nodes of the node i. This is a "distributed" filter, called 'Kalman-Consensus filter (KCF)', because each node i receives the partial measurement z_i only, and communicates the estimates $\hat{x}_j$ with its neighborhood under the communication network. The implementation of KCF can be seen in Figure 5.2.

The KCF estimates the state of plant in two steps: i) in the first step, local Kalman filtering is performed on each sensor node to track the observable state of the target, and ii) in the second step, each sensor node fuses the estimates of all

its neighbors locally to get an improved estimate by using consensus algorithm.

Unfortunately, this idea has a few drawbacks as follows.

- Unless (A, H_i) is observable for all $i \in \mathcal{N}$, some component of the error covariance matrix $P_i(t)$ may diverge that can be shown in Example 5.1.1. Then, this will cause some overflow error in a digital computer and make its implementation hard in practice.

- By the above observation, it is clear that each node maintains different error covariances even if the estimate $\hat{x}_i(t)$ converges to $x(t)$, and the optimal estimation property of the Kalman-Bucy filter is lost, and therefore the matrix $P_i(t)$ does not have the meaning of error covariance anymore.

- The condition (5.1.4c), $\hat{x}_i(0) = x(0)$ for all nodes, is unrealistic for estimation problem. In fact, unless it satisfies the initial conditions, a simulation shows the estimate error indeed diverges (see Example 5.1.2).

Since the boundedness of $P_i(t)$ is guaranteed under the assumption that (A, H_i) is observable, we can observe the divergence property of KCF.

Example 5.1.1. With $A = 0_{2\times 2}$ and $H = B = Q = R = P_0 = I_2$ (H_1 is the first row of H), the solution to the Riccati equation (5.1.4b) for $i = 1$ is

$$P_1 = \begin{bmatrix} 1 & 0 \\ 0 & t+1 \end{bmatrix}$$

The same phenomenon occurs also for the discrete-time version (Algorithm 3 of [OS07]). Consider $A = 2I_4$ and $H = B = Q = R = P_0 = I_4$ (H_i is the i-th row of H) under the cyclic graph (so that the node 2 has its neighbors 1 and 3). Then, it can be seen that Algorithm 3 of [OS07] results in $S_2(k) = \mathrm{diag}(1, 1, 1, 0)$, and so, $P_2(k)$ is diagonal and $p_{i,i}(k)$ $(i = 1, 2, 3)$ converges to $2+\sqrt{5}$ while $p_{4,4}(k)$ diverges as $1, 5, 21, 85, \cdots$, where $p_{i,j}(k)$ is the (i, j) component of $P_2(k)$. $\Diamond$

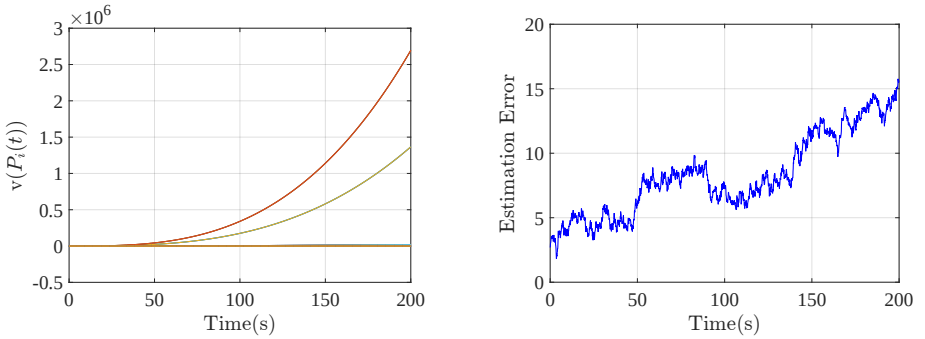

(a) Trajectories of the vectorized error covariance matrices $P_i(t)$.

(b) Filter 5's absolute estimation error of the first state, $|x^1(t) - \hat{x}_5^1(t)|$.

Figure 5.3: Simulation results of KCF with divergent $P(t)$.

Example 5.1.2. Consider the plant with process noise as

$$\begin{aligned}\dot{x} &= \begin{bmatrix} 0 & 1 & 0 & 0 \\ 0 & 0 & 0 & 0 \\ 0 & 0 & 0 & 1 \\ 0 & 0 & -1 & 0 \end{bmatrix} x + \begin{bmatrix} 0 \\ 1 \\ 0 \\ 1 \end{bmatrix} w, \quad w \sim N(0,1), \\ &=: Ax + Bw\end{aligned}$$

and the initial condition $x(0) = \mathrm{col}(0, 1, 0, 1)$. The group of N sensors can partially observe the states of the target with measurement noise; that is,

$$z_i = H_i x + v_i, \quad v_i \sim N(0,1)$$

where

$$H_i = \begin{cases} [1\ 0\ 0\ 0], & 1 \le i \le N/4, \\ [0\ 1\ 0\ 0], & N/4+1 \le i \le N/2, \\ [0\ 0\ 1\ 0], & N/2+1 \le i \le 3N/4, \\ [0\ 0\ 0\ 1], & 3N/4+1 \le i \le N. \end{cases}$$

The plant is not observable by individual sensors, but is observable by all the

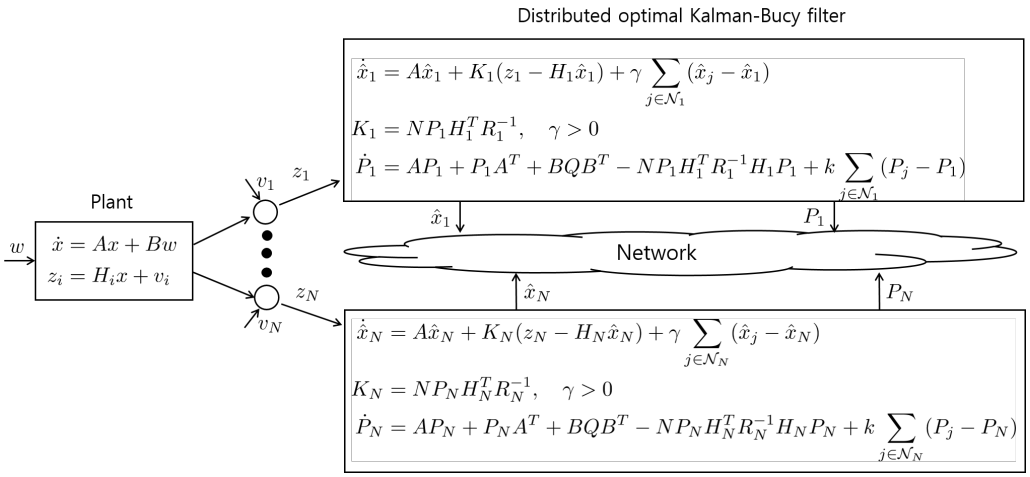

Figure 5.4: Optimal distributed Kalman-Bucy filter.

sensors. Now, the KCF [OS07] is given by (5.1.4) with the initial conditions $\hat{x}_i(0)$ are randomly determined and $P_i(0) = P_0 > 0$ for all $i \in \mathcal{N}$. We assume that the sensors ($N = 12$) are interconnected by the ring topology network and $Q = R_i = 1$ for all $i \in \mathcal{N}$. In Figure 5.3(a), since (A, H_i) is not observable, it is seen that some components of the error covariance matrices $P_i(t)$ actually diverge. In Figure 5.3(b), it is also observed that the estimation error indeed diverges. $\Diamond$

5.2 Design of Optimal Distributed Kalman-Bucy Filter

In this section, we present a modified solution which overcomes all the above drawbacks of the KCF. The proposed optimal distributed Kalman-Bucy filter (O-DKBF) is given by

$$\dot{\hat{x}}_i = A\hat{x}_i + NP_iH_i^TR_i^{-1}(z_i - H_i\hat{x}_i) + \gamma\sum_{j=1}^{N}\alpha_{ij}(\hat{x}_j - \hat{x}_i) \tag{5.2.1a}$$

$$\dot{P}_i = AP_i + P_iA^T + BQB^T - NP_iH_i^TR_i^{-1}H_iP_i + k\sum_{j=1}^{N}\alpha_{ij}(P_j - P_i) \tag{5.2.1b}$$

where $\hat{x}_i \in \mathbb{R}^n$ is the i-th state, $\gamma > 0$ and $k > 0$ represent the coupling strengths, and α_{ij} is the (i, j)-entry of the adjacency matrix of the given network.

Here, the initial conditions $\hat{x}_i(0)$ and $P_i(0) > 0$ can be anything and all differ-

ent. It is noted that the modifications from (5.1.4) are as follows: i) the number of the agents, N, appears in the gains in (5.2.1a) and (5.2.1b), ii) the diffusive coupling gain matrix is changed by I_n in (5.2.1a), and iii) more importantly, the error covariance matrix is communicated in (5.2.1b).

Remark 5.2.1. As seen in Figure 5.4, the communication of error covariance causes more information exchanged between nodes. The amount of information exchanged between two nodes is $2(n+(n+1)n/2) = n^2+3n$. For a cyclic network of N nodes, it becomes $(n^2+3n)N$. On the other hand, if each node is dispersed in location and all the information is gathered by a center to use the CKBF, the information delivered to the center is pN, and the estimated information delivered to each node is nN. Therefore, in terms of the amount of exchanged information, distributed filtering has no benefits over the centralized one. However, in wireless sensor network for example, each node has limited power so that they can only communicate with their neighbors. ◊

Our approach is to view (5.2.1) as a group of "heterogeneous" agents for $i \in \mathcal{N}$. (It is heterogeneous because $H_i^T R_i^{-1} H_i$ is not the same among the agents.) To analyze the behavior of heterogeneous agents, we employ the notion of *averaged dynamics* proposed in Section 3.2. The way to compute the averaged dynamics of (5.2.1b) is to compute the "average of vector fields" of all agents after replacing the state of each agent ($\hat{x}_i$ and P_i in our case) by a common state (say, x_s and S). Then, the dynamics about the common state is the averaged dynamics with its initial condition is also an average of the initial conditions of all agents. (See Section 3.2 for more details.) In our case, by the fact that $(1/N)\sum_{i=1}^N N H_i^T R_i^{-1} H_i = H^T R^{-1} H$, the averaged dynamics is obtained as

$$\begin{aligned}
\dot{x}_s &= Ax_s + SH^T R^{-1} H(x - x_s) + S\sum_{i=1}^N H_i^T R_i^{-1} v_i \\
&= Ax_s + SH^T R^{-1}(z - Hx_s), \qquad (5.2.2a) \\
\dot{S} &= AS + SA^T + BQB^T - S\left(\sum_{i=1}^N H_i^T R_i^{-1} H_i\right) S \\
&= AS + SA^T + BQB^T - SH^T R^{-1} HS \qquad (5.2.2b)
\end{aligned}$$

with the averaged initial conditions (*i.e.,* $x_s(0) = (1/N)\sum_{i=1}^N \hat{x}_i(0)$ and $S(0) = (1/N)\sum_{i=1}^N P_i(0)$). According to Section 3.3, with sufficiently large coupling gains (γ and k in our case), the behavior of multi-agent system (5.2.1) becomes close to the solution of the averaged dynamics (5.2.2). And, fortunately, we note that the averaged dynamics is nothing but the CKBF. However, a few technical assumptions in Chapter 3 are not satisfied for our case, and so, we present an independent analysis in this chapter.

Remark 5.2.2. The averaged dynamics is a conceptual one, and thus, it is natural that the averaged dynamics (5.2.2) is not the same as any of (5.2.1) even when $\hat{x}_i(t) = \hat{x}_j(t)$ and $P_i(t) = P_j(t)$ for all $i, j \in \mathcal{N}$ and $t \geq 0$. $\Diamond$

Remark 5.2.3. (Optimal recovery problem). The above averaged O-DKBF (5.2.2) is the same as the CKBF (5.1.3) for the plant (5.1.1) with a sensing model $z = Hx + v$. It follows from Lemma 5.1.1(c) that there exists the positive definite solution $S^* > 0$ to the algebraic Riccati equation of (5.2.2b), and the error covariance matrix $S(t)$ of (5.2.2) is bounded even when the plant system is neutrally stable or unstable. Thus, $P_i(t) \to S(t)$ as $t \to \infty$ for all $i \in \mathcal{N}$ ensures that $P_i(t) \to S^*$ as $t \to \infty$ for all $i \in \mathcal{N}$ and all $P_i(t)$, $i \in \mathcal{N}$, are bounded even when (A, H_i) is not observable which cannot be guaranteed in KCF (5.1.4). In addition, if $\hat{x}_i(t) \to x_s(t)$ as $t \to \infty$, then we can expect that the proposed filter (5.2.1) can recover the optimality of the centralized Kalman-Bucy filter in the sense that the distributed filter estimate $\hat{x}_i(t)$ and the error covariance matrix $P_i(t)$ converge to $x_s(t)$ and $S(t)$ of the averaged O-DKBF, respectively. $\Diamond$

Remark 5.2.4. An internal model requirement is necessary and sufficient for asymptotically synchronized behavior of heterogeneous agents [WSA11]. It means that without global information of the matrix $H^T R^{-1} H$, it can hardly be obtained that $P_i(t) \to S(t)$ as $t \to \infty$ for all $i \in \mathcal{N}$. In [BFL11], in order to estimate the constant value of $H^T R^{-1} H$ and achieve optimal filtering by distributed scheme, the number of node N and the structure of the network (all the eigenvalues of the Laplacian matrix) are assumed to be known to all filters in advance. In this section, instead of assuming that all filters know the structure of the network in advance, we will show that all $P_i(t)$ approximately converge to $S(t)$ and the

strong coupling makes the trajectories $P_i(t)$ of arbitrarily close to $S(t)$. $\Diamond$

5.2.1 Robustness of Heterogeneous Agents with Locally Lipschitz Nonlinearity

In order to consider the differential Riccati equation (5.2.1b) as a group of heterogeneous multi-agent systems, we need to reformulate the problem for the agent having locally Lipschitz nonlinearity, because Assumption 3.5.1 is not satisfied for the quadratic matrix equation in (5.2.1b).

We recall a group of N dynamic objects (3.5.1) with coupling input (3.5.4) represented by

$$\dot{x}_i = f_i(t, x_i) + k \sum_{j=1}^{N} \alpha_{ij}(x_j - x_i), \quad i \in \mathcal{N}, \tag{5.2.3}$$

where $f_i : [0, \infty) \times \mathbb{R}^n \to \mathbb{R}^n$ is a nonlinear vector valued function, and $x_i \in \mathbb{R}^n$ is the state.

Assumption 5.2.1. (Locally Lipschitz nonlinearity). The function $f_i(t, x_i)$ of the individual system (5.2.3) is bounded with respect to x_i, uniformly in t, continuously differentiable and the Jacobian matrix $[\partial f_i/\partial x_i]$ is bounded on a compact convex set $\Omega \subset \mathbb{R}^n$, uniformly in t; *i.e.*, there exist a non-decreasing function $M : \mathbb{R}_{\geq 0} \to \mathbb{R}_{\geq 0}$ and constant $L > 0$ such that, $\forall a \in \Omega,\ \forall t \geq 0,\ \forall i \in \mathcal{N}$,

$$|f_i(t, a)| \leq M(|a|), \quad \left\| \frac{\partial f_i}{\partial x_i}(t, a) \right\| \leq L. \tag{5.2.4}$$

$\Diamond$

By letting $x := \mathrm{col}(x_1, \ldots, x_N)$ and $f(t, x) := \mathrm{col}(f_1(t, x_1), \ldots, f_N(t, x_N))$, the inequality (5.2.4) leads to

$$|f(t, (1_N \otimes I_n)a)| \leq \sqrt{N} M(|a|), \quad \left\| \frac{\partial f}{\partial x}(t, b) \right\| \leq L \tag{5.2.5}$$

for all $t \geq 0$, $a \in \Omega$, and $b \in \Omega^N \subset \mathbb{R}^{nN}$ where Ω^N is the N-th Cartesian power of the set Ω.

Let $s(t)$ be the solution of the following *averaged dynamics* of the agents (5.2.3)

$$\begin{aligned}\dot{s} &= \frac{1}{N}\sum_{i=1}^{N} f_i(t,s) = \frac{1}{N}(1_N^T \otimes I_n) f\big(t, (1_N \otimes I_n)s\big) \\ &=: \bar{f}(t,s).\end{aligned} \tag{5.2.6}$$

with the averaged initial condition $s(0) = \sum_{i=1}^{N} x_i(0)/N$.

Assumption 5.2.2. The origin $s = 0$ of the averaged dynamics (5.2.6) is a globally exponentially stable equilibrium point. ◊

At a consequence of Assumption 5.2.2, there is a continuously differentiable function $W_1 : [0,\infty) \times \mathbb{R}^n \to \mathbb{R}$ that satisfies the inequalities

$$c_1|s|^2 \le W_1(t,s) \le c_2|s|^2 \tag{5.2.7a}$$

$$\frac{\partial W_1}{\partial t} + \frac{\partial W_1}{\partial s}\bar{f}(t,s) \le -c_3|s|^2 \tag{5.2.7b}$$

$$\left\| \frac{\partial W_1}{\partial s} \right\| \le c_4|s| \tag{5.2.7c}$$

for some positive constants c_1, c_2, c_3, and c_4. In fact, Assumption 5.2.2 is more restrictive than Assumption 3.5.2 in the sense that the origin $s = 0$ is an equilibrium point for (5.2.6), but it is not necessary in (3.5.5). However, it can be seen from [Kha02, Theorem 4.15] that Assumption 3.5.2 implies Assumption 5.2.2, but not vice versa when the origin $s = 0$ is an equilibrium point for (3.5.5).

The following theorem shows the robustness of consensus and synchronization against heterogeneity of multi-agent systems and will play a key role to show the ultimate boundedness of $x_i(t)$.

Theorem 5.2.1. Take $r > 0$ such that $B_r \subset \Omega$. Under Assumptions 5.2.1, 3.1.2, and 5.2.2, there exists a class-$\mathcal{K}$ function σ and for every initial state $x_i(0)$, satisfying $|x_i(0)| \le \sqrt{\underline{c}/(N\bar{c})}r,\ \forall i \in \mathcal{N}$, where $\underline{c} := \min\{c_1, 1/2\}$ and $\bar{c} := \max\{c_2, 1/2\}$, there is $T \ge 0$ such that the solutions of (5.2.3) satisfy

$$|x_i(t)| \le \sigma\left(\frac{1}{k\lambda_2 - L}\right), \quad \forall t \ge T,\ \forall k > \bar{K},\ \forall i \in \mathcal{N}$$

where $\sigma(\chi) := M(0)\sqrt{N\bar{c}\omega(\chi)/\underline{c}}$ and

$$\bar{K} := \max\left\{\frac{3L^2(c_4+1)^2+4c_3L}{4c_3\lambda_2}, \left(\lambda_2\omega^{-1}\left(\frac{\underline{c}^2r^2}{N\bar{c}^2M^2(0)}\right)\right)^{-1}+\frac{L}{\lambda_2}\right\}.$$

In particular, the class-$\mathcal{K}$ function ω is given by

$$\omega(\chi) = \begin{cases} 0, & \chi = 0 \\ \frac{4\chi}{c_3-3a^2\chi}, & 0<\chi\leq\frac{4c_3}{c_3^2+20a^2} \\ \frac{(c_3^2+8a^2)\chi^2}{(c_3-3a^2\chi)^2}, & \frac{4c_3}{c_3^2+20a^2}<\chi<\frac{c_3}{3a^2} \end{cases}$$

where $a := -L(c_4+1)/2$. ◊

Remark 5.2.5. (Semi-global ultimate boundedness). In Theorem 5.2.1, for any a *priori* given (arbitrarily large) compact convex set Ω of the state space, we can find a threshold $\bar{K}$ of the coupling gain k such that the solutions $x_i(t)$ of (5.2.3) can be ultimately bounded with initial condition, $|x_i(0)| \leq \sqrt{\underline{c}/(N\bar{c})}r,\ \forall i \in \mathcal{N}$. Note that r can be arbitrarily large as long as $B_r \subset \Omega$. Therefore, for all initial conditions in some arbitrarily large but compact subset, the solutions of (5.2.3) are semi-globally ultimately bounded. ◊

Proof. The dynamics of the stacked system of (5.2.3) is written as

$$\dot{x} = -k(\mathcal{L}\otimes I_n)x + f(t,x). \tag{5.2.8}$$

By the coordinate transformation in (2.2.1)

$$\xi = \begin{bmatrix}\xi_1 \\ \tilde{\xi}\end{bmatrix} = (W\otimes I_n)x = \begin{bmatrix}\frac{1}{N}1_N^T\otimes I_n \\ R^T\otimes I_n\end{bmatrix}x \tag{5.2.9}$$

where $\tilde{\xi} = \mathrm{col}(\xi_2,\ldots,\xi_N)$, the overall system (5.2.8) is transformed into

$$\begin{aligned}\dot{\xi}_1 &= \left(\frac{1}{N}1_N^T\otimes I_n\right) f\left(t,(1_N\otimes I_n)\xi_1+(Q\otimes I_n)\tilde{\xi}\right) \\ \dot{\tilde{\xi}} &= -k(\Lambda\otimes I_n)\tilde{\xi}+(R^T\otimes I_n)f\left(t,(1_N\otimes I_n)\xi_1+(Q\otimes I_n)\tilde{\xi}\right),\end{aligned} \tag{5.2.10}$$

because $x = (W^{-1} \otimes I_n)\xi = [1_N \otimes I_n, Q \otimes I_n]\xi$. Let a Lyapunov function be

$$V(\xi) = W_1(t, \xi_1) + \frac{1}{2}\tilde{\xi}^T\tilde{\xi},$$

and from (5.2.7a), the Lyapunov function satisfies the following inequality

$$\underline{c}|\xi|^2 \le V(\xi) \le \bar{c}|\xi|^2 \tag{5.2.11}$$

where $\underline{c} = \min\{c_1, 1/2\}$ and $\bar{c} = \max\{c_2, 1/2\}$. The time derivative of V along (5.2.10) becomes

$$\begin{aligned}
\dot{V} = {} & \frac{\partial W_1}{\partial t} + \frac{\partial W_1}{\partial \xi_1}\left[\left(\frac{1}{N}1_N^T \otimes I_n\right) f\left(t, (1_N \otimes I_n)\xi_1\right)\right] \\
& + \frac{\partial W_1}{\partial \xi_1}\left(\frac{1}{N}1_N^T \otimes I_n\right)\left[f\left(t, (1_N \otimes I_n)\xi_1 + (Q \otimes I_n)\tilde{\xi}\right) - f\left(t, (1_N \otimes I_n)\xi_1\right)\right] \\
& - k\tilde{\xi}^T(\Lambda \otimes I_n)\tilde{\xi} + \tilde{\xi}^T(R^T \otimes I_n)\Big[f\big(t, (1_N \otimes I_n)\xi_1 + (Q \otimes I_n)\tilde{\xi}\big) \\
& - f\big(t, (1_N \otimes I_n)\xi_1\big)\Big] + \tilde{\xi}^T(R^T \otimes I_n)\left[f\big(t, (1_N \otimes I_n)\xi_1\big) - f(t, 0)\right] \\
& + \tilde{\xi}^T(R^T \otimes I_n)f(t, 0).
\end{aligned}$$

By the mean-value theorem in Lemma 3.5.1, we obtain

$$\begin{aligned}
\dot{V} = {} & \frac{\partial W_1}{\partial t} + \frac{\partial W_1}{\partial \xi_1}\bar{f}(t, \xi_1) + \frac{\partial W_1}{\partial \xi_1}\left(\frac{1}{N}1_N^T \otimes I_n\right)\frac{\partial f}{\partial x}(t, z)(Q \otimes I_n)\tilde{\xi} \\
& - k\tilde{\xi}^T(\Lambda \otimes I_n)\tilde{\xi} + \tilde{\xi}^T(R^T \otimes I_n)\frac{\partial f}{\partial x}(t, w)(Q \otimes I_n)\tilde{\xi} \\
& + \tilde{\xi}^T(R^T \otimes I_n)\frac{\partial f}{\partial x}(t, (1_N \otimes I_n)q)(1_N \otimes I_n)\xi_1 + \tilde{\xi}^T(R^T \otimes I_n)f(t, 0)
\end{aligned}$$

in which, $z \in \mathbb{R}^{nN}$ and $w \in \mathbb{R}^{nN}$ are some points on the line segment connecting $(1_N \otimes I_n)\xi_1 + (Q \otimes I_n)\tilde{\xi}$ and $(1_N \otimes I_n)\xi_1$, and $q \in \mathbb{R}^n$ is a point on the line segment connecting ξ_1 and 0. Since $x = (1_N \otimes I_n)\xi_1 + (Q \otimes I_n)\tilde{\xi}$ and $\xi_1 = (1_N^T \otimes I_n)x/N$, we have

$$z,\ w \in l\left\{x, \left(\frac{1}{N}1_N 1_N^T \otimes I_n\right)x\right\},\ \text{and } q \in l\left\{\left(\frac{1}{N}1_N^T \otimes I_n\right)x, 0\right\}$$

where $l\{x, y\} := \{\theta x + (1-\theta)y : 0 \le \theta \le 1\}$. By the construction of $l\{x, y\}$ and

the convex property of Ω, it can be easily obtained that

$$x_i \in \Omega,\ \forall i \in \mathcal{N} \quad \Rightarrow \quad z, w, (1_N \otimes I_n)q \in \Omega^N,$$

and it is seen by (5.2.5) that

$$\left\|\frac{\partial f}{\partial x}(t,z)\right\| \le L,\ \left\|\frac{\partial f}{\partial x}(t,w)\right\| \le L,\ \left\|\frac{\partial f}{\partial x}(t,1_N \otimes I_n q)\right\| \le L.$$

Therefore, using (5.2.7) and the fact that $\|Q\| = \sqrt{N}$ and $\|R\| = 1/\sqrt{N}$, it follows that

$$\begin{aligned}
\dot{V} &\le -c_3|\xi_1|^2 + \left\|\frac{\partial W_1}{\partial \xi_1}\right\| \left\|\frac{1_N^T \otimes I_n}{N}\right\| \left\|\frac{\partial f}{\partial x}(t,z)\right\| \|Q \otimes I_n\|\,|\tilde{\xi}| \\
&\quad - k\lambda_2|\tilde{\xi}|^2 + \left\|R^T \otimes I_n\right\| \left\|\frac{\partial f}{\partial x}(t,1_N \otimes I_n q)\right\| \|1_N \otimes I_n\|\,|\xi_1||\tilde{\xi}| \\
&\quad + \left\|R^T \otimes I_n\right\| \left\|\frac{\partial f}{\partial x}(t,w)\right\| \|Q \otimes I_n\|\,|\tilde{\xi}|^2 + \left|(R^T \otimes I_n) f(t,0)\right| |\tilde{\xi}| \\
&\le -c_3|\xi_1|^2 + L(c_4+1)|\xi_1||\tilde{\xi}| - (k\lambda_2 - L)|\tilde{\xi}|^2 + M(0)|\tilde{\xi}| \\
&= -\begin{bmatrix} |\xi_1| \\ |\tilde{\xi}| \end{bmatrix}^T \begin{bmatrix} c_3 & -\frac{L(c_4+1)}{2} \\ -\frac{L(c_4+1)}{2} & k\lambda_2 - L \end{bmatrix} \begin{bmatrix} |\xi_1| \\ |\tilde{\xi}| \end{bmatrix} + M(0)|\tilde{\xi}|.
\end{aligned}$$

With $p = c_3,\ a = -L(c_4+1)/2,\ \kappa := k\lambda_2 - L$ and $\theta(t) := M(0)$, Lemma 3.3.1 can be employed to find the region for $\dot{V} < 0$. By Lemma 3.3.1, it is seen that

$$\dot{V} < -h|\xi|^2, \quad \text{if } |\xi|^2 > M^2(0)\omega(1/\kappa) \tag{5.2.12}$$

for all

$$k > \frac{3L^2(c_4+1)^2}{4c_3\lambda_2} + \frac{L}{\lambda_2} =: k_1.$$

Let Ω_ξ^N be a transformed compact convex set such that

$$\Omega_\xi^N := \{\xi \in \mathbb{R}^{nN} : \xi = (W \otimes I_n)x,\ x \in \Omega^N\}.$$

From the properties of Ω^N, it can be easily shown that Ω_ξ^N is a compact convex

set. Moreover, since $\|W \otimes I_n\| = 1/\sqrt{N}$, it follows that

$$x \in B_r^N := \{x \in \mathbb{R}^{nN} : |x| \leq r\} \;\Rightarrow\; \xi = (W \otimes I_n)x \in B_{r_1}^N$$

where $r_1 := r/\sqrt{N}$. The fact that $B_r \subset \Omega$ ensures that $B_r^N \subset \Omega^N$ and $B_{r_1}^N \subset \Omega_\xi^N$. From the left inequality (5.2.11), we have

$$\xi \in L_V(c) := \{\xi \in \mathbb{R}^{nN} : V(\xi) \leq c\} \;\Rightarrow\; |\xi| \leq \sqrt{\frac{c}{\underline{c}}}$$

Taking $c := \underline{c} r_1^2$ ensures that the level set $L_V(c)$ is in the interior of $B_{r_1}^N$; that is $L_V(c) \subset B_{r_1}^N$. From the right inequality of (5.2.11), it follows that

$$|\xi| \leq \sqrt{\frac{c}{\bar{c}}} \;\Rightarrow\; V(\xi) \leq \bar{c}|\xi|^2 \leq c \;\Leftrightarrow\; \xi \in L_V(c).$$

Thus, taking $r_2 := \sqrt{c/\bar{c}}$ ensures that $B_{r_2}^N \subset L_V(c)$. Note that $B_{r_2}^N$ is the set of initial conditions of ξ and it can be arbitrarily enlarged by increasing r. Now we will find the ultimate bound on ξ. From the left inequality of (5.2.11), we have

$$|\xi| \leq \rho(k) \;\Rightarrow\; V(\xi) \leq \bar{c}\rho^2(k) =: \epsilon(k) \;\Leftrightarrow\; \xi \in L_V(\epsilon(k))$$

where $\rho(k) := M(0)\sqrt{\omega\,(1/\kappa)}$. Consequently, from the left inequality of (5.2.11), we have

$$\xi \in L_V(\epsilon(k)) \;\Leftrightarrow\; V(\xi) \leq \epsilon(k) \;\Rightarrow\; |\xi| \leq \sqrt{\frac{\epsilon(k)}{\underline{c}}}.$$

Therefore, taking $b(k) := \sqrt{\epsilon(k)/\underline{c}}$ ensures that

$$B_{\rho(k)}^N \subset L_V(\epsilon(k)) \subset B_{b(k)}^N.$$

To obtain $B_{b(k)}^N \subset B_{r_2}^N$, we must have $\sqrt{\epsilon(k)/\underline{c}} < \sqrt{c/\bar{c}}$. Thus, if we choose $k > 0$ such that

$$k > \left(\lambda_2 \omega^{-1}\left(\frac{c\underline{c}}{\bar{c}^2 M^2(0)}\right)\right)^{-1} + \frac{L}{\lambda_2} =: k_2,$$

then we can see that the relationship between sets is obtained as

$$B^N_{\rho(k)} \subset L_V(\epsilon(k)) \subset B^N_{b(k)} \subset B^N_{r_2} \subset L_V(c) \subset B^N_{r_1} \subset \Omega^N_\xi.$$

Moreover, from (5.2.12), if $k > \bar{K} = \max\{k_1, k_2\}$, then all trajectories starting in $L_V(c)$ enter $L_V(\epsilon(k))$ within a finite time T. The ultimate bound on ξ can be taken as

$$b(k) = \sqrt{\frac{\bar{c}}{\underline{c}}} M(0) \sqrt{\omega\left(\frac{1}{k\lambda_2 - L}\right)}$$

with every initial state $\xi(0)$ satisfying $|\xi(0)| \leq \sqrt{\underline{c}/(N\bar{c})}r$. It follows from (5.2.9) that

$$|x_i(0)| \leq \sqrt{\frac{\underline{c}}{N\bar{c}}} r, \ \forall i \in \mathcal{N} \ \Rightarrow \ |\xi(0)| \leq \sqrt{\frac{\underline{c}}{N\bar{c}}} r.$$

Finally, since

$$x = (W^{-1} \otimes I_n)\xi = [1_N \otimes I_n, \ Q \otimes I_n]\xi,$$

and by the fact that $\|1_N \otimes I_n, \ Q \otimes I_n\| \leq \sqrt{N}$, we have

$$|x_i| \leq |x| \leq \sqrt{N}|\xi|.$$

Therefore, for any $i \in \mathcal{N}$, there exists $T \geq 0$ (dependent on $x_i(0), \ \forall i \in \mathcal{N}$) such that

$$|x_i(t)| \leq M(0) \sqrt{\frac{N\bar{c}}{\underline{c}} \omega\left(\frac{1}{k\lambda_2 - L}\right)}, \ \forall t \geq T, \tag{5.2.13}$$

if $k > \bar{K}$ and $|x_i(0)| \leq \sqrt{\underline{c}/(N\bar{c})}r, \ \forall i \in \mathcal{N}$. □

5.2.2 Stability Analysis

With proper vectorization, the coupled differential Riccati equation (5.2.1b) can be considered as a heterogeneous multi-agent systems in (5.2.3). The vectoriza-

tions of (5.2.1b) and (5.2.2b) are obtained as

$$\mathrm{v}(\dot{P}_i) = g_i(\mathrm{v}(P_i)) + k\sum_{j=1}^{N}\alpha_{ij}\left(\mathrm{v}(P_j) - \mathrm{v}(P_i)\right) \tag{5.2.14a}$$

$$\mathrm{v}(\dot{S}) = \bar{g}(\mathrm{v}(S)) \tag{5.2.14b}$$

where

$$\begin{aligned} g_i(\mathrm{v}(P_i)) &:= (I_n \otimes A + A \otimes I_n)\,\mathrm{v}(P_i) + \mathrm{v}(BQB^T) - N(I_n \otimes P_i H_i^T R_i^{-1} H_i)\mathrm{v}(P_i), \\ \bar{g}(\mathrm{v}(S)) &:= (I_n \otimes A + A \otimes I_n)\,\mathrm{v}(S) + \mathrm{v}(BQB^T) - (I_n \otimes SH^T R^{-1} H)\mathrm{v}(S). \end{aligned}$$

Since for any $n \times n$ matrix X, $|\mathrm{v}(X)|$ is the same as the Frobenius norm of X, it always holds that $\|X\| \le \|X\|_F = |\mathrm{v}(X)|$. From the fact that $\|I_n \otimes X\| = \|X \otimes I_n\| = \|X\|$ for arbitrary matrix X, we have

$$\begin{aligned} |g_i(\mathrm{v}(X))| &\le \bar{A}|\mathrm{v}(X)| + |\mathrm{v}\left(BQB^T\right)| + N\bar{H}|\mathrm{v}(X)|^2 \\ &=: \bar{M}(|\mathrm{v}(X)|) \end{aligned} \tag{5.2.15}$$

where $\bar{A} := \|I_n \otimes A + A \otimes I_n\|$, $\bar{H} := \max_{i\in\mathcal{N}}\left\{\left\|H_i^T R_i^{-1} H_i\right\|\right\}$. Defining derivatives of matrices with respect to matrices is accomplished by vectorizing the matrices, so $dF(A)/dA$ is considered as $d\mathrm{v}(F(A))/d\mathrm{v}(A)$. Therefore, from the simple product (Theorem 9 in [MN85]), it follows that, for all $\mathrm{v}(X) \in \Omega^n \subset \mathbb{R}^{n^2}$ where Ω^n is the n-th Cartesian power of the set Ω,

$$\begin{aligned} \left\|\frac{\partial g_i}{\partial \mathrm{v}(P_i)}(\mathrm{v}(X))\right\| &\le \bar{A} + 2N\|X\|\left\|H_i^T R_i^{-1} H_i\right\| \\ &\le \bar{A} + 2N\bar{\Omega}\bar{H} =: L \end{aligned} \tag{5.2.16}$$

where $\bar{\Omega} := \max_{\mathrm{v}(X)\in\Omega^n}\{|\mathrm{v}(X)|\}$. Note that L increases as the compact convex set Ω^n enlarges. Now, by letting $x_i(t) := \mathrm{v}(P_i(t)) - \mathrm{v}(S^*)$ and $s(t) := \mathrm{v}(S(t)) - \mathrm{v}(S^*)$,

$\forall i \in \mathcal{N}$, the transformed system can be seen as

$$\begin{aligned}\dot{x}_i &= g_i(x_i + \mathrm{v}(S^*)) + k\sum_{j=1}^{N}\alpha_{ij}\,(x_j - x_i)\\ &=: f_i(x_i) + k\sum_{j=1}^{N}\alpha_{ij}\,(x_j - x_i) \qquad (5.2.17a)\\ \dot{s} &= \bar{g}(s + \mathrm{v}(S^*)) =: \bar{f}(s) \qquad (5.2.17b)\end{aligned}$$

with respect to the bound function M[3] and the constant L in (5.2.16). We note that the origin $s = 0$ is an equilibrium point for (5.2.17b). By using the result of Theorem 5.2.1, we can show the ultimate boundedness of the error covariance matrix.

Lemma 5.2.2. Take $r > 0$ such that $B_r^n := \{x \in \mathbb{R}^{n^2} : |x| \le r\} \subset \Omega^n$. Under Assumptions 5.1.1 and 3.1.2, there exists a class-$\mathcal{K}$ function σ and for every initial state $P_i(0)$ satisfying $\|P_i(0) - S^*\| \le \sqrt{\underline{c}/(nN\bar{c})}r$ and $P_i(0) > 0$, $\forall i \in \mathcal{N}$, there is $T_1 \ge 0$ such that the solutions of the coupled differential Riccati equation (5.2.1b) satisfy

$$\|P_i(t) - S^*\| \le \sigma\left(\frac{1}{k\lambda_2 - L}\right),\ \forall t \ge T_1,\ \forall k > \bar{K},\ \forall i \in \mathcal{N}$$

where $\underline{c}$, $\bar{c}$, $\bar{K}$, and σ are the same as defined in Theorem 5.2.1. ◊

Remark 5.2.6. It follows from the initial condition bound, $\sqrt{\underline{c}/(nN\bar{c})}r$, that the initial condition of $P_i(t)$ seems like it should be located near S^*. However, the initial condition $P_i(0)$ can be any positive definite matrix by increasing the radius r of the ball. As a result, in order to contain the ball B_r^n, the compact convex set Ω^n may need to be enlarged, and thus the bound L of the Jacobian matrix increases as well. Even though the minimal coupling strength $\bar{K}$ increases as the constant L increases, a sufficiently large k ensures that all $P_i(t)$ approximately converge to the solution S^* for all initial conditions. ◊

Proof. In order to use the result of Theorem 5.2.1, we only need to show that the origin $s = 0$ is a globally exponentially stable equilibrium point of the system

[3]The bound function M^* can be obtained from (5.2.15), *i.e.,* for a matirx X, $|f_i(\mathrm{v}(X))| \le \bar{M}(|\mathrm{v}(X) + \mathrm{v}(S^*)|) =: M(|\mathrm{v}(X)|)$

(5.2.17b). We recall here the well-known result in [AM71] as follows.

Consider the equations

$$\begin{bmatrix} \dot{X} \\ \dot{Y} \end{bmatrix} = \begin{bmatrix} -A^T & H^T R^{-1} H \\ BQB^T & A \end{bmatrix} \begin{bmatrix} X \\ Y \end{bmatrix} =: \mathcal{H} \begin{bmatrix} X \\ Y \end{bmatrix} \tag{5.2.18}$$

with initial conditions $X(0) = I$ and $Y(0) = S(0) =: S_0$. Since $S_0 = \sum_{i=1}^{N} P_i(0)/N$, we have $S_0 > 0$. Assumption 5.1.1 and $S_0 > 0$ ensure that the solution $S(t)$ of the averaged differential Riccati equation (5.2.1b) satisfies $S(t) > 0$ for all $t \geq 0$ (Theorem 5.1 in [BJ68]). Then, the solution of (5.2.18) has the property that $X^{-1}(t)$ exists and that $S(t) = Y(t)X^{-1}(t)$.

The matrix $\mathcal{H}$ is the so-called 'Hamiltonian matrix', and it has no imaginary eigenvalue, given Assumption 5.1.1. It follows that if γ is an eigenvalue of $\mathcal{H}$, then so is $-\gamma$ [LS95]. Thus, there exists a real Θ such that $\Theta^{-1}\mathcal{H}\Theta = \text{diag}(-\Gamma, \Gamma)$ where Γ is a block diagonal matrix containing the 1×1 blocks $[\gamma_i]$ with $\gamma_i < 0$, or 2×2 blocks

$$\begin{bmatrix} \gamma_i & \mu_i \\ -\mu_i & \gamma_i \end{bmatrix} \text{ with } \gamma_i < 0.$$

Then, define new matrices $\hat{X}(t)$ and $\hat{Y}(t)$ by

$$\begin{bmatrix} \hat{X} \\ \hat{Y} \end{bmatrix} = \Theta^{-1} \begin{bmatrix} X \\ Y \end{bmatrix}.$$

It follows that

$$\begin{bmatrix} \dot{\hat{X}} \\ \dot{\hat{Y}} \end{bmatrix} = \begin{bmatrix} -\Gamma & 0 \\ 0 & \Gamma \end{bmatrix} \begin{bmatrix} \hat{X} \\ \hat{Y} \end{bmatrix},$$

and therefore,

$$\begin{bmatrix} \hat{X}(0) \\ \hat{Y}(t) \end{bmatrix} = \begin{bmatrix} e^{\Gamma t} & 0 \\ 0 & e^{\Gamma t} \end{bmatrix} \begin{bmatrix} \hat{X}(t) \\ \hat{Y}(0) \end{bmatrix}.$$

From the coordinate transformation, we have

$$I = X(0) = \theta_{11}\hat{X}(0) + \theta_{12}\hat{Y}(0) \tag{5.2.19a}$$

$$S_0 = Y(0) = \theta_{21}\hat{X}(0) + \theta_{22}\hat{Y}(0). \tag{5.2.19b}$$

We multiply (5.2.19a) by S_0, and subtract this from (5.2.19b), then we have $\hat{Y}(0) = D\hat{X}(0)$ where $D := -(\Theta_{22} - S_0\Theta_{12})^{-1}(\Theta_{21} - S_0\Theta_{11})$, and Θ_{ij} is the (i,j)-block of Θ. Now, using $S(t) = Y(t)X^{-1}(t)$, we obtain

$$S(t) = \left(\Theta_{21} + \Theta_{22}e^{\Gamma t}De^{\Gamma t}\right)\left(\Theta_{11} + \Theta_{12}e^{\Gamma t}De^{\Gamma t}\right)^{-1}.$$

It follows from $e^{\Gamma t} \to 0$ as $t \to \infty$, that

$$\lim_{t\to\infty} S(t) = \Theta_{21}\Theta_{11}^{-1} = S^*.$$

Note that the solution $S(t)$ converges to S^* at an exponential rate equal to twice the smallest real part of any eigenvalue of $-\Gamma$ and is independent of the initial condition S_0 as long as $S_0 > 0$. In addition, the exponential convergence of the solution $S(t)$ can be also seen from [CWW94].

Now, we restrict our concern to the convex set of the positive definite matrix which is the interior of the positive semidefinite cone. Then, in this convex set, $S(t)$ is invariant (*i.e.*, $S_0 > 0$ implies $S(t) > 0$ for all $t \geq 0$), and therefore it is seen that the origin $s = \mathrm{v}(S) - \mathrm{v}(S^*) = 0$ is a globally exponentially stable equilibrium point of (5.2.17b) with respect to the convex set of the positive definite matrix. Therefore, the assumptions of Theorem 5.2.1 are hold, and for any initial state $\|P_i(0) - S^*\| \leq \sqrt{\underline{c}/(nN\bar{c})}r,\ \forall i \in \mathcal{N}$, it follows that, $\forall t \geq T_1,\ \forall i \in \mathcal{N}$,

$$\begin{aligned}\|P_i(t) - S^*\| &\leq |\mathrm{v}(P_i(t)) - \mathrm{v}(S^*)| = |x_i(t)| \\ &\leq \sigma\left(\frac{1}{k\lambda_2 - L}\right).\end{aligned}$$

□

Lemma 5.2.2 guarantees that there exist a class-$\mathcal{K}$ function σ and $T_1 \geq 0$ such

that for any $\epsilon/2 > 0$,

$$\|P_i(t) - S^*\| \leq \sigma\left(\frac{1}{k\lambda_2 - L}\right) \leq \frac{\epsilon}{2}, \quad \forall t \geq T_1,\ \forall k > \bar{K},\ \forall i \in \mathcal{N}.$$

Moreover, it follows from the exponential convergence in Lemma 5.2.2 that there exists $T_2 \geq 0$ such that

$$\|S(t) - S^*\| \leq \frac{\epsilon}{2}, \quad \forall t \geq T_2.$$

Thus, combining these two results by triangular inequality with $T := \max\{T_1, T_2\}$, for any $\epsilon > 0$, there is a sufficiently large k such that

$$\|P_i(t) - S(t)\| \leq \epsilon, \quad \forall t \geq T,\ \forall i \in \mathcal{N}.$$

Now, let $\tilde{x}_i = \hat{x}_i - x_s$ be the error of i-th filter with respect to x_s and $\tilde{x}_s = x_s - x$ be the estimation error of the averaged O-DKBF. From the fact that $\hat{x}_j - \hat{x}_i = \tilde{x}_j - \tilde{x}_i$ and thus, by letting $e_i := \mathrm{col}(\tilde{x}_i, \tilde{x}_s)$, the error dynamics of (5.2.1a) and (5.2.2a) can be written as

$$\dot{e}_i = G_i(t)e_i + \gamma \sum_{j=1}^{N} \alpha_{ij}(e_j - e_i) \tag{5.2.20}$$

where

$$G_i(t) := \begin{bmatrix} A - NP_i(t)H_i^T R_i^{-1} H_i & -NP_i(t)H_i^T R_i^{-1} H_i + S(t)H^T R^{-1} H \\ 0 & A - S(t)H^T R^{-1} H \end{bmatrix}.$$

By letting $e := \mathrm{col}(e_1, \ldots, e_N)$, the group dynamics (5.2.20) can be written as[4]

$$\dot{e} = Ge - \gamma(\mathcal{L} \otimes I_{2n})e \tag{5.2.21}$$

where $G := \mathrm{diag}\,(G_1, \ldots, G_N)$. It follows from the definitions of $\tilde{x}_i$ and $\tilde{x}_s$ that the i-th estimation error, $\tilde{e}_i := \hat{x}_i - x$, can be converged to zero (without noise), if $\tilde{x}_i(t) \to 0$ and $\tilde{x}_s(t) \to 0$ as $t \to \infty$.

[4]We dropped the time index of the time-varying matrices for simplicity of notation.

Now, we are ready to apply this result to the main theorem of this chapter with the fact that by the exponential stability result of Lemma 5.1.1(b), there exist positive matrices $\Phi(t)$ and $\Psi(t)$ such that

$$0 < \eta_1 I_n \leq \Phi(t) \leq \eta_2 I_n, \quad 0 < \eta_3 I_n \leq \Psi(t), \quad \forall t \geq 0,$$

which satisfies the differential matrix equality,

$$-\dot{\Phi}(t) = \Phi(t)\left(A - S(t)H^T R^{-1} H\right) + \left(A - S(t)H^T R^{-1} H\right)^T \Phi(t) + \Psi(t), \quad \forall t \geq 0, \tag{5.2.22}$$

where $\eta_1,\ \eta_2$ and η_3 are positive constants.

The following theorem shows that with strong coupling, the estimates of the O-DKBF (5.2.1) asymptotically converge to the state of the plant without noise.

Theorem 5.2.3. (Stability analysis). Consider a plant system (5.1.1) with sensing model (5.1.2) and the O-DKBF (5.2.1). Suppose that every initial state $P_i(0)$ of (5.2.1b) satisfies the assumptions of Lemma 5.2.2. Under Assumptions 5.1.1 and 3.1.2, the origin $\tilde{e}_i = 0,\ \forall i \in \mathcal{N}$ of the estimation error dynamics (without noise) $\tilde{e}_i = \hat{x}_i - x,\ \forall i \in \mathcal{N}$, is globally asymptotically stable if the coupling strengths satisfy that

$$\begin{aligned} \gamma &> \frac{\bar{G}}{\lambda_2} + \frac{\epsilon \bar{G}}{2}\left(2\eta_2 + \frac{1}{\lambda_2}\right) \\ k &> \max\left\{\bar{K}, \left(\bar{\sigma}^{-1}\left(\frac{\eta_3}{16\eta_2 N \bar{H}}\right)\right)^{-1}\right\} \end{aligned} \tag{5.2.23}$$

where $\bar{G} := \max_{t\geq 0}\{\|G(t)\|\}$, $\epsilon > (\bar{G}/\eta_3)\,(2\eta_2 + 1/\lambda_2)$, $\bar{\sigma}\,(1/k) := \sigma\,(1/(k\lambda_2 - L))$, and $\bar{K}$, $\bar{H}$, and σ are the same as defined in Theorem 5.2.1 and Lemma 5.2.2.

$\Diamond$

Remark 5.2.7. As long as the scale and the structure of the network are fixed, the thresholds of the coupling strengths in (5.2.23) are fixed, too. Thus, with γ and k sufficiently large, it can be obtained that all $\hat{x}_i(t) \to x(t)$ as $t \to \infty$. $\Diamond$

Proof. By the coordinate transformation in (2.2.1)

$$\xi = \begin{bmatrix} \xi_1 \\ \tilde{\xi} \end{bmatrix} = (W \otimes I_{2n})e = \begin{bmatrix} \frac{1}{N} 1_N^T \otimes I_{2n} \\ R^T \otimes I_{2n} \end{bmatrix} e$$

where $\tilde{\xi} = \mathrm{col}(\xi_2, \ldots, \xi_N)$, the group dynamics (5.2.21) is transformed into

$$\dot{\xi}_1 = (I_2 \otimes A - SH^T R^{-1} H)\xi_1 + \begin{bmatrix} -\Delta & \Delta \\ 0 & 0 \end{bmatrix} \xi_1 + \left(\frac{1}{N} 1_N^T \otimes I_{2n} \right) G(Q \otimes I_{2n})\tilde{\xi} \tag{5.2.24a}$$

$$\dot{\tilde{\xi}} = -\gamma(\Lambda \otimes I_{2n})\tilde{\xi} + (R^T \otimes I_{2n})G(1_N \otimes I_{2n})\xi_1 + (R^T \otimes I_{2n})G(Q \otimes I_{2n})\tilde{\xi} \tag{5.2.24b}$$

where $\Delta := \sum_{i=1}^N (P_i - S)H_i^T R_i^{-1} H_i$. Now, we use

$$V(\xi_1, \tilde{\xi}) = \xi_1^T (I_2 \otimes \Phi)\xi_1 + \frac{1}{2}\tilde{\xi}^T (\Lambda^{-1} \otimes I_{2n})\tilde{\xi}$$

as a Lyapunov function. By calculating $\dot{V}$, It is seen by (5.2.22) that

$$\begin{aligned}
\dot{V} &= \xi_1^T (I_2 \otimes \dot{\Phi})\xi_1 + \dot{\xi}_1^T (I_2 \otimes \Phi)\xi_1 + \xi_1^T (I_2 \otimes \Phi)\dot{\xi}_1 + \frac{1}{2}\dot{\tilde{\xi}}^T (\Lambda^{-1} \otimes I_{2n})\tilde{\xi} \\
&\quad + \frac{1}{2}\tilde{\xi}^T (\Lambda^{-1} \otimes I_{2n})\dot{\tilde{\xi}} \\
&= -\xi_1^T (I_2 \otimes \Psi)\xi_1 + 2\xi_1^T (I_2 \otimes \Phi) \begin{bmatrix} -\Delta & \Delta \\ 0 & 0 \end{bmatrix} \xi_1 \\
&\quad + 2\xi_1^T (I_2 \otimes \Phi) \left(\frac{1}{N} 1_N^T \otimes I_{2n} \right) G(Q \otimes I_{2n})\tilde{\xi} \\
&\quad - \gamma \tilde{\xi}^T \tilde{\xi} + \tilde{\xi}^T (\Lambda^{-1} R^T \otimes I_{2n})G(1_N \otimes I_{2n})\xi_1 + \tilde{\xi}^T (\Lambda^{-1} R^T \otimes I_{2n})G(Q \otimes I_{2n})\tilde{\xi}.
\end{aligned}$$

The time T_1 and the class-$\mathcal{K}$ function $\bar{\sigma}$ can be found in Lemma 5.2.2, and also from the exponential convergent property in Lemma 5.2.2, there exists $T_2 \geq 0$ such that

$$\|S(t) - S^*\| \leq \frac{\eta_3}{16N\eta_2 \bar{H}}, \quad \forall t \geq T_2.$$

Hence, it follows with $k > \bar{K}$ that

$$\begin{aligned}\|P_i(t) - S(t)\| &\leq \|P_i(t) - S^*\| + \|S^* - S(t)\| \\ &\leq \bar{\sigma}\left(\frac{1}{k}\right) + \frac{\eta_3}{16N\eta_2\bar{H}}, \quad \forall t \geq T = \max\{T_1, T_2\}.\end{aligned} \tag{5.2.25}$$

By Young's inequality and (5.2.25), we have

$$\begin{aligned}\dot{V} &\leq -\xi_1^T(I_2 \otimes \Psi)\xi_1 + 4\|\Phi\| \sum_{i=1}^{N} \|P_i - S\|\|H_i^T R_i^{-1} H_i\||\xi_1|^2 \\ &\quad + \frac{2}{N}\bar{G}\|\Phi\| \left\|1_N^T\right\| \|Q\||\tilde{\xi}||\xi_1| - \gamma|\tilde{\xi}|^2 + \bar{G}\|\Lambda^{-1}\|\|R^T\||1_N||\xi_1||\tilde{\xi}| \\ &\quad + \bar{G}\|\Lambda^{-1}\|\|R^T\|\|Q\||\tilde{\xi}|^2 \\ &\leq -\left\{\frac{3\eta_3}{4} - 4N\eta_2\bar{H}\bar{\sigma}\left(\frac{1}{k}\right) - \frac{\bar{G}}{2\epsilon}\left(2\eta_2 + \frac{1}{\lambda_2}\right)\right\}|\xi_1|^2 \\ &\quad - \left\{\gamma - \frac{\bar{G}}{\lambda_2} - \frac{\epsilon\bar{G}}{2}\left(2\eta_2 + \frac{1}{\lambda_2}\right)\right\}|\tilde{\xi}|^2, \quad \forall t \geq T.\end{aligned}$$

Choosing

$$\begin{aligned}\gamma &> \frac{\bar{G}}{\lambda_2} + \frac{\epsilon\bar{G}}{2}\left(2\eta_2 + \frac{1}{\lambda_2}\right), \\ k &> \max\left\{\bar{K}, \left(\bar{\sigma}^{-1}\left(\frac{\eta_3}{16\eta_2 N\bar{H}}\right)\right)^{-1}\right\},\end{aligned}$$

and $\epsilon > (\bar{G}/\eta_3)\,(2\eta_2 + 1/\lambda_2)$ ensure that $\dot{V}(\xi_1, \tilde{\xi})$ is negative definite. Hence, for a fixed $T \geq 0$, there exist $\beta_1 > 0$ and $\mu_1 > 0$ such that

$$|\xi(t)| \leq \beta_1|\xi(T)|e^{-\mu_1(t-T)}, \quad \forall t \geq T \geq 0. \tag{5.2.26}$$

It means that for each $\epsilon_1 > 0$, there is $\delta_1(\epsilon_1) > 0$ such that

$$|\xi(T)| < \delta_1(\epsilon_1) \quad \Rightarrow \quad |\xi(t)| < \epsilon_1, \quad \forall t \geq T \geq 0. \tag{5.2.27}$$

Let us consider the transformed system (5.2.24) as $\dot{\xi} = \tilde{A}(t)\xi$. Lemma 5.1.1 and Lemma 5.2.2 ensure that $P_i(t)$ and $S(t)$ are bounded for all $i \in \mathcal{N},\ t \geq 0$, and it follows that there exists $\zeta \geq 0$ such that $\|\tilde{A}(t)\| \leq \zeta,\ \forall t \geq 0$. Gronwall-Bellman

inequality to the function $|\xi(t)|$ results in

$$|\xi(t)| \leq |\xi(0)|e^{\zeta t}. \tag{5.2.28}$$

From the inequalities (5.2.26) and (5.2.28), we obtain that

$$|\xi(0)| < \delta_1(\epsilon_1)e^{-\zeta T} \quad \Rightarrow \quad |\xi(T)| < \delta_1(\epsilon_1), \quad \forall t \geq T \geq 0 \tag{5.2.29}$$

Thus, by (5.2.29) and (5.2.27), the equilibrium point $\xi = 0$ is stable. Since for any initial condition, $|\xi(T)|$ is bounded by $|\xi(0)|e^{\zeta T}$, it follows from (5.2.26) that $\xi(t) \to 0$ as $t \to \infty$. Therefore, we conclude that the origin of (5.2.20) is globally asymptotically stable. Since $e = [1_N \otimes I_n,\ Q \otimes I_n]\xi$, due to the fact that $\xi(t) \to 0$ as $t \to \infty$ implies that $e_i(t) \to 0,\ \forall i \in \mathcal{N}$ as $t \to \infty$. Finally, $\tilde{x}_i \to 0,\ \forall i \in \mathcal{N}$ and $\tilde{x}_s \to 0$ as $t \to \infty$ ensure that $\hat{x}_i(t) \to x(t),\ \forall i \in \mathcal{N}$ as $t \to \infty$. □

5.2.3 Flexible Sensor Network

Until now, we proposed the O-DKBF (5.2.1) due to achieve optimality of the CKBF (5.1.3). However, the proposed O-DKBF is not a completely distributed one because the information of the number of nodes N is required. In Theorem 5.2.3, it also be seen that the thresholds, which γ and k should be larger than, are dependent of the number of nodes as well. In this circumstance, it is difficult to deal with the expansion and reduction of the nodes. However, the thresholds can be simply large enough, and so, if one knows the maximum number of nodes, one can compute γ and k that work with any number of nodes below the maximum. So, we then present another type of flexible distributed Kalman-Bucy filter (F-DKBF) in this section; that is,

$$\dot{\hat{x}}_i = A\hat{x}_i + P_i H_i^T R_i^{-1}(z_i - H_i\hat{x}_i) + \gamma \sum_{j=1}^{N} \alpha_{ij}(\hat{x}_j - \hat{x}_i) \tag{5.2.30a}$$

$$\dot{P}_i = AP_i + P_iA^T + BQB^T - P_iH_i^TR_i^{-1}H_iP_i + k\sum_{j=1}^{N}\alpha_{ij}(P_j - P_i). \tag{5.2.30b}$$

Note that the proposed filter (5.2.30) is no more dependent of the number of node N. The averaged distributed Kalman-Bucy filter of (5.2.30) can be obtained as

$$\dot{x}_s = Ax_s + \frac{1}{N}SH^TR^{-1}(z - Hx_s) \tag{5.2.31a}$$

$$\dot{S} = AS + SA^T + BQB^T - \frac{1}{N}SH^TR^{-1}HS \tag{5.2.31b}$$

with the initial conditions $x_s(0) = \sum_{i=1}^{N} \hat{x}_i(0)/N$ and $S(0) = \sum_{i=1}^{N} P_i(0)/N$.

Remark 5.2.8. (Suboptimality problem). Since the averaged F-DKBF (5.2.31) is scaled from R to NR (or R_i to NR_i for all $i \in \mathcal{N}$), the error covariance matrix $S(t)$ of (5.2.31b) does not converge to that of the CKBF (5.1.3). Instead, it converges to the error covariance of (5.1.3) with the noise covariance matrix NR, *i.e.,* $S(t) \to S^*$ as $t \to \infty$ where $S^* > 0$ is the solution to the algebraic Riccati equation of (5.2.31b). Therefore, even if $P_i(t) \to S(t)$ and $\hat{x}_i(t) \to x_s(t)$ as $t \to \infty$ for all $i \in \mathcal{N}$, the proposed F-DKBF (5.2.30) cannot achieve optimality but suboptimality. ◊

As was formulated in Section 5.2.2, a similar approach is used in this section. It follows from the vectorizations of (5.2.30b) and (5.2.31b) that

$$\mathrm{v}(\dot{P}_i) = h_i(\mathrm{v}(P_i)) + k\sum_{j=1}^{N} \alpha_{ij}\left(\mathrm{v}(P_j) - \mathrm{v}(P_i)\right) \tag{5.2.32a}$$

$$\mathrm{v}(\dot{S}) = \bar{h}(\mathrm{v}(S)) \tag{5.2.32b}$$

where

$$h_i(\mathrm{v}(P_i)) := (I_n \otimes A + A \otimes I_n)\,\mathrm{v}(P_i) + \mathrm{v}(BQB^T) - (I_n \otimes P_iH_i^TR_i^{-1}H_i)\mathrm{v}(P_i),$$

$$\bar{h}(\mathrm{v}(S)) := (I_n \otimes A + A \otimes I_n)\,\mathrm{v}(S) + \mathrm{v}(BQB^T) - \left(I_n \otimes \frac{1}{N}SH^TR^{-1}H\right)\mathrm{v}(S).$$

By letting $x_i(t) := \mathrm{v}(P_i(t)) - \mathrm{v}(S^*)$ and $s(t) := \mathrm{v}(S(t)) - \mathrm{v}(S^*)$, $\forall i \in \mathcal{N}$, the

transformed system (5.2.32) can be rewritten as

$$\begin{aligned}\dot{x}_i &= h_i(x_i + \mathrm{v}(S^*)) + k\sum_{j=1}^{N}\alpha_{ij}\,(x_j - x_i)\\ &=: f_i(x_i) + k\sum_{j=1}^{N}\alpha_{ij}\,(x_j - x_i) \qquad (5.2.33a)\\ \dot{s} &= \bar{h}(s + \mathrm{v}(S^*)) =: \bar{f}(s) \qquad (5.2.33b)\end{aligned}$$

with respect to the bound function M and the constant L (which are obtained from (5.2.15) and (5.2.16)) such that

$$\begin{aligned}|f_i(\mathrm{v}(X))| &\le \bar{A}|\mathrm{v}(X) + \mathrm{v}(S^*)| + |\mathrm{v}\left(BQB^T\right)| + \bar{H}|\mathrm{v}(X) + \mathrm{v}(S^*)|^2\\ &=: M(|\mathrm{v}(X)|),\\ \left\|\frac{\partial f_i}{\partial \mathrm{v}(P_i)}(\mathrm{v}(X))\right\| &\le \bar{A} + 2\|X\|\left\|H_i^T R_i^{-1} H_i\right\| \le \bar{A} + 2\bar{\Omega}\bar{H}\\ &=: L, \quad \forall \mathrm{v}(X) \in \Omega^n \subset \mathbb{R}^{n^2}\end{aligned}$$

where $\bar{\Omega} = \max_{\mathrm{v}(X)\in\Omega^n}\{|\mathrm{v}(X)|\}$. Now, by letting $\tilde{x}_i = \hat{x}_i - x_s$ and $e_i := \mathrm{col}(\tilde{x}_i, \tilde{x}_s)$, the error dynamics of can be written as

$$\dot{e}_i = F_i e_i + \gamma\sum_{j=1}^{N}\alpha_{ij}(e_j - e_i) \qquad (5.2.34)$$

where

$$F_i := \begin{bmatrix} A - P_i H_i^T R_i^{-1} H_i & -P_i(t) H_i^T R_i^{-1} H_i + \frac{1}{N} S H^T R^{-1} H \\ 0 & A - \frac{1}{N} S H^T R^{-1} H \end{bmatrix}.$$

By letting $e := \mathrm{col}(e_1, \ldots, e_N)$, the group dynamics can be written as

$$\dot{e} = Fe - \gamma(\mathcal{L} \otimes I_{2n})e \qquad (5.2.35)$$

where $F := \mathrm{diag}\,(F_1, \ldots, F_N)$.

Suboptimal state estimation with the F-DKBF (5.2.30) is shown in the fol-

lowing corollary.

Corollary 5.2.4. Consider a plant system (5.1.1) with sensing model (5.1.2) and the F-DKBF (5.2.30). Suppose that every initial state $P_i(0)$ of (5.2.30b) satisfies the assumptions of Lemma 5.2.2. Under Assumptions 5.1.1 and 3.1.2, the origin $\tilde{e}_i = 0,\ \forall i \in \mathcal{N}$ of the estimation error dynamics (without noise) $\tilde{e}_i = \hat{x}_i - x,\ \forall i \in \mathcal{N}$, is globally asymptotically stable if the coupling strengths satisfy that

$$\begin{aligned} \gamma &> \frac{\bar{F}}{\lambda_2} + \frac{\epsilon \bar{F}}{2}\left(2\eta_2 + \frac{1}{\lambda_2}\right) \\ k &> \max\left\{\bar{K}, \left(\bar{\sigma}^{-1}\left(\frac{\eta_3}{16\eta_2 \bar{H}}\right)\right)^{-1}\right\} \end{aligned} \tag{5.2.36}$$

where $\bar{F} := \max_{t\geq 0}\{\|F(t)\|\}$, and $\bar{K}$, $\bar{H}$, and $\bar{\sigma}$ are the same as defined in Theorems 5.2.1 and 5.2.3. ♢

The proof of Corollary 1 directly follows from Lemma 5.2.2 and Theorem 5.2.3 with R and R_i replaced with NR and NR_i, respectively.

Remark 5.2.9. (Design of flexible network). In (5.2.36), the thresholds of the coupling gains γ and k are dependent on λ_2. As mentioned in Section 2.2, it depends both on the topology of the graph and the number N of the nodes. For example, for the path graph with unit weights, increasing N decreases λ_2 (because $\lambda_2 = 2(1 - \cos(\pi/N))$ in Table 2.1). It means that γ and k may need to be increased when N is increased. In order to deal with the expansion and reduction of scale, we consider the maximum number of nodes. If the number of nodes is bounded above by N^*, then we can consider the worst scenario of the network (path topology with N^* nodes). Under the assumption that the rest parameters are bounded with respect to the worst network and the upper bounds are known, the thresholds can be computed with respect to the worst network. Hence, γ and k can work with any numbers of nodes below N^* and any topology which is connected. ♢

5.3 Simulation Results

In this section, we recall the same sensor network model in Example 5.1.2. Thus, we reconsider the plant system with process noise as

$$\dot{x} = \begin{bmatrix} 0 & 1 & 0 & 0 \\ 0 & 0 & 0 & 0 \\ 0 & 0 & 0 & 1 \\ 0 & 0 & -1 & 0 \end{bmatrix} x + \begin{bmatrix} 0 \\ 1 \\ 0 \\ 1 \end{bmatrix} w, \quad w \sim N(0,1),$$

and the initial condition $x(0) = x_0$. The group of N sensors can partially observe the states of the target with measurement noise; that is,

$$z_i = H_i x + v_i, \quad v_i \sim N(0,1)$$

where

$$H_i = \begin{cases} [1\ 0\ 0\ 0], & 1 \le i \le N/4, \\ [0\ 1\ 0\ 0], & N/4+1 \le i \le N/2, \\ [0\ 0\ 1\ 0], & N/2+1 \le i \le 3N/4, \\ [0\ 0\ 0\ 1], & 3N/4+1 \le i \le N. \end{cases}$$

Note that the plant is controllable and not observable by individual sensors, but observable by all the sensors. The initial condition of the target is given by $x_0 = \mathrm{col}(0,1,0,1)$, and that of the distributed Kalman-Bucy filter $\hat{x}_i(0)$ are randomly determined[5]. Moreover, the initial conditions of the coupled differential Riccati equation are any positive definite matrices; that is $P_i(0) > 0$, $\forall i \in \mathcal{N}$. Noise covariance matrix are the identity matrices, that is, $Q, R_i = 1$ for all $i \in \mathcal{N}$ in this case.

[5]In Example 5.1.2, it is observed that the KCF in [OS07] cannot deal with the randomly determined initial values

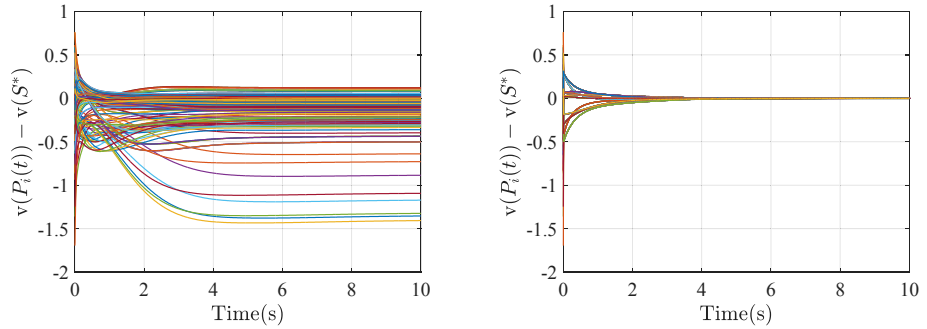

(a) $k = 3$ (b) $k = 50$

Figure 5.5: Trajectories of 4-sensor errors between vectorized error covariance matrices $P_i(t)$ of O-DKBF and the vectorized solution S^* to the algebraic Riccati equation of CKBF. $\mathrm{v}(P_i(t)) - \mathrm{v}(S^*)$ are depicted as solid curves.

5.3.1 Optimal Recovery

We assume that the sensors ($N = 12$) are interconnected by the ring topology network. In order to evaluate the performance of the proposed algorithms, we compare the estimation error of the state for the following three kinds of Kalman-Bucy filters: i) CKBF, ii) O-DKBF, and iii) F-DKBF.

The effect of strong coupling k is seen rather clearly by comparing Figure 5.5(a) with 5.5(b) and Figure 5.6(a) with 5.6(b), respectively. It is observed that the strong coupling k makes the entries of the error covariance matrix $P_i(t)$ of O-DKBF in (5.2.1) close to the solution S^* of the algebraic Riccati equation of CKBF and the level of estimation error of O-DKBF become lower. Thus, it can be seen from the simulation that O-DKBF can achieve the optimality of the CKBF when $k \to \infty$. In Figure 5.6, it is also observed that F-DKBF yields a larger estimation error than O-DKBF because the error covariance matrix of F-DKBF cannot approximately converge to that of CKBF even when $k \to \infty$.

5.3.2 Various Network Topologies

In this section, we simulate the case of various network topologies including expansion and reduction of scale. Here, we assume that the maximum number of

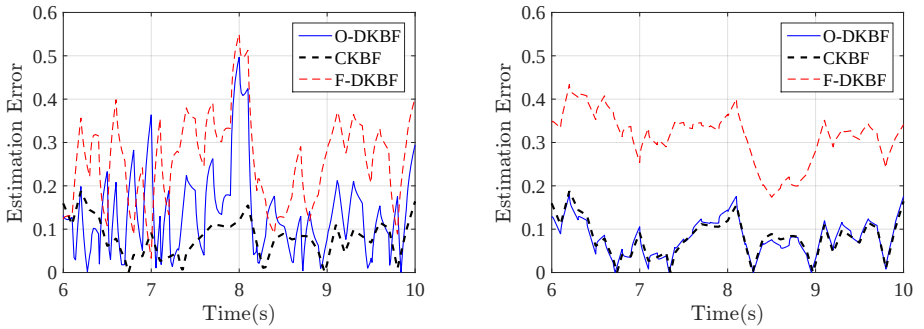

(a) $\gamma = 10$, $k = 3$ (b) $\gamma = 10$, $k = 50$

Figure 5.6: A comparison of filter 3's absolute estimation error of the first state, $|x^1(t) - \hat{x}_3^1(t)|$, between three different Kalman-Bucy filters. Estimation error of CKBF is depicted as black thick dashed curve. O-DKBF and F-DKBF are given as the blue thin solid curve and the red thin dashed curve, respectively.

nodes is $N^* = 12$. As mentioned in Remark 5.2.9, the worst network with respect to N^* is a path topology with 12 nodes. In this case, the algebraic connectivity of the graph is $\lambda_2 = 2(1 - \cos(\pi/12))$, and thus the thresholds of γ and k can be determined with respect to λ_2 and N^*. To see the effect of flexible sensor network, we compare 4 cases of different communication networks with F-DKBF: i) path topology with $N = 12$, ii) path topology with $N = 4$, iii) all-to-all topology with $N = 12$, and iv) all-to-all topology with $N = 4$. We note that path and all-to-all topologies are extreme cases of connected network.

It is observed from Figure 5.7(a) that even though we consider the worst network topology, the proposed F-DKBF can estimate the states of the plant with $\gamma = 10$ and $k = 50$. The result of expansion and reduction of scale is seen by comparing Figure 5.7(a) with (b), and (c) with (d), respectively. Furthermore, by comparing (a) with (c), and (b) with (d), it is seen that the F-DKBF is robust against various network topologies which are connected.

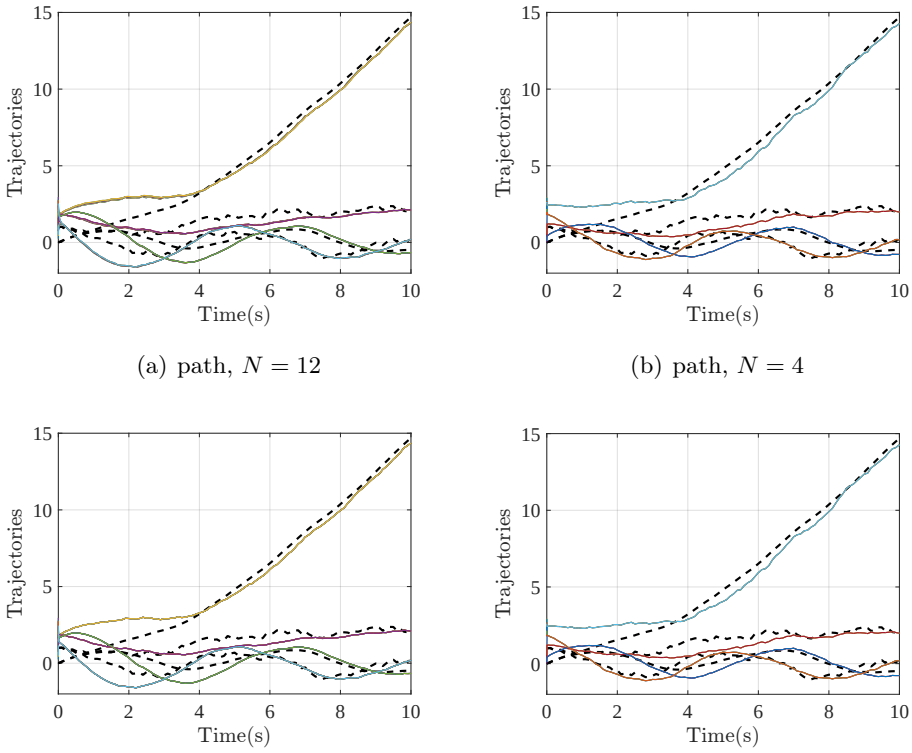

(a) path, $N = 12$

(b) path, $N = 4$

(c) all-to-all, $N = 12$

(d) all-to-all, $N = 4$

Figure 5.7: Trajectories $\hat{x}_i(t)$ of N-sensor network with F-DKBF which have coupling strength $\gamma = 10$ and $k = 50$ are depicted as solid curves, and the trajectory $x(t)$ of plant system is given as the black dashed curve.

Chapter 6

Conclusions

6.1 Summary and Discussion

We started this dissertation with the observation that the consensus and synchronization are everywhere and the robustness is a very significant property in consensus and synchronization problems. In view of this, the objectives of this dissertation was to contribute to an improved analysis theoretic understanding of robustness underlying consensus and synchronization.

The problems of consensus and synchronization are dealt with the diffusive couplings between agents which is the phenomena occurring consecutively in nature. In order to effectively handle the diffusive coupling, some definitions and results of algebraic graph theory are presented in Chapter 2. By the proposed transformation, we can see that the solvability of the consensus and synchronization problems result in the stabilizability problem of certain $(N-1)$ subsystems.

Throughout this dissertation, we have considered the robustness of multi-agent systems, which has inherent heterogeneities from the nature. Averaged dynamics is the most important notion to deal with heterogeneous multi-agent systems. For this reason, the averaged dynamics constituted the main theme in this dissertation. In Chapter 3, the group behavior of the heterogeneous multi-agent systems can be represented by the averaged dynamics under strong coupling condition. Moreover, the averaging effect in the averaged dynamics ensures that a large number of agent enhances the robustness of the group behavior against randomly determined variations, in Chapter 4. As stated in Chapter 5, distributed

sensor network is the one of the most important application area to use the concept of the averaged dynamics. By using this, we recovered the optimality of the centralized Kalman-Bucy filter in distributed sense.

In Chapter 3, we found out that strong coupling is the one of two main ingredients in robustness of diffusively connected multi-agent systems against heterogeneities. In particular, all trajectories of the agents converge (approximately) to that of averaged dynamics, and thus the error are ultimately bounded by the class-$\mathcal{K}$ function of coupling gain k. Another ingredient in robustness against the heterogeneities from the random variations was a large number of agents. In Chapter 4, we focused on the robustness of the averaged dynamics, and therefore we presented the notion of expected averaged dynamics. Finally, we showed that strong coupling and a large number of agents both enhance robustness of the networked group behavior.

A framework for achieving optimal filtering of distributed sensor network has been proposed in Chapter 5, when the sensors can obtain the partial state (not observable) of the plant and exchange the estimations through the network. In order to achieve optimal estimation, we presented the design and analysis of the distributed Kalman-Bucy filter and proved that strong coupling enforces the trajectories of each error covariance matrix tend to that of the centralized Kalman-Bucy filter by considering the averaged distributed Kalman-Bucy filter. Flexible sensor network was implemented by completely distributed Kalman-Bucy filter which can achieve the suboptimality.

Throughout this dissertation, we considered a general nonautonomous multi-agent system model which has Lipschitz nonlinearity. In Chapters 3 and 4, the function $f_i(t, x_i)$ of the individual system is globally Lipschitz in x_i, and locally Lipschitz nonlinearity was dealt with in Chapter 5. Therefore, LTI and LTV with bounded system matrix are the special cases of this system.

6.2 Further Issues

Some further issues regarding the topics of this dissertation are listed as follows.

i) One of the main assumptions of this dissertation is that the communication

network is constrained to be fixed, undirected, and unweighted. Researches on the general network model are further studies, including time-varying, directed, and weighted graph model [Kim12, WSA11], and so on. In particular, if we consider the concept of *uniformly connectedness* [Mor05] of a time-varying graph, then we can deal with the situation when the agents leave and join the group. In this case, the averaged dynamics cannot represent the group behavior any more, since the collective behavior is determined by the network structure, *e.g.,* leader-follow topology, weighted averaged consensus, and so on.

ii) The other main assumption is the stability of the averaged dynamics. In order to show that the trajectories of all agents converge approximately to that of averaged dynamics, the global stability condition, (*e.g,* contraction property, or negative definiteness of the Jacobian matrix, etc), was required in this dissertation. However, some oscillator model, including Van der Pol oscillator, cannot satisfy this global stability assumption. In [WS05], semi-contraction property has been proposed, and thus the authors proved that two coupled identical Van der Pol oscillators are synchronized under strong coupling. It may be very interesting to carry this idea over to stability of the averaged dynamics. Another extension of the assumption in averaged dynamics may concern the incremental properties such as incremental stability [Ang02], incremental dissipativity [LHZ14], and so on.

iii) In Chapter 4, we considered the deterministic system which cannot guarantee the stochastic variations, *e.g.,* white Gaussian noise. It means that once the random variables are drawn (or, realized) when the system is created, it remains deterministic. Thus, it is natural to expand the system dynamics and consider stochastic differential equation.

iv) Throughout this dissertation, state diffusive coupling is considered. However, it might be interesting to ask what are the distinctive features of different coupling mechanisms and how do these features affect the results presented in this dissertation. Usually, it is difficult to achieve the consensus and synchronization via output diffusive coupling [SSB09, KSS11, Wie10].

They presented diffusive couplings extended by dynamic compensators in order to overcome various limitations inherent to static diffusive couplings, and thereby allowing for increased system and topological complexity of the network.

v) In Chapter 5, the proposed distributed Kalman-Bucy filter causes more communication bandwidth than Kalman-Consensus filter in [OS07], because it needs the diffusive coupling of the error covariance matrix. From the vectorization of the error covariance matrix, the additional amount of information exchanged between two nodes is $2n^2$. In fact, for a symmetric matrix the vectorized vector contains more information than is strictly necessary. In this case, half-vectorization is sometimes more useful than the vectorization. Since the error covariance matrix is symmetric, the additional amount of information is $n(n+1)$ by half-vectorization.

APPENDIX

A.1 Ultimate boundedness lemma in Section 3.3.

Claim: Let

$$\rho_\kappa(x,y) = -\begin{bmatrix}|x|\\|y|\end{bmatrix}^T \begin{bmatrix}p & a\\ a & \kappa\end{bmatrix}\begin{bmatrix}|x|\\|y|\end{bmatrix} + \theta(t)|y|$$

with $x \in \mathbb{R}^l$, $y \in \mathbb{R}^m$, $p > 0$, $\theta(t) \geq 0$, and a is a constant. Then, there are a class-$\mathcal{K}$ function r and a positive number c such that

$$\rho_\kappa(x,y) \leq -c(|x|^2 + |y|^2) \quad \text{if } |x|^2 + |y|^2 > \theta^2(t) r(1/\kappa)$$

for all $\kappa > 3a^2/p$.

Proof. With $\kappa > 3a^2/p$, note that

$$\begin{aligned}
&\rho_\kappa(x,y) + \frac{p}{2}|x|^2 + \frac{a^2}{p}|y|^2 \\
&= -p|x|^2 - 2a|x||y| - \kappa|y|^2 + \theta(t)|y| + \frac{p}{2}|x|^2 + \frac{a^2}{p}|y|^2 \\
&= -\frac{p}{2}\left(|x| + \frac{2a}{p}|y|\right)^2 - \left(\kappa - \frac{3a^2}{p}\right)|y|^2 + \theta(t)|y| \\
&= -\frac{p}{2}X^2 - \delta(\kappa)|y|^2 + \theta(t)|y| = -\delta(\kappa)\left(\frac{p}{2\delta(\kappa)}X^2 + |y|^2\right) + \theta(t)|y| \\
&\leq -\delta(\kappa)|Y_\kappa|^2 + \theta(t)|Y_\kappa|
\end{aligned}$$

where $X := |x| + (2a/p)|y|$, $\delta(\kappa) := \kappa - 3a^2/p$, and $Y_\kappa := [\sqrt{p/2\delta(\kappa)}X, |y|]^T$. The last inequality holds because $|Y_\kappa| \geq |y|$. Therefore, it follows that if $|Y_\kappa| \geq$

$\theta(t)/\delta(\kappa)$, then $\rho_k(x,y) \leq -c(|x|^2+|y|^2)$ with $c := \min\{p/2, a^2/p\}$. Now, it is seen that

$$|x|^2+|y|^2 = \left(X - \frac{2a}{p}|y|\right)^2 + |y|^2 \leq 2X^2 + \frac{8a^2}{p^2}|y|^2 + |y|^2$$
$$\leq \max\left\{\frac{4\delta(\kappa)}{p}, \frac{8a^2}{p^2}+1\right\}\left(\frac{p}{2\delta(\kappa)}X^2 + |y|^2\right) =: \eta(\kappa)|Y_\kappa|^2.$$

With $\eta(\kappa)/\delta^2(\kappa)$ being monotonically decreasing to zero as $\kappa \to \infty$ for $\kappa > 3a^2/p$, define a class-$\mathcal{K}$ function $r : [0, p/3a^2) \to [0,\infty)$ as follows:

$$r(\chi) = \begin{cases} 0, & \chi = 0 \\ \frac{\eta(1/\chi)}{\delta^2(1/\chi)}, & 0 < \chi < \frac{p}{3a^2} \end{cases} = \begin{cases} 0 & \chi = 0 \\ \frac{4\chi}{p-3a^2\chi}, & 0 < \chi \leq \frac{4p}{p^2+20a^2} \\ \frac{(p^2+8a^2)\chi^2}{(p-3a^2\chi)^2}, & \frac{4p}{p^2+20a^2} < \chi < \frac{p}{3a^2} \end{cases}$$

in which, if $a = 0$, the number $p/3a^2$ is considered as ∞.

Therefore, if $|x|^2+|y|^2 > \theta^2(t) r(1/\kappa)$, then

$$|Y_\kappa|^2 \geq \frac{1}{\eta(\kappa)}\left(|x|^2+|y|^2\right) > \frac{\theta^2(t)}{\eta(\kappa)} r\left(\frac{1}{\kappa}\right) \geq \frac{\theta^2(t)}{\eta(\kappa)}\frac{\eta(\kappa)}{\delta^2(\kappa)} = \left(\frac{\theta(t)}{\delta(\kappa)}\right)^2$$

which completes the proof. □

BIBLIOGRAPHY

[Aiz76] Y. Aizawa. Synergetic approach to the phenomena of mode-locking in nonlinear systems. *Progress of Theoretical Physics*, 56(3):703–716, 1976.

[AM71] B. D. O. Anderson and J. B. Moore. *Linear optimal control*, volume 197. Prentice-Hall Englewood Cliffs, 1971.

[Ang02] D. Angeli. A lyapunov approach to incremental stability properties. *IEEE Transactions on Automatic Control*, 47(3):410–421, 2002.

[Apo74] T. M. Apostol. *Mathematical analysis*. Addison–Wesley Publishing Company, 1974.

[ASSC02] I. F Akyildiz, W. Su, Y. Sankarasubramaniam, and E. Cayirci. A survey on sensor networks. *IEEE Communications magazine*, 40(8):102–114, 2002.

[AWJ+15] J. H. Abel, L. A. Widmer, P. C. John, J. Stelling, and F. J. Doyle. A coupled stochastic model explains differences in cry knockout behavior. *IEEE Life Sciences Letters*, 1(1):3–6, 2015.

[AYSS08] T. C. Aysal, M. E. Yildiz, A. D. Sarwate, and A. Scaglione. Broadcast gossip algorithms: Design and analysis for consensus. In *Proceedings of the 47th IEEE Conference on Decision and Control*, pages 4843–4848, 2008.

[BFL11] H. Bai, R. A. Freeman, and K. M. Lynch. Distributed kalman filtering using the internal model average consensus estimator. In *Pro-*

ceedings of the 2011 American Control Conference, pages 1500–1505, 2011.

[Big93] N. Biggs. *Algebraic Graph Theory*. Cambridge, 2nd ed. edition, 1993.

[BJ68] R. S. Busy and P. D. Joseph. Filtering for stochastic process with applica tion to guidance. *NY: Interscience Publishers*, 1968.

[Bol02] B. Bollobas. *Modern Graph Theory*. Graduate Texts in Mathematics. Springer, corrected edition, 2002.

[Bon76] J. A. Bondy. *Graph Theory With Applications*. North Holland, 1976.

[BS11] J. Bouvrie and J. J. Slotine. Synchronization and redundancy: implications for robustness of neural learning and decision making. *Neural computation*, 23(11):2915–2941, 2011.

[Buc88] J. Buck. Synchronous rhythmic flashing of fireflies. ii. *Quarterly review of biology*, pages 265–289, 1988.

[CHZ02] M. Chu, H. Haussecker, and F. Zhao. Scalable information-driven sensor querying and routing for ad hoc heterogeneous sensor networks. *International Journal of High Performance Computing Applications*, 16(3):293–313, 2002.

[CMKB02] J. Cortes, S. Martinez, T. Karatas, and F. Bullo. Coverage control for mobile sensing networks. In *Proceedings of the IEEE International Robotics and Automation*, volume 2, pages 1327–1332, 2002.

[CWW94] F. M. Callier, J. Winkin, and J. L. Willems. Convergence of the time-invariant riccati differential equation and lq-problem: mechanisms of attraction. *International journal of control*, 59(4):983–1000, 1994.

[DA07] N. M. M. De Abreu. Old and new results on algebraic connectivity of graphs. *Linear algebra and its applications*, 423(1):53–73, 2007.

[DB12] F. Dorfler and F. Bullo. Synchronization and transient stability in power networks and nonuniform kuramoto oscillators. *SIAM Journal on Control and Optimization*, 50(3):1616–1642, 2012.

[DDBL15] P. DeLellis, M. Di Bernardo, and D. Liuzza. Convergence and synchronization in heterogeneous networks of smooth and piecewise smooth systems. *Automatica*, 56:1–11, 2015.

[DdBR11] P. DeLellis, M. di Bernardo, and G. Russo. On QUAD, Lipschitz, and Contracting Vector Fields for Consensus and Synchronization of Networks. *IEEE Transactions on Circuits and Systems I: Regular Papers*, 58(3):576–583, 2011.

[DdG09] P. DeLellis, M. diBernardo, and F. Garofalo. Novel decentralized adaptive strategies for the synchronization of complex networks. *Automatica*, 45(5):1312–1318, 2009.

[Die06] R. Diestel. *Graph theory*. Graduate Texts in Mathematics. Springer, 3rd edition, 2006.

[DW05] H. F. Durrant-Whyte. Data fusion in sensor networks. In *IPSN*, volume 2, 2005.

[EGHK99] D. Estrin, R. Govindan, J. Heidemann, and S. Kumar. Next century challenges: Scalable coordination in sensor networks. In *Proceedings of the 5th annual ACM/IEEE International conference on Mobile computing and networking*, pages 263–270. ACM, 1999.

[Fie73] M. Fiedler. Algebraic connectivity of graphs. *Czechoslovak mathematical journal*, 23(2):298–305, 1973.

[Fie89] M. Fiedler. Laplacian of graphs and algebraic connectivity. *Banach Center Publications*, 25(1):57–70, 1989.

[FM04] J. A. Fax and R. M. Murray. Information Flow and Cooperative Control of Vehicle Formations. *IEEE Transactions on Automatic Control*, 49(9):1465–1476, 2004.

[FOSPP06] E. Franco, R. Olfati-Saber, T. Parisini, and M. M. Polycarpou. Distributed fault diagnosis using sensor networks and consensus-based

filters. In *Proceedings of the 45th IEEE Conference on Decision and Control*, pages 386–391, 2006.

[FYL06] R. A. Freeman, P. Yang, and K. M. Lynch. Stability and convergence properties of dynamic average consensus estimators. In *Proceedings of the 45th IEEE Conference on Decision and Control*, 2006.

[FZ09] F. Fagnani and S. Zampieri. Average consensus with packet drop communication. *SIAM Journal on Control and Optimization*, 48(1):102–133, 2009.

[GDW94] S. Grime and H. F. Durrant-Whyte. Data fusion in decentralized sensor networks. *Control engineering practice*, 2(5):849–863, 1994.

[Geo13] J. George. Networked sensing and distributed kalman-bucy filtering based on dynamic average consensus. In *Proceedings of the IEEE Distributed Computing in Sensor Systems*, pages 175–182, 2013.

[GR01] C. Godsil and G. Royle. *Algebraic Graph Theory*. Graduate Texts in Mathematics 207. Springer-Verlag New York, 1 edition, 2001.

[Gro04] L. Gross. *Handbook of graph theory*. Discrete mathematics and its applications. CRC Press, 1 edition, 2004.

[Hal97] J. K. Hale. Diffusive coupling, dissipation, and synchronization. *Journal of Dynamics and Differential Equations*, 9(1):1–52, 1997.

[HBSM04] S. Hubbard, P. Babak, S. T. Sigurdsson, and K. G. Magnússon. A model of the formation of fish schools and migrations of fish. *Ecological Modelling*, 174(4):359–374, 2004.

[HC06] D. J. Hill and G. Chen. Power systems as dynamic networks. In *Proceedings of the IEEE International Symposium on Circuits and Systems*, pages 722–725, 2006.

[HHK10] S. Y. Ha, T. Ha, and J. H. Kim. On the complete synchronization of the kuramoto phase model. *Physica D: Nonlinear Phenomena*, 239(17):1692–1700, 2010.

[HJ12] R. A. Horn and C. R. Johnson. *Matrix analysis*. Cambridge university press, 2012.

[Hol06] M. J. Holroyd. *Synchronizability and connectivity of discrete complex systems*. PhD thesis, Citeseer, 2006.

[HRL88] H. R. Hashemipour, S. Roy, and A. J. Laub. Decentralized structures for parallel kalman filtering. *IEEE Transactions on Automatic Control*, 33(1):88–94, 1988.

[IM08] E. M. Izhikevich and J. Moehlis. Dynamical systems in neuroscience: The geometry of excitability and bursting. *SIAM review*, 50(2):397, 2008.

[IMC14] A. Isidori, L. Marconi, and G. Casadei. Robust output synchronization of a network of heterogeneous nonlinear agents via nonlinear regulation theory. *IEEE Transactions on Automatic Control*, 59(10):2680–2691, 2014.

[JLM03] A. Jadbabaie, J. Lin, and A. S. Morse. Coordination of groups of mobile autonomous agents using nearest neighbor rules. *IEEE Transactions on Automatic Control*, 48(6):988–1001, 2003.

[JMB05] S. Janson, M. Middendorf, and M. Beekman. Honeybee swarms: how do scouts guide a swarm of uninformed bees? *Animal Behaviour*, 70(2):349–358, 2005.

[KA15] B. Y. Kim and H. S. Ahn. Consensus of multi-agent systems with switched linear dynamics. In *Proceedings of the 10th Asian Control Conference*, pages 1–6, 2015.

[Kha02] H. K. Khalil. *Nonlinear systems*, volume 3rd edition. Prentice hall, 2002.

[KHHPB07] J. Kim, P. Heslop-Harrison, I. Postlethwaite, and D. G. Bates. Stochastic noise and synchronisation during dictyostelium aggregation make camp oscillations robust. *PLoS Comput Biol*, 3(11):e218, 2007.

[Kim12] H. Kim. *Consensus and synchronization among output-coupled identical and non-identical linear systems through fast switching network.* PhD thesis, Ph. D. thesis, Seoul National University, Department of Electrical Engineering and Computer Science, South Korea, 2012.

[KKYS13] J. Kim, J. S. Kim, J. Yang, and H. Shim. Robustness of synchronization in heterogeneous multi-agent systems. In *Proceedings of the 12th European Control Conference*, pages 3821–3826, 2013.

[KS15] J. Kim and H. Shim. Robust Synchronization for High-Order Heterogeneous Multi-Agent Systems. In *Proceedings of the First International Symposium on Swarm Behavior and Bio-Inspired Robotics*, pages 293–294, 2015.

[KSBS13] H. Kim, H. Shim, J. Back, and J. H. Seo. Consensus of output-coupled linear multi-agent systems under fast switching network: averaging approach. *Automatica*, 49(1):267–272, 2013.

[KSS11] H. Kim, H. Shim, and J. H. Seo. Output consensus of heterogeneous uncertain linear multi-agent systems. *IEEE Transactions on Automatic Control*, 56(1):200–206, 2011.

[Kur75] Y. Kuramoto. Self-entrainment of a population of coupled non-linear oscillators. In *Proceedings of the International Symposium on Mathematical Problems in Theoretical Physics*, pages 420–422. Springer, 1975.

[KYKS12] J. Kim, J. Yang, J. S. Kim, and H. Shim. Practical consensus for heterogeneous linear time-varying multi-agent systems. In *Proceedings of the 12th IEEE International Control, Automation and Systems*, pages 23–28, 2012.

[KYS+] J. Kim, J. Yang, H. Shim, J. S. Kim, and J. H. Seo. Robustness of Synchronization of Heterogeneous Agents by Strong Coupling and A Large Number of Agents. *IEEE Transactions on Automatic Control.*

[LHZ14] T. Liu, D. J. Hill, and J. Zhao. Incremental-dissipativity-based output synchronization of dynamical networks with switching topology. In *Proceedings of the 53rd IEEE Conference on Decision and Control*, pages 4591–4596, 2014.

[Lin06] Z. Lin. *Coupled dynamic systems: From structure towards stability and stabilizability*. PhD thesis, University of Toronto, 2006.

[LJ08] P. Lin and Y. Jia. Average consensus in networks of multi-agents with both switching topology and coupling time-delay. *Physica A: Statistical Mechanics and its Applications*, 387(1):303–313, 2008.

[LS95] F. L. Lewis and V. L. Syrmos. *Optimal control*. John Wiley & Sons, 1995.

[LS04] A. N. Langville and W. J. Stewart. The kronecker product and stochastic automata networks. *Journal of computational and applied mathematics*, 167(2):429–447, 2004.

[LWK+07] A. C. Liu, D. K. Welsh, C. H. Ko, H. G. Tran, E. E. Zhang, A. A Priest, E. D. Buhr, O. Singer, K. Meeker, I. M. Verma, et al. Intercellular coupling confers robustness against mutations in the scn circadian clock network. *Cell*, 129(3):605–616, 2007.

[LXP07] F. L. Lewis, L. Xie, and D. Popa. *Optimal and robust estimation: with an introduction to stochastic control theory*, volume 29. CRC press, 2007.

[ME10] M. Mesbahi and M. Egerstedt. *Graph Theoretic Methods in Multiagent Networks (Princeton Series in Applied Mathematics)*. Princeton Series in Applied Mathematics. Princeton University Press, 2010.

[Mer95] R. Merris. A survey of graph laplacians. *Linear and Multilinear Algebra*, 39(1-2):19–31, 1995.

[MMS91] P. C. Matthews, R. E. Mirollo, and S. H. Strogatz. Dynamics of a large system of coupled nonlinear oscillators. *Physica D: Nonlinear Phenomena*, 52(2):293–331, 1991.

[MN85] J. R. Magnus and H. Neudecker. Matrix differential calculus with applications to simple, hadamard, and kronecker products. *Journal of Mathematical Psychology*, 29(4):474–492, 1985.

[Moh91] B. Mohar. The Laplacian Spectrum of Graphs. *Graph Theory, Combinatorics, and Applications, Vol. 2*, 2:871–898., 1991.

[Moh92] B. Mohar. Laplace eigenvalues of graphs—a survey. *Discrete Mathematics*, 109(1):171–183, 1992.

[Mor05] L. Moreau. Stability of multiagent systems with time-dependent communication links. *IEEE Transactions on Automatic Control*, 50(2):169–182, 2005.

[MPA10] U. Münz, A. Papachristodoulou, and F. Allgöwer. Delay robustness in consensus problems. *Automatica*, 46(8):1252–1265, 2010.

[New00] M. W. Newman. *The Laplacian spectrum of graphs*. PhD thesis, Citeseer, 2000.

[OBH09] S. Ostojic, N. Brunel, and V. Hakim. Synchronization properties of networks of electrically coupled neurons in the presence of noise and heterogeneities. *Journal of computational neuroscience*, 26(3):369–392, 2009.

[OS05] R. Olfati-Saber. Ultrafast consensus in small-world networks. In *Proceedings of the 2005 American Control Conference*, pages 2371–2378. IEEE, 2005.

[OS07] R. Olfati-Saber. Distributed kalman filtering for sensor networks. In *Proceedings of the 46th IEEE Conference Decision and Control*, pages 5492–5498, 2007.

[OSFM07] R. Olfati-Saber, A. Fax, and R. M. Murray. Consensus and cooperation in networked multi-agent systems. *Proceedings of the IEEE*, 95(1):215–233, 2007.

[OSM04] R. Olfati-Saber and R. M. Murray. Consensus Problems in Networks of Agents With Switching Topology and Time-Delays. *IEEE Transactions on Automatic Control*, 49(9):1520–1533, 2004.

[OSS05] R. Olfati-Saber and J. S Shamma. Consensus filters for sensor networks and distributed sensor fusion. In *Proceedings of the 44th IEEE Conference on Decision and Control*, pages 6698–6703, 2005.

[PLS+07] D. A. Paley, N. E. Leonard, R. Sepulchre, D. Grünbaum, and J. K. Parrish. Oscillator models and collective motion. *IEEE Transactions on Control Systems*, 27(4):89–105, 2007.

[PS07] Q. C. Pham and J. J. Slotine. Stable concurrent synchronization in dynamic system networks. *Neural networks : the official journal of the International Neural Network Society*, 20(1):62–77, 2007.

[PTS09] Q. C. Pham, N. Tabareau, and J. J. Slotine. A contraction theory approach to stochastic incremental stability. *IEEE Transactions on Automatic Control*, 54(4):816–820, 2009.

[QWH08] Z. Qu, J. Wang, and R. A. Hull. Cooperative control of dynamical systems with application to autonomous vehicles. *IEEE Transactions on Automatic Control*, 53(4):894–911, 2008.

[RB08] W. Ren and R. W. Beard. *Distributed consensus in multi-vehicle cooperative control*. Springer, 2008.

[RBA07] W. Ren, R. W. Beard, and E. M. Atkins. Information consensus in multivehicle cooperative control. *IEEE Control systems magazine*, 2(27):71–82, 2007.

[RDW91] B. S. Rao and H. F. Durrant-Whyte. Fully decentralised algorithm for multisensor kalman filtering. In *Proceedings of the IEE Control Theory and Applications*, volume 138, pages 413–420. IET, 1991.

[RDWS93] B. S. Rao, H. F. Durrant-Whyte, and J. A. Sheen. A fully decentralized multi-sensor system for tracking and surveillance. *The International Journal of Robotics Research*, 12(1):20–44, 1993.

[Rey87] C. W. Reynolds. Flocks, herds and schools: A distributed behavioral model. In *Proceedings of the ACM SIGGRAPH computer graphics*, volume 21, pages 25–34. ACM, 1987.

[SM88] S. H. Strogatz and R. E. Mirollo. Phase-locking and critical phenomena in lattices of coupled nonlinear oscillators with random intrinsic frequencies. *Physica D: Nonlinear Phenomena*, 31(2):143–168, 1988.

[SPL08] R. Sepulchre, D. A. Paley, and N. E. Leonard. Stabilization of planar collective motion with limited communication. *IEEE Transactions on Automatic Control*, 53(3):706–719, 2008.

[SSB09] J. H. Seo, H. Shim, and J. Back. Consensus of high-order linear systems using dynamic output feedback compensator: Low gain approach. *Automatica*, 45(11):2659–2664, 2009.

[Str00] S. H. Strogatz. From kuramoto to crawford: exploring the onset of synchronization in populations of coupled oscillators. *Physica D: Nonlinear Phenomena*, 143(1):1–20, 2000.

[Str03] S. Strogatz. *Sync: The emerging science of spontaneous order*. Hyperion, 2003.

[TS11] K. Thulasiraman and M. N. Swamy. *Graphs: theory and algorithms*. John Wiley & Sons, 2011.

[TS13] N. Tabareau and J. J. Slotine. Contraction analysis of nonlinear random dynamical systems. *arXiv preprint arXiv:1309.5317*, 2013.

[TSP10] N. Tabareau, J. J. Slotine, and Q. C. Pham. How synchronization protects from noise. *PLoS computational biology*, 6(1):e1000637, 2010.

[Tun08a] S. E. Tuna. LQR-based coupling gain for synchronization of linear systems. *arXiv preprint arXiv:0801.3390*, (ii):1–9, 2008.

[Tun08b] S. E. Tuna. Synchronizing linear systems via partial-state coupling. *Automatica*, 44(8):2179–2184, 2008.

[VCBJ+95] T. Vicsek, A. Czirók, E. Ben-Jacob, I. Cohen, and O. Shochet. Novel type of phase transition in a system of self-driven particles. *Physical review letters*, 75(6):1226, 1995.

[Wie10] P. Wieland. *From static to dynamic couplings in consensus and synchronization among identical and non-identical systems*. Logos Verlag Berlin GmbH, 2010.

[Win67] A. T. Winfree. Biological rhythms and the behavior of populations of coupled oscillators. *Journal of theoretical biology*, 16(1):15–42, 1967.

[WS98] D. J. Watts and S. H. Strogatz. Collective dynamics of 'small-world'networks. *nature*, 393(6684):440–442, 1998.

[WS05] W. Wang and J. J. Slotine. On partial contraction analysis for coupled nonlinear oscillators. *Biological cybernetics*, 92(1):38–53, 2005.

[WSA11] P. Wieland, R. Sepulchre, and F. Allgöwer. An internal model principle is necessary and sufficient for linear output synchronization. *Automatica*, 47(5):1068–1074, 2011.

[Wu05] C. W. Wu. Algebraic connectivity of directed graphs. *Linear and Multilinear Algebra*, 53(3):203–223, 2005.

[XJZY11] D. Xiwang, X. Jianxiang, S. Zongying, and Z. Yisheng. Consensus for high-order time-delayed swarm systems with uncertainties and external disturbances. In *Proceedings of the 30th IEEE Control Conference*, pages 4852–4859, 2011.

[YG05] R. D. Yates and D. J. Goodman. *Probability and stochastic processes: a friendly introduction for electrical and computer engineers*, volume 2. John Wiley & Sons, 2005.

[YKK15] J. Yoo, W. Kim, and H. J. Kim. Distributed estimation using online semi-supervised particle filter for mobile sensor networks. *IET Control Theory and Applications*, 9(3):418–427, 2015.

[ZHL11] J. Zhao, D. J. Hill, and T. Liu. Synchronization of Dynamical Networks With Nonidentical Nodes: Criteria and Control. *IEEE Transactions on Circuits and Systems I: Regular Papers*, 58(3):584–594, 2011.

[ZHL12] J. Zhao, D. J. Hill, and T. Liu. Global bounded synchronization of general dynamical networks with nonidentical nodes. *IEEE Transactions on Automatic Control*, 57(10):2656–2662, 2012.

국문초록

Robust Consensus and Synchronization in Heterogeneous Multi-Agent Systems

이종 다개체 시스템의 상태 일치 및 동기화에 대한 강인성 연구

상태 일치 (consensus) 또는 동기화 (synchronization) 모두 집단 내 각 개체들의 의견이 어떤 관점에서 모두 합의를 보이는 것과 관련이 있고 이 현상들은 시스템들이 상호 작용하는 생물 물리학이나 사회과학, 공학 분야와 같은 여러 집단에서 종종 발견이 된다. 새들이 무리를 지어 움직이는 현상이나 물고기들의 군집 유영, 벌들의 무리 현상들은 자연에서 나타나는 매우 흥미로운 현상들이다. 때때로 상태 일치 이론은 사회 현상을 설명하는 좋은 도구로 쓰이게 되고 특히 공학적인 관점에서 보면 상태 일치와 동기화연구는 매우 많은 응용분야와 관련이 있다. 예를 들어 센서 네트워크, 무인 자동차, 군집 로봇 제어, 이동 통신 시스템 등과 같은 분야들이 좋은 예시가 될 수 있다.

특히 생물 물리학 분야에서는 상호 연결된 시스템에서 상태 일치와 동기화가 외부로부터의 교란 (perturbation)에 대해서 강인성을 보장해 준다는 내용은 잘 알려진 사실이고 이는 여러 연구들의 실험과 시뮬레이션으로부터 입증되어 왔다. 따라서 본 논문에서는 다개체 시스템 (multi-agent systems) 의 강인한 상태 일치와 동기화에 대한 내용을 전개한다. 여기서 다개체 시스템이란 다수의 이종 동적 시스템들이 네트워크 통신을 통해 특정 정보를 교환하며 상호작용하는 시스템을 말한다. 각 개체들의 상호 연결이 정해진 특정 네트워크에서 상태 일치와 동기화 문제를 다루게 되는데 여기서 특정 네트워크라 함은 그래프로 모델이 된 통신 구조와 개별 개체들의 동역학 특성이 비선형 상미분 방정식으로 이루어진 네트워크를 지칭한다.

본 논문은 크게 두 가지 연구로 나눌 수 있는데 첫 번째 연구는 동기화가 어떤 방식으로 상호 연결된 다개체 시스템을 이종성 (heterogeneity) 과 임의의 변이 (random variation) 로부터 강인하게 지켜주는지에 대해서 다루게 될 것이다. 사실, 강인성은 동기화 자체로부터가 아니라 동기화를 이끄는 두 가지 특정 요인에 의한 것으로부터 나온다는 사실을 강조할 필요가 있다. 즉, "많은 수"의 개체들이 "상호 연결" 된 것이 중요하다는 것이다. 따라서 이를 수학적으로 증명하고 그 내용은

다음과 같다. (가) 개체들 사이의 이종성이 매우 큰 상황에서도 각 개체들의 궤적이 상호 연결 강도가 클수록 다른 개체들과 가까워지게 되고 실용적 동기화 (practical synchronization) 들 달성하게 된다. (나) 개체들의 수가 많으면 많을수록 달성된 동기화 현상이 각 개체들의 변이들에 대해서 영향을 덜 받게 된다.

일반적으로 이종 네트워크에서의 상태 일치와 동기화 문제들은 단일 개체를 제어할 때보다 어려운 본질적인 복잡성을 내포하고 있다. 가령 전체 개체수의 많고 적음으로 인한 복잡도, 개별 시스템 동역학의 복잡성, 다수 시스템들로 이루어진 네트워크 위상 구조의 복잡도 등이 존재하게 된다. 따라서 본 논문에서는 이종 다는체 시스템의 군집 행동을 잘 이해할 수 있는 평균 동역학 (averaged dynamics) 개념을 새로이 제시한다.

본 논문의 두 번째 연구에서는 강인한 상태 일치와 동기화의 응용 연구로서 최적의 분산 센서 네트워크 구현을 위한 설계 방법을 제시한다. 비록 중앙 집중형 칼만-부시 필터 (centralized Kalman-Bucy filter) 가 최적의 필터라는 것이 최적 제어 이론 (optimal control theory) 연구들에서 잘 알려져 있지만, 분산 센서 네트워크에서는 분산 기법을 이용하여 대상 시스템의 상태를 추정하는 것이 본질적인 문제이기 때문에 이는 효율적이지 않게 된다. 분산형 칼만-부시 필터 (distribued Kalman-Bucy filter) 의 설계는 기존의 강인한 상태 일치와 동기화 문제를 달성하는 것과 같은 맥락에 있기 때문에 본 논문에서는 중앙 집중형 칼만-부시 필터의 최적성을 분산 기법을 이용하여 달성하기 위한 평균 분산형 칼만-부시 필터 (averaged distributed Kalman-Bucy filter) 개념을 제시하고 제안한 알고리즘이 강한 상호 연결 하에서는 실제로 각 개체의 오차 공분산 행렬 (error covariance matrix) 이 중앙 집중형 칼만-부시 필터의 오차 공분산 행렬로 근접하게 가까워진다는 것을 보이게 된다. 따라서 분산 기법을 통해 중앙 집중형 칼만-부시 필터의 최적성을 복구 할 수 있게 된다. 또한 센서 네트워크 크기를 늘이고 줄일 수 있는 유연한 분산형 칼만-부시 필터 (flexible distributed Kalman-Bucy filter) 를 제시하고 시뮬레이션을 통해 제시한 설계 기법들의 성능을 검증한다.

주요어 : 다개체 시스템, 상태 일치, 동기화, 강인성, 평균 동역학, 분산 센서 네트워크, 분산형 칼만-부시 필터

학 번 : 2010–20777